JOURNAL OF FOOD PROCESS ENGINEERING

D.R. HELDMAN
and
R.P. SINGH
COEDITORS

FOOD & NUTRITION PRESS, INC.

VOLUME 19, NUMBER 3 SEPTEMBER 1996

JOURNAL OF FOOD PROCESS ENGINEERING

All articles for publication and inquiries regarding publication should be sent to DR. D.R. HELDMAN, COEDITOR, *Journal of Food Process Engineering*, Food Science/Engineering Unit, University of Missouri-Columbia, 235 Agricultural/Engineering Bldg., Columbia, MO 65211 USA; or DR. R.P. SINGH, COEDITOR, *Journal of Food Process Engineering*, University of California, Davis, Department of Agricultural Engineering, Davis, CA 95616 USA.

All subscriptions and inquiries regarding subscriptions should be sent to Food & Nutrition Press, Inc., 6527 Main Street, P.O. Box 374, Trumbull, CT 06611 USA.

One volume of four issues will be published annually. The price for Volume 19 is $149.00, which includes postage to U.S., Canada, and Mexico. Subscriptions to other countries are $172.00 per year via surface mail, and $183.00 per year via airmail.

Subscriptions for individuals for their own personal use are $119.00 for Volume 19, which includes postage to U.S., Canada and Mexico. Personal subscriptions to other countries are $142.00 per year via surface mail, and $153.00 per year via airmail. Subscriptions for individuals should be sent directly to the publisher and marked for personal use.

The *Journal of Food Process Engineering* is listed in *Current Contents/Agriculture, Biology & Environmental Sciences (CC/AB)*, and SciSearch, and Research Alert.

The *Journal of Food Process Engineering* (ISSN:0145-8876) is published quarterly (March, June, September and December) by Food & Nutrition Press, Inc.—Office of Publication is 6527 Main Street, P.O. Box 374, Trumbull, Connecticut 06611 USA.

Second class postage paid at Bridgeport, CT 06602.

POSTMASTER: Send address changes to Food & Nutrition Press, Inc., 6527 Main Street, P.O. Box 374, Trumbull, Connecticut 06611 USA.

JOURNAL OF FOOD PROCESS ENGINEERING

JOURNAL OF FOOD PROCESS ENGINEERING

Journal of FOOD PROCESS ENGINEERING

VOLUME 19
NUMBER 3

Coeditors: D.R. HELDMAN
R.P. SINGH

FOOD & NUTRITION PRESS, INC.
TRUMBULL, CONNECTICUT 06611 USA

ISSN 0145-8876

Printed in the United States of America

CONTENTS

FLUID-TO-PARTICLE CONVECTIVE HEAT TRANSFER COEFFICIENT AS EVALUATED IN AN ASEPTIC PROCESSING HOLDING TUBE SIMULATOR

G.B. AWUAH, H.S. RAMASWAMY[1], B.K. SIMPSON and J.P. SMITH

Department of Food Science and Agricultural Chemistry
Macdonald Campus of McGill University
21,111 Lakeshore Rd, Ste Anne de Bellevue
Quebec, Canada, H9X 3V9

Accepted for Publication May 26, 1995

ABSTRACT

A pilot scale aseptic processing holding tube simulator was fabricated for evaluating fluid-to-particle convective heat transfer coefficients at temperatures up to 110C. The simulator was calibrated to give carrier fluid flow rate as a function of CMC concentration, temperature, pump rpm and pipe diameter. Fluid-to-particle heat transfer coefficients (h_{fp}) were estimated with model and real food particles held stationary in a moving liquid. Data were gathered under various conditions: CMC concentration (0 - 1.0% w/w), flow rate (1.0 - 1.9 × $10^{-4}m^3/s$) and particle size (diameter: 21 and 25.4 mm; length: 24 and 25.4 mm). Depending on operating conditions, average heat transfer coefficients (h_{fp}) ranged from 100 to 700 W/m^2C with corresponding Biot numbers (Bi) ranging from 10 to 50. CMC concentration, fluid temperature and flow rate, as well as their interactions, had significant effect ($p < 0.05$) on h_{fp} for both Teflon and potato particles. Some differences were observed with respect to the associated h_{fp} for Teflon and potatoes due probably to differences in their structural/textural characteristics. Heat transfer coefficient associated with cooling were significantly lower ($p < 0.05$) than those associated with heating.

INTRODUCTION

High temperature short time (HTST) sterilization has long been demonstrated to be effective in minimizing nutrient and quality factor degradation and, therefore, highly favored over traditional processing of heterogenous foods in metal, glass and plastic containers. The concept has resulted in commercialization of aseptic processing of liquid foods. However, commercialization of

[1]To whom all correspondence should be addressed.

Journal of Food Process Engineering **19** (1996) 241–267. *All Rights Reserved.*

low-acid (pH > 4.6) foods containing discrete particles larger than 3.2 mm in major dimension still remain to be accomplished (Chandarana and Gavin 1989), particularly in North America, where federal regulations require stringent proof of process adequacy through microbiological verification/validation. Mathematical modelling serves as an important tool in reducing the number and cost of experiments required in designing, validating, and, optimizing processing systems (Clark 1978; Maesmans *et al.* 1992). Several researchers (Sastry 1986; Larkin 1989; Chandarana and Gavin 1989; Skjoldebrand and Ohlsson 1993) have proposed mathematical procedures for predicting heat transfer to particles and computer simulation programs for process evaluation. The effectiveness of these models and programs in predicting adequate processes depend on the accuracy of input thermophysical and boundary value parameters.

Dignan *et al.* (1989) listed critical factors needed in modelling heat transfer and lethality distribution in continuously processed low-acid particulate foods as: particle size/distribution, the convective heat transfer coefficient and residence time distribution both in the heat exchanger and holding tube. According to Larkin (1990), examining critical control factors depends not only on whether the parameters influence the process, but the extent to which these factors affect the process. Using an implicit Crank-Nicolson finite difference method to simulate an aseptic system, Lee *et al.* (1990) demonstrated that particle size, shape, particle thermal properties and residence time distribution within the scraped surface heat exchanger (SSHE) and the holding tube influenced the minimum process time required to achieve a 6 log-cycle reductions of *Clostridium sporogenes* PA3679. The authors found that the effect on the minimum process time was significant when the fluid-to-particle heat transfer coefficient (h_{fp}) ranged between 50 to 500 W/m^{2}C, but leveled out beyond 500 W/m^{2}C. The physical significance is that minor changes in h_{fp} beyond 500 W/m^{2}C does not greatly affect the holding tube length/processing time required to achieve a given F_o. As Larkin (1990) demonstrated, a change in h_{fp} from 175 to 181 W/m^{2}C in the holding tube could result in more than 5% increase in accumulated F_o. Since the Biot number associated with aseptic processing of foods are most likely to be below 40, the convective heat transfer coefficient may present one of the rate limiting parameters in process design (Heldman and Singh 1981). Proven to be highly influential and significant in process evaluation through simulations, the fluid-to-particle heat transfer coefficients in both the heat exchanger and holding tube probably are the most important but difficult parameters to be determined experimentally (Dignan *et al.* 1989; Heldman 1989).

Two approaches have been used for estimating h_{fp} at elevated temperatures; the "indirect approach" which utilizes time-temperature integrators (TTI) such as immobilized enzymes or microorganisms (Hunter 1972; Heppell 1985), and the "direct approach" which uses time-temperature data gathered directly from

a particle (Sastry 1986; Alhamdan *et al.* 1990; Chandarana *et al.* 1990; Zuritz *et al.* 1990; Awuah *et al.* 1993). Aside from the fact that the TTIs depend on the reliability and reproducibility of systems whose kinetics need to be accurately established, placing the TTIs in particles which provide high Biot number heating conditions would make them respond more to thermal diffusivity rather than h_{fp} (Maesmans *et al.* 1992).

Several studies have been carried out on the evaluation of h_{fp} under simulated aseptic processing conditions (Sastry *et al.* 1989, 1990; Alhamdan *et al.* 1990; Zuritz *et al.* 1990; Mwangi *et al.* 1993; Awuah *et al.* 1993; Astrom and Bark 1994; Cacace *et al.* 1994; Balasubramaniam and Sastry 1994a,b; Zitoun and Sastry 1994a,b) with only a few carried out at temperatures in excess of 100C (Chandarana *et al.* 1988, 1990; Chang and Toledo 1989; Balasubramaniam and Sastry 1994b). Under high temperature processing conditions, the relative velocity between the particle and the carrier fluid may vary depending on the characteristics of both the fluid and system. The objectives of this research work were to (1) fabricate a pilot-scale aseptic processing holding tube simulator for carrying out heat transfer studies, (2) evaluate the performance of the simulator in relation to gathering heat penetration data for routine estimation of fluid-to-particle convective heat transfer coefficients (3) study the individual and combined effects of fluid concentration (apparent viscosity), temperature and flow rate on h_{fp} under simulated aseptic processing conditions and (4) investigate h_{fp} associated with the cooling of heat treated particles, since data related to cooling may play an important role in quality optimization. The studies were conducted with finite cylindrical particles due to paucity of experimental data associated with such particles in the literature.

MATERIALS AND METHODS

Construction of the Simulator

The simulator was constructed with the following salient features: (1) a heat exchanger and a reservoir, (2) steam inlet controls for temperature regulation, (3) a positive displacement pump, (4) a holding tube equipped with a by-pass mechanism for carrier fluid temperature stabilization, (5) a mechanism for rapid cooling of heated samples, (6) a readily accessible compartment for mounting model/food particles, (7) a device for holding the particle along the geometric center of the holding tube in either parallel or perpendicular direction with respect to fluid flow, (8) a flow meter for measuring fluid flow rates and (9) a safety valve to release excess pressure from the system. Copper pipes and brass plates were chosen for construction of most parts on the basis of strength, workability and cost. Figure 1 shows a schematic diagram of the simulator

which consisted mainly of either a 5.1 cm (2 in.) or 7.6 cm (3 in.) internal diameter copper pipe equipped with a by-pass and mounted on a metal framework (not shown in diagram). The piping network was insulated to reduce heat losses to the surrounding, and inclined upward at an angle of ~ 1.2° as per requirement. A standard steam jacketed kettle was used to heat the fluid which was recirculated back into the kettle using a variable-speed sine pump (Model SPS 20, Systron Proquip, Pointe Claire, PQ) through the system. A special lid having two openings was secured onto the steam kettle with G-clamps. One of the openings facilitated the filing of the system with cold fluid, while the other served as a return port for the fluid to be reheated. Aside from heating the cold fluid to a predetermined temperature, the steam kettle served as an on-line reservoir for the 90 L capacity unit. The steam kettle was shielded from other components of the simulator with plexiglass for safety reasons.

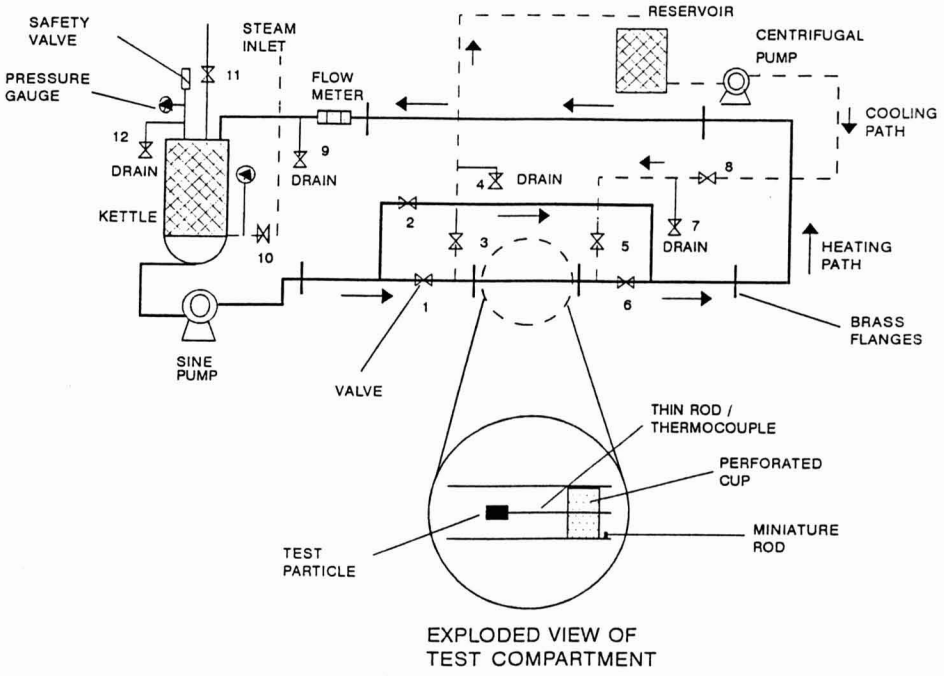

FIG. 1. A SCHEMATIC DIAGRAM OF THE PILOT SCALE SIMULATOR (NOT DRAWN TO SCALE)

A minimum pipe length (24 times the tube diameter) was provided before and after the test compartment to minimize fluid distortions. A flow meter (Model FTB-5005, Omega Engineering Inc., Stamford, CT) located on the return path measured the volumetric through flow rate. Five Teflon-insulated 30 AWG copper-constantan thermocouples were installed at several locations on the piping network with brass thermocouple receptacles (Type C-5.2, Ecklund-Harrison Technologies Inc., Cape Coral, FL). The temperature of the fluid in the steam kettle and in the test compartment were continuously monitored with thermocouple thermometers (Model 650, Omega Engineering Inc., Stamford, CT) for manually adjusting the steam flow. In addition to the heating network, a "cooling loop" including a cold water reservoir, valves and a variable-speed centrifugal pump (Micropump, Cole Parmer Instrument Co., Chicago, IL) enabled heated samples to be cooled *in-situ*.

Test Compartment and Sample Holder

The test compartment (Fig. 1) consisted of approximately 30 cm long copper pipe welded onto brass plates (flanges). Four holes were drilled on each flange for coupling the test compartment to the holding tube. A hole was punched at the exit of the test compartment and sealed off with a miniature (1.27 cm long) brass rod which protruded into the compartment, purposely, to support the sample holder from sliding out during fluid flow. Two Teflon-insulated 36 AWG copper-constantan thermocouples were attached to the entrance and exit of the test compartment to monitor fluid temperature. The sample holder consisted of (1) a perforated cylindrical cup, which was carefully dimensioned and slotted to fit the test compartment by sliding along the miniature brass rod and turning to lock and (2) approximately 15 cm long brass rod with copper rings welded at its tip to hold a test sample. The brass rod was threaded at the other end and connected to the perforated cup by means of a miniature nut.

Operation of the Simulator

During preheating, the test compartment was isolated by diverting the fluid through the by-pass and back into the kettle. This was achieved by keeping the ball valve #2 open and valves #1 and #6 closed (Fig. 1). The system was stabilized with the recirculating fluid until the desired temperature was obtained. The temperature of the fluid was thereafter adjusted by manual regulation of the steam inlet valve. Prior to each experimental run, the test compartment was taken out of the system and fitted with the perforated-cup sample-holder combination which ensured flexibility and proper positioning of test samples along the central axis of the tube. On achieving the desired system temperature, the test compartment was attached and secured in place. Valve #1 was opened and valve #2 was simultaneously closed to allow fluid into the test compartment.

All valves except #1, #5 and #7 remained closed as the test compartment was filled up with the hot fluid. This procedure drove any resident fluid out of the compartment through valve #7. Once the test compartment was full, valve #6 was opened and valve #5 was simultaneously closed to let the fluid flow back into the kettle to be reheated. Time-temperature data were continuously gathered at predetermined time intervals. Once heating was completed, valve #2 was opened while valves #1 and #6 were closed, allowing the fluid to be diverted back into the kettle. Valves #3 and #5 were gradually opened to release excess pressure from the system through the drain. Cooling was initiated by opening valve #8 and simultaneously closing the valve #7 to pump the cold fluid into the test chamber using a variable-speed centrifugal pump (Micropump, Cole Parmer Instrument Co., Chicago, IL).

Data Acquisition System

All thermocouples were connected to a data acquisition system which consisted of (1) a personal computer (2) a Dash-8, 8 analog input channels featuring a high-speed, 12-bit, successive-approximation A/D converter with 35 μs maximum conversion time and data throughput rate of approximately 30 kHz, and (3) an EXP-16 expansion multiplexer which provided 16 thermocouple input channels (Metra-Byte Corp., Tauton, MA).

Evaluation of Heat Transfer Coefficient (h_{fp})

Fluid-to-particle convective heat transfer coefficients were estimated (h_{fp}) using a modified rate method (Ramaswamy *et al.* 1983) which utilizes the heating rate index (f_h), estimated from the straight line portion of the semi-logarithmic plot of temperature ratio against time, for back calculating the h_{fp}. The theoretical background involved with calculating the heat transfer coefficient by the rate method is detailed in Ramaswamy *et al.* (1983). This method was chosen on the basis of appropriateness for use and its nonrestrictive nature with respect to thermocouple placement in test materials. An *initial estimate* of the heat transfer coefficient was made using "the lumped capacity approach"; a value of f_h or f_c was then calculated and compared with its experimental counterpart. The estimated h_{fp} is then sequentially varied until the calculated f_h or f_c value matched the experimental value, thus giving the h_{fp} value associated with the test run. An iterative computer program based on simplified equations developed by Ramaswamy *et al.* (1982) was used for calculating the roots of the characteristic functions involved.

Test Materials and CMC Preparation

Potatoes (purchased from a local market and stored in a refrigerator at 5C)

and Teflon (Small Parts Inc., Miami Lakes, FL) were used for the study. Cylinders of potato were punched out using a cork borer of known diameter and the required length was cut with a knife. A pinhole was made along the axis of the particle to coincide with the central plane. A Teflon-insulated 30 AWG copper-constantan thermocouple was attached to a toothpick and pushed along the pinhole until it traveled an equivalent distance made with the pin. The point of entry was then sealed off with epoxy glue and left to dry within 3-5 min. This approach reduced chances of water leaking into the sample along the thermocouple wire. For Teflon particles, appropriate lengths were cut from a Teflon rod and a hole was drilled along its axis to predetermined depths using a drilling machine. Teflon-insulated 30 AWG copper-constantan thermocouples were inserted into the holes and secured with epoxy glue. All thermocouples were calibrated against an ASTM mercury-in-glass thermometer prior to installation. Test particles (positioned with axis perpendicular to carrier fluid) were held along the central axis of the tube using a specially designed sample holder which offered minimum resistance to the carrier fluid. Temperature history of test samples were simultaneously gathered and stored on a personal computer at 5 s intervals.

Two concentrations (0.5 and 1.0% w/w) of food grade carboxymethylcellulose (Pre-hydrated CMC PH-2500, TIC Gum Inc., Belcamp, MD) were prepared by adding water to a known quantity of CMC powder in a variable speed mixer (Hobart Model D-300, Hobart Canada Inc., Mississauga, ON). Thorough mixing was carried out to ensure complete dissolution of CMC. The solution was adjusted to the desired concentration in a 90 L plastic container and left overnight until use.

Rheological and Thermal Properties

High temperature rheological data were obtained using a rotational viscometer Model RV20 (Haake Mess-Technik, Karlsruhe, Germany) coupled to an M-S OSC measuring head and a D100/300 sensor, and modelled with the classical power law equation for the downward linear-ramp shearing curve (Abdelrahim and Ramaswamy 1995). The model parameters measured from the upward ramp shearing curve would represent the rheological behavior of "virgin" sample while those from the downward ramp are representative of a test sample that has gone through a certain shear history. The power-law parameters from the downward ramp were considered more appropriate for the present work since, in the experimental set-up, the carrier fluid was continuously recirculated. Effective mean CMC apparent viscosity values were obtained, as detailed in Skelland (1967), using the following relationship:

$$\mu_{mean} = [2^{n-2}m\ [(3n+1)/n]^n n\ (\frac{D_t}{V})^{1-n}]\ /\ (3n-1)$$

where n, m, D_t and V represented fluid behavior index, consistency coefficient (Pa.s), diameter of tube (m) and average linear velocity (m/s) of the carrier fluid (volumetric flow rate divided by the cross sectional area), respectively. The thermal conductivity and heat capacity of CMC were computed from the equations given by Heldman and Singh (1981). Thermophysical properties for potato and Teflon are given elsewhere (Awuah *et al.* 1993, 1995).

Experimental Design and Data Analysis

To study the effect of both system and product parameters, a 3^3 full factorial design involving fluid concentration (0, 0.5 and 1.0% w/w CMC), flow rate (1.0, 1.5, and 1.9 $\times$ 10^{-4} m^3/s), and temperature (90, 100, and 110C) was conducted with 25.4 mm diameter by 25.4 mm length Teflon and 21 mm diameter by 24 mm length potato samples. The temperature range of 90-110C was selected primarily to include the transition zone from the nonpressurized (90-100C) to pressurized (100-110C) heating conditions. Heat transfer coefficients associated with cooling of heated potato particles were estimated at selected conditions: initial temperatures (90, 100 and 110C), and flow rate (1.0, 1.53, 1.61, 1.62, and 1.71 $\times$ 10^{-4} m^3/s). The particle is held stationary, and hence these fluid velocities represent the difference in velocity between the fluid and the particle. The convectional fluid flow rate under commercial processing conditions is about 10 gallons per min. The range of fluid to particle velocity ratios reported in literature (Chandarana *et al.* 1990; Dutta and Sastry 1990; Sastry 1986) generally lies between 0.8 to 1.2. At an average fluid flow rate of 10 gallons per min, this translates to a maximum difference in velocity between the fluid and particle of 2 gallons per min which is about the midpoint of the fluid flow rate range employed in the study (1.5 to 2.5 gallons per min). Cooling medium was water at 20C. All experiments were replicated at least five times.

In order to facilitate data handling and visual comparison of temperature profiles, all time-temperature data were normalized with respect to initial and medium temperatures (Schultz and Olson 1940). As follows from theory, such normalization does not influence the evaluated f_h which is the basis of the present studies for h_{fp} determination. Due to unequal number of observations within the same treatment, mean values of the heat transfer coefficient as affected by various processing conditions were analyzed using Least Significance Difference (LSD) multiple comparison procedure (Steel and Torrie 1960). Since a finite cylinder has two Biot numbers (related to cylindrical and cross sectional surfaces), a *characteristic* dimension (d_{cd}) estimated as the diameter of a sphere having the same volume as a finite cylinder (d_{cd} = 1.15d) was used in calculating the representative Biot number ($Bi = h_{fp}d_{cd}/k_p$). The 15% increase in the characteristic dimension was redefined to include particle length as

follows: $d_{cd} = d\ (1 + 0.15d/L)$: where d and L represent the diameter and length of a finite cylinder respectively.

RESULTS AND DISCUSSION

Performance Testing of the Simulator

Since uniform fluid flow profiles were essential in heat transfer studies, adequate pipe lengths were provided before and after the test compartment to reduce disturbances due to pipe bends. The clamping mechanism allowed the system to be operated at a maximum pressure of 15 psig and 115C. This constraint was imposed by the "soft" components (especially the scraper gate) of the positive displacement sine pump. The location of the thermocouples and visual observation of the fluid temperatures allowed excellent control of system temperature manually. In general, a 2C drop in temperature was found between the exit of the jacketed steam kettle via the holding tube back to the steam kettle, covering a total pipe length of approximately 5 m. This indicated that pipe insulation was very effective in reducing heat losses to the surrounding. Stabilizing the simulator to the desired operating temperature took between 30 to 50 min depending on fluid concentration and data collection was initiated prior to exposing the compartment to the hot fluid. Figure 2 shows time-temperature plots of data gathered from a stationary particle in a typical experiment. A constant fluid temperature could be maintained over the heating period and heating was carried out till the particle center temperature approached that of the fluid.

Calibration of the Simulator

It was observed that for a given pump speed (rpm), the volumetric through flow rate measured with the flow meter varied for different fluid concentrations and temperatures. This observation could be attributed to slip between the pump's rotor, scrapper gate, and housing resulting in a reduced fluid output for less viscous fluids. This observation indicated qualitatively that fluid concentration was temperature dependent, with fluid apparent viscosity decreasing with increasing temperature. Therefore, fluid flow rates were recorded for three CMC concentrations (0, 0.5 and 1.0% w/w), three temperatures (90, 100 and 110C), and three pump speeds (120, 160 and 190 rpm) and for two pipe diameters (5.08 and 7.62 cm nominal diameter). The influence of the above factors and their interactions was assessed with a General Linear Model (GLM) procedure of the Statistical Analysis System (SAS). As indicated in Table 1, pump speed rpm (n), fluid concentration (C), temperature (T), pipe diameter (D) and their interactions had significant influence ($p < 0.005$) on measured flow rate. Using stepwise multiple regression, the required flow rate (R in m^3/s $\times$

10^4) for predetermined levels of concentration (C in dimensionless %; i.e., 0.005 and 0.01 to represent 0.5% and 1%, respectively), temperature (T in °C), pump speed (n, in rpm) and pipe diameter (D, in m) was obtained as:

$$R = 0.13D + 8.4 \times 10^{-2} C \times T + 1.5 \times 10^{-2} n - 0.25 C \times D - 1.4\ 10^{-3} D \times n - 0.61$$

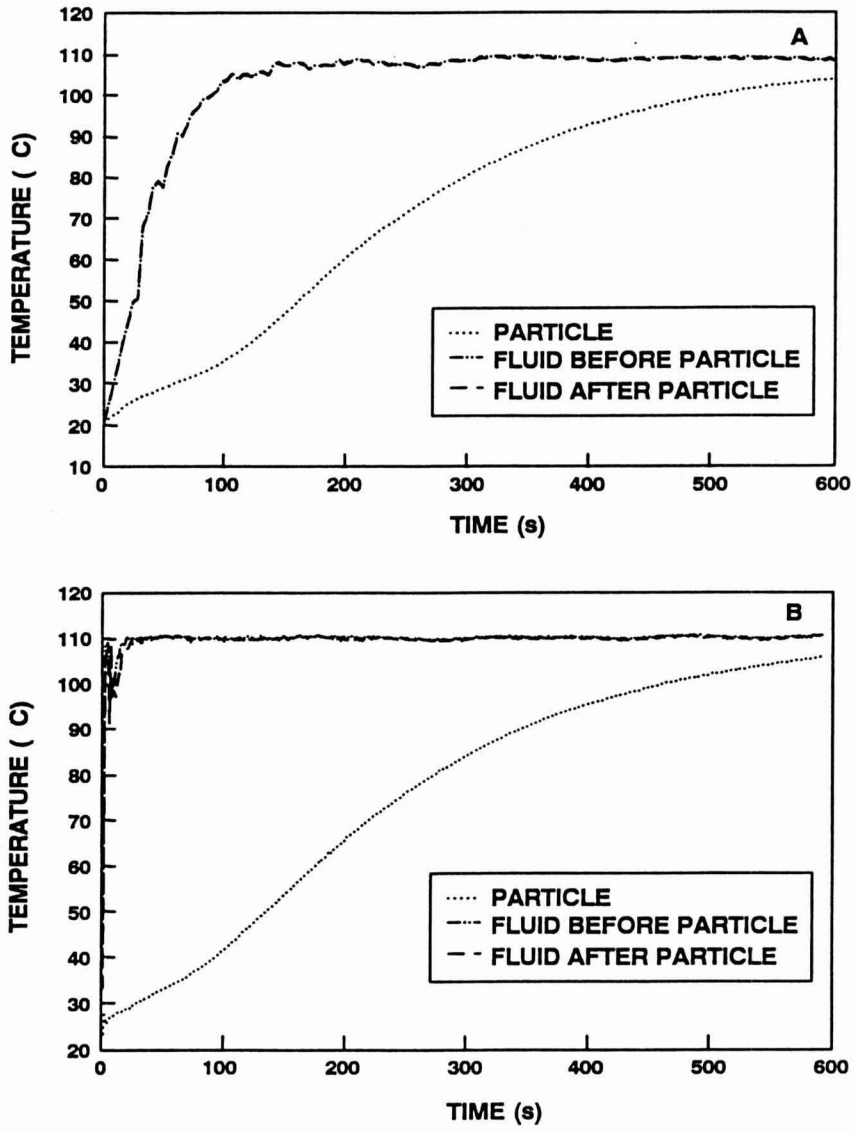

FIG. 2. HEAT PENETRATION CURVES FOR HEATING A 25.4 MM DIAMETER AND 25.4 MM LONG TEFLON PARTICLE AT 110C

TABLE 1.
ANALYSIS OF VARIANCE OF FACTORS INFLUENCING FLUID FLOW RATE

Source	dF	Sum of Squares	Mean Square	F
Model	25	45.33	1.81	267.27*
Main effects				
Concentration (C)	2	3.16	1.58	233.14*
Temperature (T)	2	1.27	0.63	93.36*
Pump speed (n)	2	24.35	12.18	1795*
Diameter (D)	1	2.31	2.31	340.16*
Interactions				
C × T	4	0.705	0.176	25.97*
C × n	4	0.148	0.0371	5.46**
C × D	2	0.59	0.30	43.63*
T × n	4	0.36	0.09	13.33*
T × D	2	0.213	0.106	15.69*
n × D	2	0.18	0.09	13.01*
Residual (error)	118	0.801	0.007	
Total	143	46.13		
R^{2b}	0.98			

[b] Coefficient of determination;
Level of significance * $p < 0.005$; Level of significance ** $p < 0.01$

A good correlation ($R^2 = 0.92$) was obtained between observed and predicted values (Fig. 3). Thus, the pump speed (rpm) needed to output a given fluid flow was generally found to be higher for low viscosity fluids as compared to higher viscosity fluids at all temperatures. Alternatively, the pump speed (rpm) required for achieving a given flow rate could also be obtained from concentration (C), temperature (T) and pipe diameter (D) using the following regression equation ($R^2 = 0.90$):

$$n = 39.4 + 5.8\ R \times D + 18.3\ C \times D + 67.5\ R - 0.63\ C \times T$$

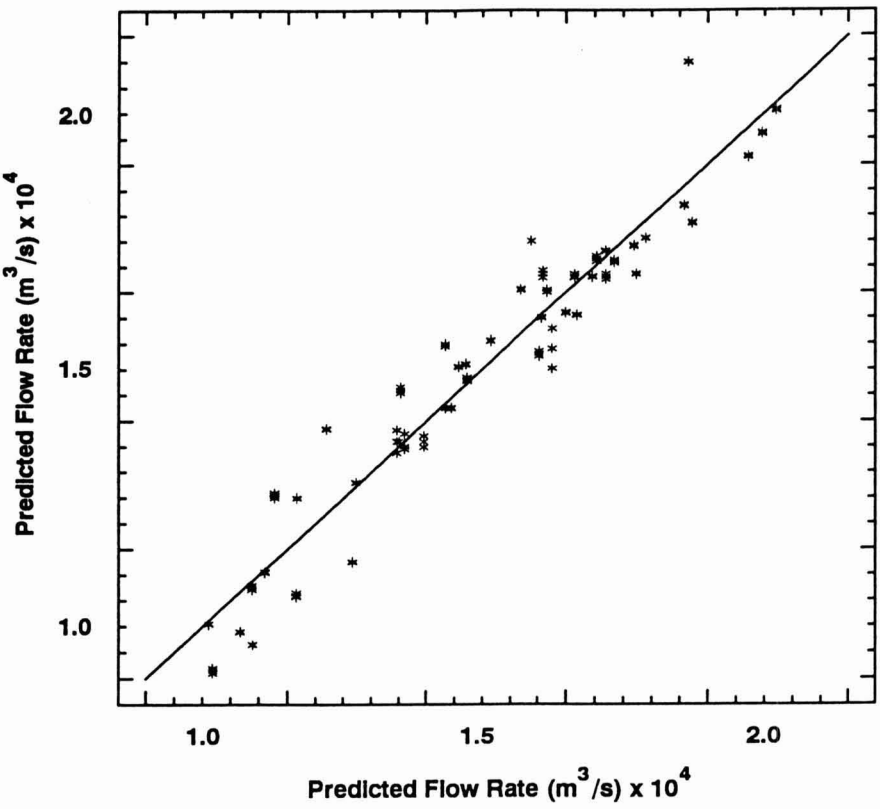

FIG. 3. PLOT OF OBSERVED VERSUS PREDICTED FLOW RATE AS A FUNCTION OF TEMPERATURE, CONCENTRATION AND PUMP RPM

Temperature Response in the Simulator

The simulator could be operated under one of the two modes for gathering heat penetration data from test samples. In the first mode of operation (referred to as M1), the test compartment was initially filled with cold fluid. The hot recirculating fluid was then let in, forcing the cold fluid out of the compartment within 120 to 150 s depending on operating temperature and fluid flow rate (Fig.

2A). Higher pressures associated with elevated temperatures contributed to reducing the "come-up" time in the compartment. Although, the test compartment goes through a transient phase prior to establishing the desired operating temperature (Fig. 2A), this mode of operation was found suitable for both low and highly conductive materials. However, the use of analytical routines for calculating heat penetration and other parametric values become limiting especially for highly conductive materials which may follow almost the same temperature profile as that of the fluid. Calculating the convective heat transfer coefficient under such situations will require numerical techniques which accommodate transient changes in medium temperatures.

In the second mode of operation (referred to as M2), the test compartment was left empty prior to exposure to the hot fluid. Filling and heating of the test compartment to operating condition was achieved much more rapidly (Fig. 2B). The fundamental requirement (i.e., a constant temperature medium) for implementing analytical routines was satisfied with the rapid exposure of test particles to the medium temperature. The fluid, however, goes through a momentary temperature drop (Fig. 2B) especially for conditions in excess of 100C due to both heat losses to the test compartment and sudden exposure to atmospheric conditions which was found necessary to evacuate entrapped air. After approximately 50 s of heating (Fig. 2B), the fluid temperature appeared to stabilize and remain constant over the rest of heating period, with an average standard deviation of $\pm$ 0.2C. It should be emphasized that achieving constant fluid temperature was easily effected with the strategic location of the visual thermometer thermocouples and manual regulation of the steam inlet valve. To stimulate the effect of relative velocities on heat transfer coefficients, turbulent eddies had to be minimized from the onset of data gathering. Hence, the use of highly conductive materials in conjunction with the mode of operation M2 appear inappropriate for estimating heat transfer coefficients.

Based on the heating characteristics of the test compartment in relation to the mode of operation, the mode M1 was found more adequate and convenient for routine estimation of heat transfer coefficients as a function of system parameters using low conductive products.

Fluid to Particle Heat Transfer Coefficients

Depending on experimental conditions, the individual value of fluid-to-particle heat transfer coefficient ranged from 100 to 500 W/m^{2}C and 230 to 700 W/m^{2}C with corresponding Biot number (Bi) ranging from 10 to 50 and 10 to 30 for Teflon and potato samples, respectively. The range of Biot numbers found in the present study falls around the range (0.1 to 40) specified for conditions involving both internal and external resistances to heat transfer (Heldman and Singh 1981). The h_{fp} values found in the present study fall in the

lower end of the overall range (100-5000 W/m^{2}C) reported in the literature (Chandarana *et al.* 1988; Chang and Toledo 1989; Alhamdan *et al.* 1990; Chandarana *et al.* 1990; Zuritz *et al.* 1990; Mwangi *et al.* 1993; Astrom and Bark 1994; Cacace *et al.* 1994; Balasubramaniam and Sastry 1994a,b; Zitoun and Sastry 1994a,b). Generally, the h_{fp} values were under the 500 W/m^{2}C mark reported as the upper limit for aseptic processing considerations (Lee *et al.* 1990). Further, the h_{fp} values from this study compares favorably with those reported in studies carried out at elevated temperatures: 239-303 W/m^{2}C (Chang and Toledo 1989); 134-669 W/m^{2}C (Balasubramaniam and Sastry 1994b).

Influence of Fluid Concentration, Temperature and Flow Rate

Dutta and Sastry (1990) pointed out that one critical factor affecting particle velocity, and therefore, the heat transfer coefficient, is fluid apparent viscosity. Higher viscosities associated with fluids, retard heat transfer rates, especially when the associated turbulence decrease the fluid-to-particle relative velocity at the interface. The impact of fluid viscosity and flow rate on h_{fp} has been reported in several studies. Most of these studies (with the exception of some, for example, Chandarana *et al.* 1988; Chang and Toledo 1989; Balasubramaniam and Sastry 1994b) were conducted at low temperatures. Such conditions ignore the combined influence of temperature and concentration on h_{fp}. Studying heat transfer to particulates under free convection situations, Awuah *et al.* (1993) highlighted the fact that the sensitivity and response of fluid viscosity to higher temperatures may shift the natural heat transfer mode from mixed to forced convection. According to Astrom and Bark (1994), aseptic simulations should be carried out with liquids of relevant apparent viscosity at the operating temperature. One major limitation to the use of higher temperatures in studying aseptic processes is the lack of data on rheological properties of carrier fluid at aseptic conditions (Abdelrahim and Ramaswamy 1995). In a review on modelling continuous sterilization of particulate foods, Sastry (1992) stressed the fact that food tissues permit free transport of mass across its boundary, and may be considered to possess higher effective thermal conductivities. He also highlighted the possibility of starch leaching out of starchy particles into the fluid, thus increasing fluid viscosity. These phenomena are most often considered to have negligible effects and, therefore, ignored in heat transfer studies. Where practical, real food materials should be used as test samples, or at least the model particle used should possess similar thermophysical properties. A material with a very different heat capacity may influence natural convection (Astrom and Bark 1994). The 3 $\times$ 3 $\times$ 3 full factorial design experiments involving CMC concentration, carrier fluid flow rate and temperature with two test samples (an inert and a food particle) in a 5.08 cm (2 in.) diameter pipe was carried out in this study to explore the above scenarios although mass transfer

aspects were not verified experimentally. CMC effective mean apparent viscosity varied from 0.021 to 0.206 Pas.

Table 2 shows the analyses of variance results for the effects of individual factors and their interactions on the h_{fp} values associated with both potato and Teflon particles of approximately same volume to surface area ratio. The results indicate that the model was highly significant ($p < 0.0001$) with an R^2 value greater than 0.95 for both samples. Examination of the data (Table 2) shows that all main factors, i.e., temperature (T), concentration (C), and flow rate (R) significantly influenced the convective heat transfer coefficient. Furthermore, the two factor interactions, T × C, T × R, and C × R and the three factor interaction (T × C × R) significantly influenced estimated h_{fp}. Based on the highly positive correlation coefficients of the main effects and their higher order interactions, estimated heat transfer coefficient can be said to be affected as the level of each factor changes.

TABLE 2.
ANALYSIS OF VARIANCE FOR THE 3×3×3 FACTORIAL DESIGN OF FACTORS INFLUENCING THE FLUID-TO-PARTICLE CONVECTIVE HEAT TRANSFER COEFFICIENT

Source	dF	SS^T	F^T	SS^P	F^P
Model	26	2419537	261***	2260081	123***
Main effects					
Temperature (T)	2	334615	469***	996623	702***
Concentration (C)	2	1039027	1458***	707589	499***
Flow rate (R)	2	412391	578***	307638	216***
Interactions					
T × C	4	169673	119***	89501	31***
T × R	4	147482	104***	51288	18***
C × R	4	124060	87***	68857	24***
T × R × C	8	192287	67***	38586	7***
Residual (error)	97^T (120^P)	34573		85083	
Total	123^T (146^P)	2454109		2345164	
R^{2h}		0.99^T		0.96^P	

[T]Teflon; [P]Potato
***Level of significance ($p < 0.0001$)
[h]Coefficient of determination

The effect plots of the influence of various parameters and some of their interactions on h_{fp} are presented in Fig. 4 to 9. The points represent the mean of all experimental values at a given level of the variable in question and the vertical bar at the mean indicate the standard deviation in h_{fp} values. Because of the averaging of values for a given parameter over the entire range of the factorial design of experiments, the effect curves don't span the full range of h_{fp} values found in the study (100-700 W/m^2C). As the number of combinations involved in the averaging decreases, the range of h_{fp} values gets broadened (see Fig. 7-9 shown for interactions). The flow rate effect generally appeared to be linear in the range studied (Fig. 4), more so with Teflon than potato particles. Values of h_{fp} increased by 50% for potato while they doubled for Teflon as the flow rate changed from 1.0×10^{-4} to 1.9×10^{-4} m^3/s. The temperature effect on h_{fp} was nonlinear with both Teflon and potato particles (Fig. 5). As the temperature increased from 90 to 100 and 110C, the h_{fp} values increased by about 80 and 90%, respectively, for Teflon. For potato samples, between 90 and 100C, h_{fp} increased by only 15%, but as the temperature increased to 110C, a 60% increase was found. The association of higher heat transfer coefficient at higher temperature may be a result of the combined effect of temperature on fluid viscosity and product thermophysical properties. With biological samples, higher temperatures may also result in rupturing/altering the interfacial/boundary layer characteristics. The release of tissue gases as suggested by Sastry (1992) may have caused thermal boundary layer disruption in the potato samples, resulting in the enhancement of the fluid-to-particle interface heat transfer coefficient. The concentration effect on h_{fp} for Teflon was much more between 0 and 0.5% CMC (54% drop) than between 0.5 and 1.0% CMC (a marginal 9% drop). For potato particles, approximately 20% drop occurred in a linear fashion for each 0.5% rise in CMC concentration (Fig. 6). The flow rate and concentration effects on h_{fp} observed in this study were somewhat more pronounced than those reported by Balasubramaniam and Sastry (1994b). Exhibited trends of h_{fp} with respect to operating variables (fluid flow rate, temperature and concentration) appear to be a little different between Teflon and potato, due probably to differences in their surface roughness, structural and textural characteristics. These trends demonstrate the presence of some interaction between system and product parameters. Hassan (1984) and Stoforos (1988) observed similar trends during processing in a retort. In Hassan's study for instance, heat transfer coefficients were found to be higher for potato as compared to Teflon in a can containing water.

Figures 7, 8, and 9 show graphically, the two-way interaction of fluid temperature, concentration and flow rate on h_{fp} for both Teflon and potato. With the exception of potato treated at 100C for flow rates between 1.5 and 1.9×10^{-4} m^3/s which had no significant differences, all other conditions showed definitive trends of the combined effects on h_{fp}, supporting the trends similar to

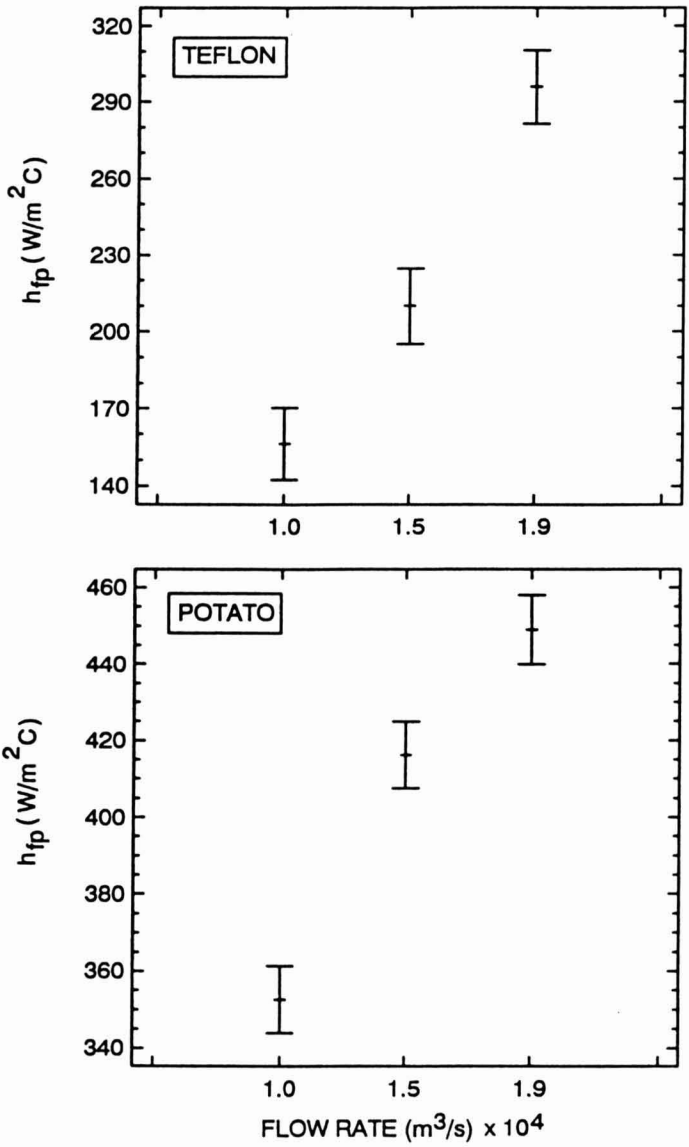

FIG. 4. HEAT TRANSFER COEFFICIENTS (h_{fp}) AS INFLUENCED BY FLOW RATE FOR HEATING TEFLON AND POTATO PARTICLES

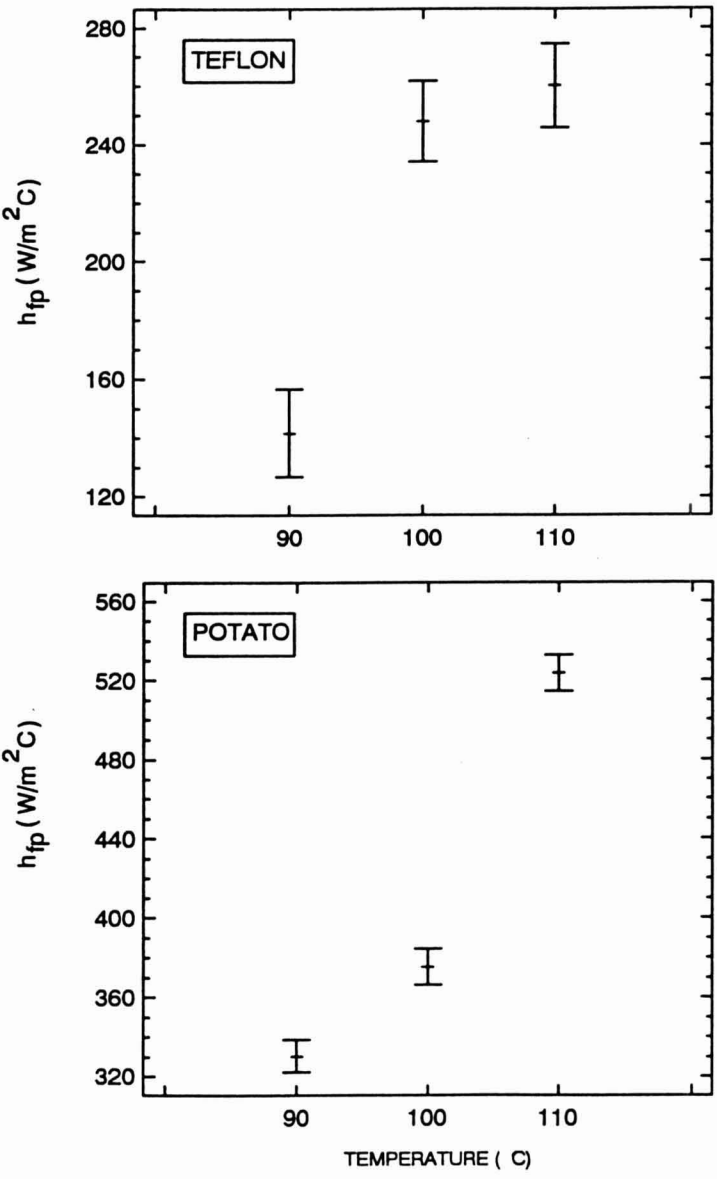

FIG. 5. HEAT TRANSFER COEFFICIENTS (h_{fp}) AS INFLUENCED BY TEMPERATURE FOR HEATING TEFLON AND POTATO PARTICLE

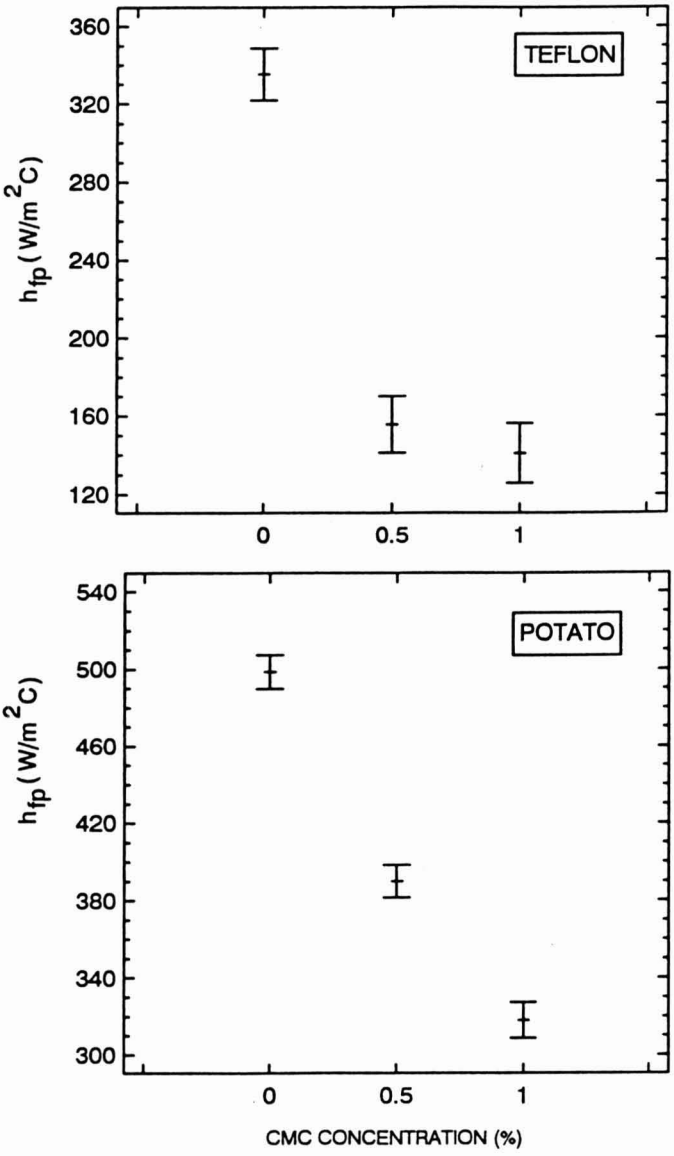

FIG. 6. HEAT TRANSFER COEFFICIENTS (h_{fp}) AS INFLUENCED BY THE FLUID CONCENTRATION FOR HEATING TEFLON AND POTATO PARTICLES

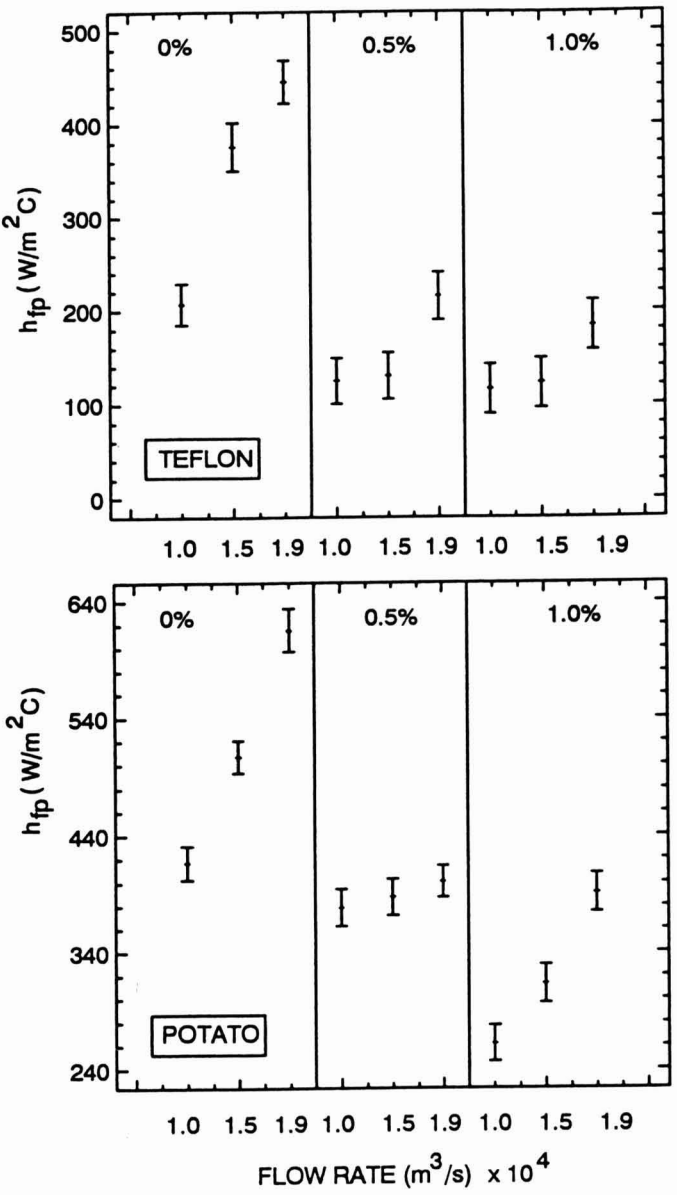

FIG. 7. HEAT TRANSFER COEFFICIENTS (h_{fp}) AS INFLUENCED BY THE INTERACTION OF FLUID CONCENTRATION AND FLOW RATE FOR HEATING TEFLON AND POTATO SAMPLES

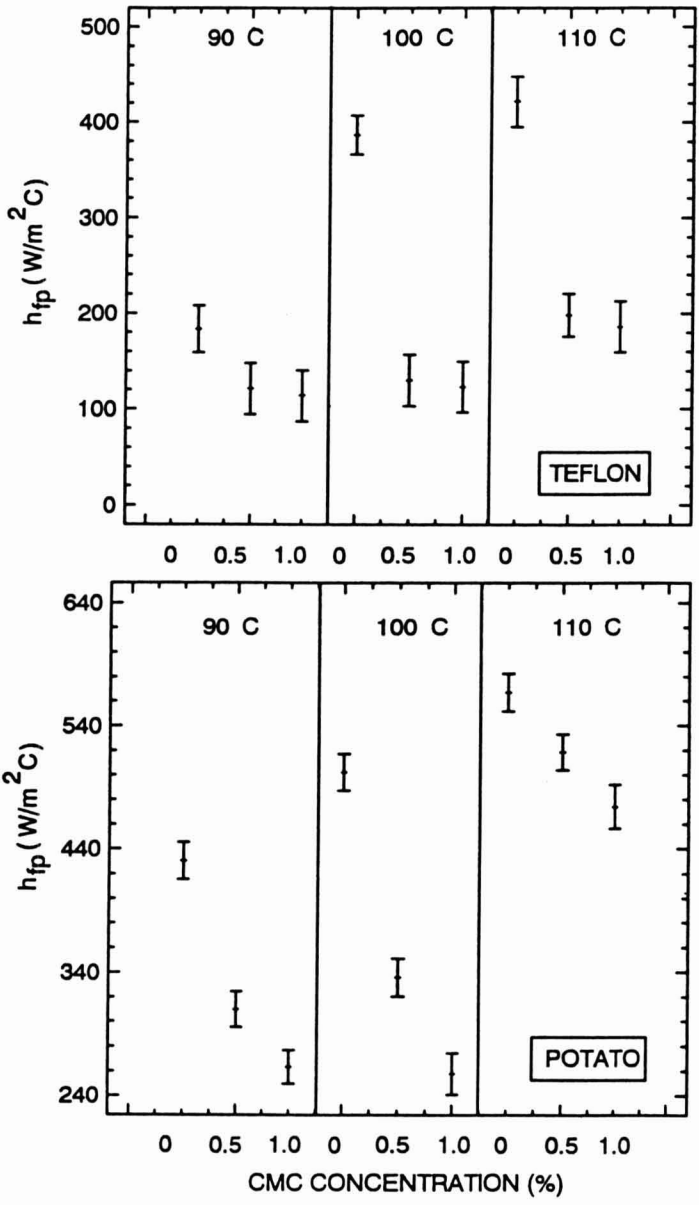

FIG. 8. HEAT TRANSFER COEFFICIENTS (h_{fp}) AS INFLUENCED BY THE INTERACTION OF FLUID TEMPERATURE AND CONCENTRATION FOR HEATING TEFLON AND POTATO PARTICLES

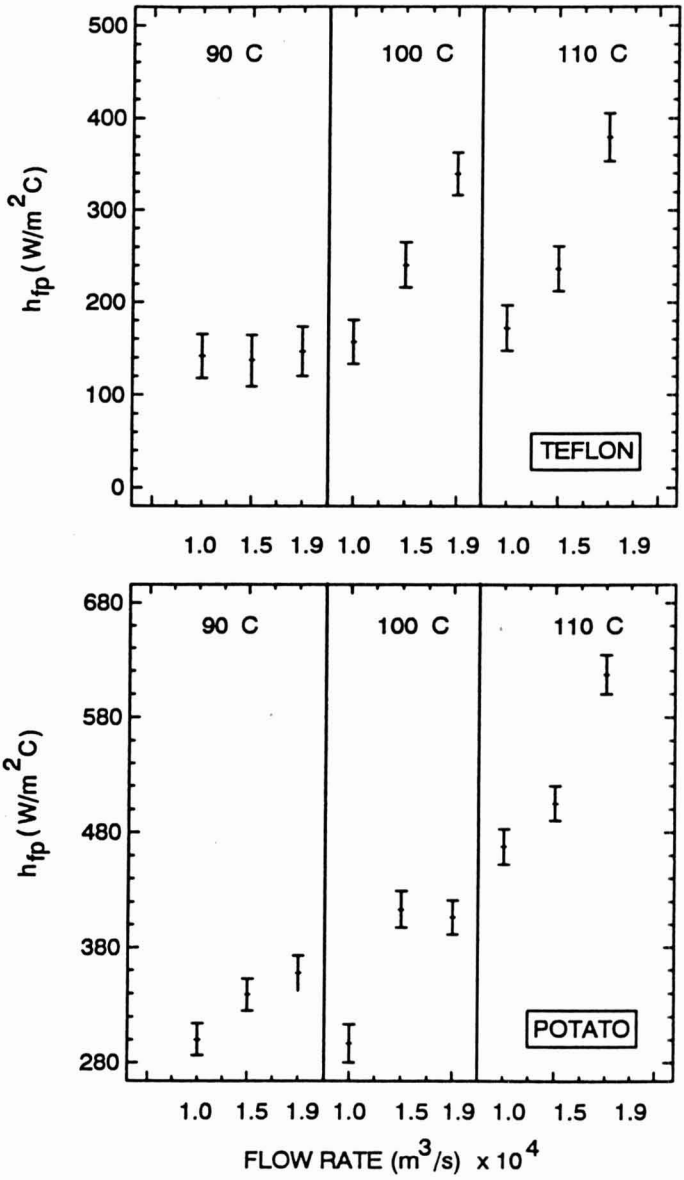

FIG. 9. HEAT TRANSFER COEFFICIENT (h_{fp}) AS INFLUENCED BY THE INTERACTION OF FLUID FLOW RATE AND TEMPERATURE FOR HEATING TEFLON AND PARTICLE PARTICLES

those discussed earlier with main effects. Another important observation is that, with Teflon the combined effect of temperature and concentration appeared to be insignificant as the fluid concentration exceeds 0.5% (Fig. 8).

Heat Transfer Coefficients Associated with Cooling Heated Samples

Irrespective of contributions made toward overall lethality during cooling and heating, the FDA recognizes only what is achieved in the holding tube alone. Contribution realized during cooling commonly serves as a safety factor (Dignan *et al.* 1989). On achieving the required lethality, quality becomes the primary goal. As such, cooling should be carried out as quickly as possible to prevent over-processing, because suspended particles cool more slowly compared to the carrier fluid. Under natural convection situations, test material assumes greater importance (Astrom and Bark 1994). Since starch gelatinizes on heating beyond 70C, structural changes occur and probably would affect the heat transfer coefficient. Table 3 shows that heat transfer coefficients associated with heating are significantly higher than for cooling ($p < 0.05$). For example, a 36% difference occurred between heating raw potato sample from 20 to 90C and

TABLE 3.
COMPARISON OF HEAT TRANSFER COEFFICIENTS ASSOCIATED WITH HEATING AND COOLING POTATO CYLINDERS IN WATER AT SELECTED INITIAL TEMPERATURES AND FLOW RATES

Flow rate (m^3/s, $\times 10^4$)	MTemp[1] (°C)	PTemp[2] (°C)	h_{fp} (W/m^2C)	Standard Deviation (W/m^2C)
Heating				
1.61	90	20	294^{c}	16
1.62	100	20	343^{b}	9
1.71	110	20	360^{a}	8
Cooling				
1.61	20	100	190^{d}	7
1.53	20	100	183^{de}	5
1.01	20	100	177^{ef}	7
1.61	20	90	189^{d}	5
1.53	20	90	170^{f}	5
1.61	20	110	189^{d}	10

[a-g] Mean values sharing the different superscript are significantly different ($p<0.05$)
[1] Heating medium temperature in 7.62 cm internal diameter pipe.
[2] Initial temperature of the particle.
Particle length and diameter are 24 and 21 mm, respectively.

cooling of heated samples from 90 to 20C. The differences can be attributed to difference in (1) the interfacial characteristics resulting from textural differences between cooked and raw potatoes, (2) lower fluid apparent viscosity associated with higher temperatures and (3) mass transfer may occur at a faster rate with raw potato. Alhamdan *et al.* (1990) also found that the average heat transfer coefficient for heating was 140 to 200% higher than for cooling. The authors used an aluminum irregular-shaped particle under natural convection conditions. The initial particle temperature prior to cooling had no significant effect ($p > 0.05$) on estimated heat transfer coefficients. Changing fluid flow rate followed the trend discussed earlier but had insignificant effect on the heat transfer coefficient.

CONCLUSIONS

A versatile holding tube simulator was fabricated for carrying out heat transfer studies using stationary particles at temperatures up to 110C. The sample holder allowed exact location of different diameter particles along the central axis of the holding tube. The simulator was calibrated to output the desired flow rate as a function of fluid concentration, temperature, pump speed, and pipe diameters. Statistical analyses indicated the above factors to significantly influence fluid discharged from the pump. Higher pump speeds were needed to maintain a given flow for less viscous fluids. Good correlations ($R^2 \geq 0.90$) were obtained between predicted and observed fluid flow rate and pump speed. Heat losses to the surrounding were generally found to be small and a constant operating temperature could be obtained without any specialized skills of the operator.

The effect of individual, as well as combined effects of fluid flow rate, temperature and CMC concentration were investigated using both model and real food particles in the form of finite cylinders. Depending on experimental conditions, h_{fp} values ranged from 100 to 700 W/m^2C for heating Teflon and potato samples, with Biot numbers ranging from 10 to 50. Temperature, concentration, flow rate and their interactions had significant influence on estimated h_{fp} of both particles. Some differences were also observed between the h_{fp} values for potato and Teflon. Heat transfer coefficients associated with cooling were lower than those found during heating.

ACKNOWLEDGEMENT

This research was supported by the Strategic Grants Program of Natural Sciences and Engineering Research Council of Canada. Financial support provided to the first author by the Canadian International Development Agency is acknowledged.

REFERENCES

ABDELRAHIM, K.A. and RAMASWAMY, H.S. 1995. High temperature/pressure rheology of carboxymethylcellulose (CMC). Food Res. Intl. *28*, 285–290.

ALHAMDAN, A., SASTRY, S.K. and BLAISDELL, J.L. 1990. Natural convection heat transfer between water and an irregular-shaped particle. Trans. ASAE 33(2), 620.

ASTROM, A. and BARK, G. 1994. Heat transfer between fluid particles in aseptic processing. J. Food Eng. *21*, 97–125.

AWUAH, G.B., RAMASWAMY, H.S. and SIMPSON, B.K. 1993. Surface heat transfer coefficients associated with heating food particles in CMC solutions. J. Food Process Engineering *16*, 39–57.

AWUAH, G.B., RAMASWAMY, H.S. and SIMPSON, B.K. 1995. Comparison of two methods for evaluating fluid-to-surface heat transfer coefficient. Food Res. Intl. *28*, 261–271.

BALASUBRAMANIAM, V.M. and SASTRY, S.K. 1994a. Liquid-to-particle heat transfer coefficient in non-Newtonian carrier medium during continuous tube flow. J. Food Eng. *23*, 169–187.

BALASUBRAMANIAM, V.M. and SASTRY, S.K. 1994b. Convective heat transfer at particle-liquid interface in continuous tube flow at elevated temperatures. J. Food Sci. *59*, 675–681.

CACACE, D., PALMIERI, L., PIRONE, G., MASI, P. and CAVELLA. 1994. Biological validation of mathematical modeling of thermal processing of particulate foods: the influence of heat transfer coefficient determination. J. Food Eng. *23*, 51:68.

CHANDARANA, D.I. and GAVIN, A. III. 1989. Establishing thermal processes for heterogenous foods to be processed aseptically: a theoretical comparison of process development methods. J. Food Sci. *54*, 198–204.

CHANDARANA, D.I., GAVIN, A. III. and WHEATON, F.W. 1988. Particle/fluid interface heat transfer during aseptic processing of foods. ASAE Paper No. 88-6599. American Society of Agricultural Engineers, St. Joseph, MI.

CHANDARANA, D.I., GAVIN, A. III. and WHEATON, F.W. 1990. Particle/fluid interface heat transfer under UHT conditions at low particle/fluid relative velocities. J . Food Process Engineering *13*, 191–206.

CHANG, S.K. and TOLEDO, R.T. 1989. Heat and simulated sterilization of particulate solids in a continuously flowing system. J. Food Sci. *54*, 1017–1023, 1030.

CLARK, P.J. 1978. Mathematical modelling in sterilization processes. Food Technol. *32*(3), 73–75.

DIGNAN, D.M., BERRY, R., PFLUG, I.J. and GARDINE, T.D. 1989. Safety considerations in establishing aseptic processes for low-acid foods containing particulates. Food Technol. *43*(3), 118–121.

DUTTA, B. and SASTRY, S.K. 1990. Velocity distribution of food particle suspensions in holding tube flow: distribution characteristics of and fastest-particle velocities. J. Food Sci. *55*, 1703–1710.

HASSAN, B.H. 1984. Heat Transfer Coefficients for Particles in Axially Rotating Cans. Ph.D thesis. Dept. of Agricultural Engineering. Univ. of California, Davis, CA.

HELDMAN, D.R. 1989. Establishing aseptic thermal processes for low-acid foods containing particulates. Food Technol. *43*(3), 122–123.

HELDMAN, D.R. and Singh, R.P. 1981. *Food Process Engineering*. Van Nostrand Reinhold/AVI, New York.

HEPPELL, N.J. 1985. Measurement of liquid-solid heat transfer coefficient during continuous sterilization of liquids containing solids. Paper presented at the 4th Int. Conference on Engineering and Food, July 7–10. Edmonton, AB, Canada.

HUNTER, G.M. 1972. Continuous sterilization of liquid media containing suspended particles. Food Technol. in Australia, *24*, 158–165.

LARKIN, J.W. 1989. Use of a modified Ball's formula method to evaluate aseptic processing of foods containing particulates. Food Technol. *43*(3), 124–131.

LARKIN, J.W. 1990. Mathematical analysis of critical parameters in aseptic particulate processing systems. J. Food Process Engineering *13*, 155–167.

LEE, J.H., SINGH, R.K. and LARKIN, J.W. 1990. Determination of lethality and processing time in a continuous sterilization system containing particulates. J. Food Eng. *11*, 67–92.

MAESMANS, G., HENDRICKX, M., DECORDT, S., FRANSIS, A. and TOBBACK, P. 1992. Fluid-to-particle heat transfer coefficient determination of heterogeneous foods: A review. J. Food Processing and Preserv. *16*, 29–69.

MWANGI, J.M., RIZVI, S.S.H. and DATTA, A.K. 1993. Heat transfer to particles in shear flow: application in aseptic processing. J. Food Eng. *19*, 55–74.

RAMASWAMY, H.S., LO, K.V. and TUNG, M.A. 1982. Simplified equations for transient temperatures in conductive foods with convective heat transfer at the surface. J. Food Sci. *47*, 2042–2047, 2065.

RAMASWAMY, H.S., TUNG, M.A. and STARK, R. 1983. A method to measure surface heat transfer from steam/air mixtures in batch retorts. J. Food Sci. *48*, 900–904.

SASTRY, S.K. 1986. Mathematical evaluation of process schedules for aseptic processing of low-acid foods containing discrete particulate matter. J. Food Sci. *51*, 1323–1328, 1332.

SASTRY, S.K. 1992. Modelling the continuous sterilization of particulate foods. In *Mathematical Modelling of Food Processing Operations*. (S. Thorne, ed.) pp. 233–270, Elsevier Applied Science. New York.

SASTRY, S.K., HESKITT, B.F. and BLAISDELL, J.L. 1989. Convective heat transfer at particle liquid interface in aseptic processing systems. Food Technol. *43*(3), 132, 136, 143.

SASTRY, S.K., LIMA, M., BRIM, J., BRUNN, T. and HESKITT, B.F. 1990. Liquid-to-particle heat transfer during continuous tube flow: influence of flow rate and particle to tube diameter ratio. J. Food Process Engineering *13*, 239–253.

SCHULTZ, O.T. and OLSON, F.C.W. 1940. Thermal processing of foods in tin containers. III. Recent improvements in the general method of thermal process calculations - a special coordinate paper and methods of converting initial and retort temperatures. Food Res. *5*, 399.

SKELLAND, A.H.P. 1967. *Non-Newtonian Flow and Heat Transfer*. John Wiley & Sons, New York.

SKJOLDEBRAND, C. and OHLSSON, T. 1993. A computer simulation program for evaluation of the continuous heat treatment of particulate food products. Part 1: Design. J. Food Eng. *20*, 149–165.

STEEL, R.G.D and TORRIE, J.H. 1960. *Principles and Procedures of Statistics*. McGraw Hill, New York.

STOFOROS, N.G. 1988. Heat Transfer in Axially Rotating Canned Liquid/Particulate Food Systems. Ph.D thesis. Dept. of Agricultural Engineering. Univ. of California, Davis, CA.

ZITOUN, K.B. and SASTRY, S.K. 1994a. Determination of convective heat transfer between fluid and cubic particles in continuous tube flow using noninvasive experimental techniques. J. Food Process Engineering *17*, 209–228.

ZITOUN, K.B. and SASTRY, S.K. 1994b. Convective heat transfer coefficients for cubic particles in continuous tube flow using the moving thermocouple method. J. Food Process Engineering *17*, 229–241.

ZURITZ, C.A., MCCOY, S.C. and SASTRY, S.K. 1990. Convective heat transfer coefficients for irregular particles immersed in non-Newtonian fluids during tube flow. J. Food Eng. *11*, 159–179.

DIMENSIONLESS CORRELATIONS FOR MIXED AND FORCED CONVECTION HEAT TRANSFER TO SPHERICAL AND FINITE CYLINDRICAL PARTICLES IN AN ASEPTIC PROCESSING HOLDING TUBE SIMULATOR

G.B. AWUAH and H.S. RAMASWAMY[1]

Department of Food Science and Agricultural Chemistry
Macdonald Campus of McGill University
21,111 Lakeshore Rd., Ste Anne de Bellevue
Quebec, Canada, H9X 3V9

Accepted for Publication May 26, 1995

ABSTRACT

Dimensionless correlations for estimating heat transfer coefficients for spherical and finite cylinders under mixed and forced convection heat transfer regimes were individually investigated using multiple regression of statistically significant dimensionless groups. Food and model particles were subjected to heat treatments in an aseptic processing holding tube simulator (carrier fluid: 0, 0.5, and 1.0%, carboxymethyl cellulose solutions, w/w basis; temperature: 90 to 110C; flow rate 1.0 to 1.9 $\times$ 10^{-4} m^3/s). The type of test material was found to have a significant effect on the Nusselt number, and hence developed correlations. Introducing a diffusivity ratio defined as the ratio of particle-to-fluid thermal diffusivities was found to consistently improve developed models. Excellent correlations ($R^2 \geq 0.97$) were obtained between the Nusselt number and dimensionless groups for all models. Natural convection in heat transfer correlations in situations where forced convection is expected to be the dominant mechanism was accommodated.

INTRODUCTION

Aside from residence time distribution of particulates travelling in continuous heat-hold-cool systems, interfacial fluid-to-particle convective heat transfer coefficients (h_{fp}) play a key role in establishing proper processing schedules from both quality and safety standpoints (Pflug *et al.* 1990). However, h_{fp} values present one of the most difficult parameters to estimate under practical aseptic conditions (Larkin 1990).

[1]To whom correspondence should be addressed.

Journal of Food Process Engineering **19** (1996) 269–287.

Aseptic processing systems generally require a pump for feeding raw materials to the heat exchanger and the holding tube. Since carrier fluids associated with such products are generally viscous and non-Newtonian in nature, estimation of heat treatment times become more complex as a result of the dependence of residence times on particle size and density, shape, concentration of the carrier fluid and system parameters such as temperature, pressure, fluid flow rate and system configuration. Therefore, lethalities achieved by individual particles will depend on such factors as well as the relative velocities between the fluid and the particle.

The pumping mechanism associated with particulate laden products suggests forced convection as the dominant mechanism of heat transfer between the fluid and particles. However, since fluid flow rates are usually low, the mechanisms involved are complex combinations of natural and forced convection; the predominant mechanism depending on system design and operational conditions (Alhamdan and Sastry 1990). In all forced convection situations (Fand and Keswani 1973), the natural convection phenomenon continues to operate since buoyant forces resulting from density gradients persist. Since mixed convection occurs whenever there is a temperature difference between the convecting body and the fluid along with the slightest amount of forced fluid, buoyant as well as inertial forces operate simultaneously within the fluid, and in some situations, may have the same order of magnitude (Ozisik 1985; Chapman 1989). In such circumstances, heat losses should be related to a combined effect rather than either natural or forced convection alone (Fand and Keswani 1973).

Studies related to natural and forced convection about submerged particles include those by Yuge (1960) and Johnson *et al.*(1988) for spheres in air; Chandarana *et al.* (1990), Alhamdan *et al.* (1990), Alhamdan and Sastry (1990), Sastry *et al.* (1990), Zuritz *et al.* (1990) and Astrom and Bark (1994) for spherical, cube shaped, or irregular shaped particles in Newtonian or non-Newtonian fluids. In most of the above studies especially those involving non-Newtonian fluids, proposed dimensionless correlations describe the dominance of either natural or forced convection alone at relatively low operating temperatures. The conservative approach has generally been to assume zero velocity between the fluid and particle, resulting in a Nusselt number of 2.0 for spherical particles (Geankoplis 1978) and 0.3 for an infinite cylinder (Gnielinski 1983). Although several predictive models and computer software have been presented for estimating product sterility and quality optimization (Sastry 1986; Larkin 1989, Chandarana *et al.* 1989, Skjoldebrand and Ohlsson 1993), good estimates of the fluid-to-particle heat transfer coefficient is an important prerequisite for successful implementation of such models.

In dynamic flow conditions involving aseptic processing, dimensionless correlations are hard to use since the particle-to-fluid relative velocity is difficult to measure in real systems (Maesmans *et al.* 1992). Although the Nusselt

number depends primarily on fluid properties, the heat capacity and thermal conductivity of the particle material (Astrom and Bark 1994) can be expected to influence the rate of heat transfer to the fluid and to some extent enhance free convection. The existing literature shows lack of information on the combined effect of forced and natural convection to the overall transfer of heat under aseptic conditions.

The objective of this study was to develop dimensionless correlations for mixed and forced convection heat transfer to spherical and cylindrical particles processed in a pilot scale holding tube simulator operated at temperatures between 90 and 110C.

THEORETICAL CONSIDERATIONS

Analytical solution to heat transfer problems involve simultaneous solution of Navier-Stokes equations of motion and continuity, and the energy equation for four dependent variables including two-dimensional velocity components, pressure, and temperature (Burmeister 1983; Chapman 1989). The equations involved are sufficiently complex that analytical solutions can only be obtained for simple boundary conditions and geometry (Chapman 1989). From dimensional analysis, the convective heat transfer coefficient is expressed in terms of the Nusselt number (Nu), which is generally described as a function of the Reynolds (Re), Prandtl (Pr), and Grashof (Gr) numbers:

$$Nu = f(Re,Pr,Gr) \tag{1}$$

Heat transfer coefficients associated with pure forced convection are generally evaluated from the expression:

$$Nu = C+D(Re)^n(Pr)^p \tag{2}$$

where C, D, n and p are constants. The constant p varies between 0.3 and 0.4 with the lower value being commonly used (Morgan 1975). For infinite cylinders, Žhukauskas (1972) found 0.37 to be more suitable. For flow past a single spherical particle, the average heat transfer coefficient can be estimated from the following relationship (Geankoplis 1978), which is valid for Reynolds and Prandtl numbers between 1 to 70,000 and 0.6 to 400, respectively:

$$Nu = 2.0 + 0.60Re^{0.5}Pr^{1/3} \tag{3}$$

Whitaker (1972) presented a more general correlation for flow of gases and liquids across a single sphere in the form:

$$Nu = 2.0+(0.4Re^{0.5}+0.06Re^{2/3})Pr^{0.4}\left[\frac{\mu_\infty}{\mu_w}\right]^{0.25} \quad (4)$$

Equation (4) is valid for Re between 3.5 and 80000, Pr between 0.7 and 380, and μ_∞/μ_w (which is the ratio of main stream fluid viscosity to the fluid viscosity at the wall) between 1 and 3.2. For free convection on an isothermal horizontal cylinder, Churchill and Chu (1975) proposed a relationship, valid for Rayleigh number (Ra) between 10^{-4} and 10^{12}:

$$Nu^{1/2} = 0.60 + \frac{0.387Ra^{1/6}}{[1+(0.559/Pr)^{9/19}]^{8/27}} \quad (5)$$

For flow of gases and liquids over a single cylinder, Whitaker (1972) proposed the relationship:

$$Nu = [0.4Re^{0.5} + 0.06Re^{2/3}]Pr^{0.4}\left[\frac{\mu_\infty}{\mu_w}\right]^{0.25} \quad (6)$$

which is valid for Re from 40 to 10^5; Pr from 0.67 to 300; and μ_∞/μ_w from 0.25 to 5.2. Churchill and Bernstein (1977) correlated experimental data from several fluids including air, water, and liquid sodium to derive an expression for a cylinder, which is valid for Re from 100 to 10^7 and Peclet number (Re.Pr) greater than 0.2 for forced convection:

$$Nu = 0.3 + \frac{0.62Re^{1/2}Pr^{1/3}}{[1+(0.4/Pr)^{2/3}]^{1/4}}\left[1+\left[\frac{Re}{282{,}000}\right]^{5/8}\right]^{4/5} \quad (7)$$

The magnitude of the dimensionless group Gr/Re^2, describes the ratio of buoyant to inertia forces and governs the relative importance of free to forced convection. Again, it delineates free, forced, and mixed convection regimes (Ozisik 1985; Chapman 1989). Yuge (1960) indicated that forced convection dominates for flow over a sphere when the condition $Gr/Re^2 < 0.01$ is satisfied. According to Johnson *et al.* (1988), mixed convection occurs when the ratio Gr/Re^2 falls between 0.08 and 5.10. The authors performed numerical evaluation of the Navier-Stokes momentum equations and the energy equations using a finite difference procedure, and verified their analysis with experimental data obtained from an isothermal sphere submerged in a wind tunnel with air flowing vertically upward. For a horizontal cylinder in cross flow, Fand and Keswani (1973) found forced convection to dominate when $Gr/Re^2 < 0.5$, whereas natural convection dominated when the ratio exceeded 40. Between 0.5 and 2, natural convection contributed 10% to the overall heat transfer. According to the authors, both forced and natural convection are of the same order of magnitude

when the ratio falls between 2 and 40 for a cylinder. For the same order of magnitude the two mechanisms should be analyzed simultaneously (Ozisik 1985).

To make the significance of Gr/Re^2 plausible, the ratio of buoyant to inertial forces is often considered in mixed convection models. For air flow normal to a long horizontal cylinder, Oosthuizen and Madan (1970) recommended the following relationship for $100 < Re < 3000$ and $2.5 \times 10^4 < Gr < 3 \times 10^5$:

$$\frac{Nu}{Nu_{forced}} = 1 + 0.18\frac{Gr}{Re^2} - 0.011\left[\frac{Gr}{Re^2}\right]^2 \quad (8)$$

where $Nu_{forced} = 0.464Re^{1/2} + 0.0004Re$. Churchill (1977) in a critical survey on mixed convection, suggested the relationship:

$$Nu^3_{combined} = Nu^3_{forced} + Nu^3_{natural} \quad (9)$$

In order to correlate data for the region $0.5 < Gr/Re^2 < 2.0$ where forced convection contributed over 90%, Fand and Keswani (1973) considered natural convection as an additive term, but proportional to Gr/Re^2 raised to a power (m) which depends on the orientation of the fluid velocity relative to the gravitational field:

$$Nu = \left[0.255 + 0.699Re^{0.5} + C\left[\frac{Gr}{Re^2}\right]^m Gr^{0.25}\right] Pr^{0.29} \quad (10)$$

where C and m are constants ranging from -0.0240 to 0.0330 and 0.15 to 0.30, respectively.

MATERIALS AND METHODS

Materials and Experimental Conditions

Spherical Teflon, cylindrical potato and Teflon samples were prepared as detailed in Awuah *et al.* (1994, 1996), and heated at temperatures between 90 and 110C using either Newtonian or non-Newtonian fluids (0 - 1.0% w/w carboxymethyl cellulose, CMC, solutions) in two pipes of inside diameters 5.08 and 7.62 cm (2 in. and 3 in.). High temperature rheological data, obtained in the form of power law model parameters m, and n, were obtained from Abdelrahim and Ramaswamy (1995). Physical properties for potato and Teflon are as detailed in Awuah *et al.* (1993, 1994). Physical properties for water were obtained from Chapman (1989). Heat transfer coefficients were estimated with the rate method (Ramaswamy *et al.* 1983) and the Nusselt numbers were calculated from the relationship $Nu = h_{fp}\, d_{cd}/k_f$, where d_{cd} and k_f are the

characteristic dimension of the particle and thermal conductivity of the fluid respectively, as detailed in Awuah *et al.* (1993, 1994, 1996).

Characteristic Dimension

For an infinite cylinder in cross flow, the diameter (d) is generally used as the characteristic dimension, whereas the length (L) is used for axial flows (ASHRAE 1981; Žukauskas and Žiugžda 1985). For a finite cylinder, both diameter and length can be expected to influence heat transfer. King (1932) recommended using $Ld/(L+d)$ as the characteristic dimension. Sparrow and Ansari (1983) refuted King's approach on the basis that it overpredicted heat transfer coefficients by 40 to 50% for a finite cylinder with diameter-to-length ratio equal to unity. The authors suggested particle diameter (d) as the appropriate dimension. Since the diameter-to-length ratio used in the present study varied between 0.63 and 1.0, two characteristic dimensions were investigated in addition to d and $Ld/(L+d)$. Firstly, a correlation which incorporates the length of the cylinder was adopted. This was defined as the diameter of a sphere having the same volume as that of a finite cylinder which will be equal to 1.15 d, when the length (L) and diameter (d) of the cylinder are equal. The equivalent diameter is therefore 15% higher. This 15% increase in volume of the equivalent sphere was redefined to include particle length (within the range studied) as follows:

$$d_{cd} = d\left[1+\frac{0.15d}{L}\right] \tag{11}$$

The second characteristic dimension was defined as the volume-to-total surface area ratio of a cylinder, giving a simplified relationship based on its length (L) and diameter (d):

$$d_{cd}=\frac{0.5L}{\left[1+\frac{2L}{d}\right]} \tag{12}$$

Characteristic dimensions defined above were individually tested for appropriateness in correlating experimental data.

Data Analysis

The criteria suggested by Fand and Keswani (1973), Yuge (1960), and Johnson *et al.* (1988) for a cylinder and sphere were individually considered in establishing the appropriate regimes prior to data analysis. However, in view of the fact that pump-assisted circulation of the fluid was involved, forced convection was considered as first approximation neglecting natural convection,

and a modified relationship which takes particle and tube dimensions into consideration was employed.

To account for natural convection the generalized Grashof and Gr/Re^2 were simultaneously introduced and investigated as follows:

$$Nu = A + BRe^{n}Pr^{m}\left[\frac{d}{D}\right]^{r}\left[\frac{d}{L}\right]^{y} \tag{13}$$

$$Nu = A + BRe^{n}Pr^{m}Gr^{q}\left[\frac{d}{D}\right]^{r}\left[\frac{Gr}{Re^{2}}\right]^{y}\left[\frac{d}{L}\right]^{z} \tag{14}$$

where A, B, n, m, q, r, y and z are constants. Multiple regression was performed after logarithmic linearization of each model. The criteria used to evaluate accuracy of fit for each model were the coefficient of determination (R^2), the percentage average error (PAE), the percentage deviation modulus (PDM) and percentage standard deviation (PSD) defined respectively as follows:

$$PAE = \frac{1}{n}\sum_{i=1}^{n} M_i \tag{15}$$

$$PDM = \frac{1}{n}\sum_{i=1}^{n} |M_i| \tag{16}$$

$$PSD^2 = \frac{1}{n-1}\left[\sum_{i=1}^{n} M_i^2 - \frac{1}{n}\left(\sum_{i=1}^{n} M_i\right)^2\right] \tag{17}$$

where n represents the total number of data points, with Nu_{cal} and Nu_{exp} representing the predicted and experimental Nusselt numbers in the relationship $M_i = (N_{cal} - N_{exp})*100/N_{exp}$. The generalized Reynolds (GRe), Prandtl (GPr), and Grashof (GGr) were used as defined in Awuah *et al.* (1993).

RESULTS AND DISCUSSION

Characteristic Dimension

The determination coefficient (R^2), the percentage average error (PAE), the percentage deviation modulus (PDM), and the percentage standard deviation (PSD) varied from 0.98 to 0.99, -3 to 3%, 18 to 20%, and 22 to 25% respectively, as presented in Table 1 depending on the characteristic dimension used in developing the correlation. The optimum characteristic dimension was defined as the dimension which yielded the highest R^2, and low PAE, PDM and PSD values using a common model. All characteristic dimensions fitted the

experimental data well covering diameter-to-length ratios ranging from 0.625 to 1.0, with marginal differences between predicted and experimental values. Since characteristic dimension chosen affects the dimensionless groups (Re, Nu, Pr, Gr, Ra) to different orders of magnitude, care should be taken in selecting the appropriate one if comparison is to be made with published correlations. In this study, the diameter (d) was chosen as the characteristic dimension so that calculated GGr/GRe^2 for both spherical and finite cylindrical particles will have the same meaning as published by Fand and Keswani (1973) for comparison of flow regimes. However, to accommodate different sample lengths of finite cylinders, the diameter-to-particle length ratio was introduced as an additional factor in all models prior to data analysis. Nu for such particles were calculated based on volume to surface area ratio [$d_{cd} = 0.5\ L/(1+2L/d)$].

TABLE 1.
ERRORS ASSOCIATED WITH VARIOUS CHARACTERISTIC DIMENSIONS

Characteristic Dimension (d_{cd}) (m)	PAE (%)	PDM (%)	PSD (%)	R^2
d	-3.24	18.1	22.4	0.98
0.5 L/(1+(2L/d))	2.37	19.7	24.6	0.99
d (1+ 0.1447d/L)	2.37	18.1	23.1	0.98
d L/(d + L)	2.52	19.2	24.0	0.98

Traditionally, fluid physical properties are estimated at film temperatures, defined as the average of the bulk fluid and the surface temperature under steady state conditions. However, particles suspended in carrier fluids experience a transient temperature profile which becomes asymptotic to the medium temperature with time. Therefore, the bulk fluid temperature was adopted for calculating fluid physical properties. Two reference temperatures were hypothesized for calculating, in particular, the temperature difference (ΔT) associated with the generalized Grashof number. These were defined as (1) the arithmetic mean of the bulk fluid and initial temperature of the particle, and (2) the difference between the bulk fluid and the initial temperature of the particle. The validity of these temperature differences were tested with experimental data using the same model and characteristic dimension. Surprisingly, only marginal differences in R^2 (0.98 and 0.98), PAE (1.9 and 2.1%), PDM (16 and 17%) and PSD (20 and 21%) resulted from using the arithmetic mean and the difference between the bulk and sample initial temperatures, respectively. The difference between the bulk fluid and particle initial temperatures was adopted in this study

to conform with relationships used by Alhamdan and Sastry (1990) for studies on natural convection.

The generalized particle Reynolds (GRe), Grashof (GGr), and Prandtl (GPr) numbers ranged from 4.3 to 8750; 216 to 1.6×10^8; and 1.6 to 800 respectively, for finite cylindrical particles. The corresponding Nusselt number and GGr/GRe^2 ratio ranged from 2.1 to 24 and 0.88 to 31, respectively. The GGr/GRe^2 ratio obtained in the study indicates that two flow regimes can be established for a finite cylinder: the region where free convection contributes about 10% (i.e., $0.88 < GGr/GRe^2 < 2.0$) to the overall heat transfer and the region where both free and forced contribute significantly ($2 < GGr/GRe^2 < 31$).

Limiting Nusselt Number for Finite Cylinder

The limiting Nusselt number was determined using Eq. (14) as the reference model and Eq. (15), (16) and (17) as the criteria for accuracy. Predicted data compared well with experimental data when the constant A (Eq. 14) varied between 0.31 and 0.6. The optimum value found was 0.36. This value falls as expected, between 0.3 and 2.0 for an infinite cylinder and a sphere, respectively.

Forced Convection to Finite Cylinders

Since free convection contributes 10% to the overall heat transfer for $0.5 < GGr/GRe^2 < 2.0$, pure forced convection was considered, resulting in the following relationship with finite Teflon cylinder data:

$$Nu-0.36=0.0008Gre^{1.8}\left[\frac{GPr}{900}\right]^{1.66}\left[\frac{d}{D}\right]^{-2.04}\left[\frac{d}{L}\right]^{-2.0} \tag{18}$$

Although a higher R^2 (0.99) was obtained, the associated PSD (33%), PDM (27%), and PAE (5%) were quite high. Introducing the Grashof number and Gr/Re^2 ratio resulted in the relationship:

$$\frac{Nu-0.36}{GRe^{1.8}\left[\frac{GPr}{900}\right]^{3.03}}=10^{-2.87}GGr^{0.69}\left[\frac{GGr}{GRe^2}\right]^{0.83}\left[\frac{d}{D}\right]^{2}\left[\frac{d}{L}\right]^{-8.6} \tag{19}$$

with PSD, PDM and PAE changing to 26%, 21%, and 2.9%, respectively with an R^2 of 1.00. Equation 19 is valid for GGr/GRe^2 between 0.88 and 1.8; GRe between 14 and 8038 and GPr between 1.8 and 558, each dimensionless group including the particle-to-tube diameter and the particle diameter-to-length ratios contributing significantly ($p < 0.05$) to the model. The marked improvement in the model confirms observations made by Fand and Keswani (1973) with regards

to the effect of free convection even in situations where forced convection predominates the mechanism of heat transfer. Figure 1 shows the plot of a rearranged form of Eq. (19) and illustrates an excellent fit between predicted and experimental data for Teflon over the entire range of GRe. The logarithmic format has been used to cover the broad range of numerical values involved. However, the model somewhat under-predicted data for potato, giving a percentage average error (PAE) of -24%, although the percentage standard deviation (PSD) was (13%).

Two streams of data distribution can be identified with Fig. 1. The upper stream represents high Reynolds and Grashof numbers, while the lower stream represents the opposite, each distribution satisfying the GGr/GRe^2 criterion between 0.88 and 2.0 for finite cylinders. The reason for this observation is that, as the fluid temperature increases, the fluid apparent viscosity decreases while the temperature difference (ΔT) between the bulk fluid and the particle increases, hence causing a simultaneous increase in both the generalized Reynolds and Grashof numbers. The reverse trend occurs at lower temperatures. Figure 1 also shows that the Nusselt number increases with increase in the generalized Reynolds as well as the generalized Grashof numbers.

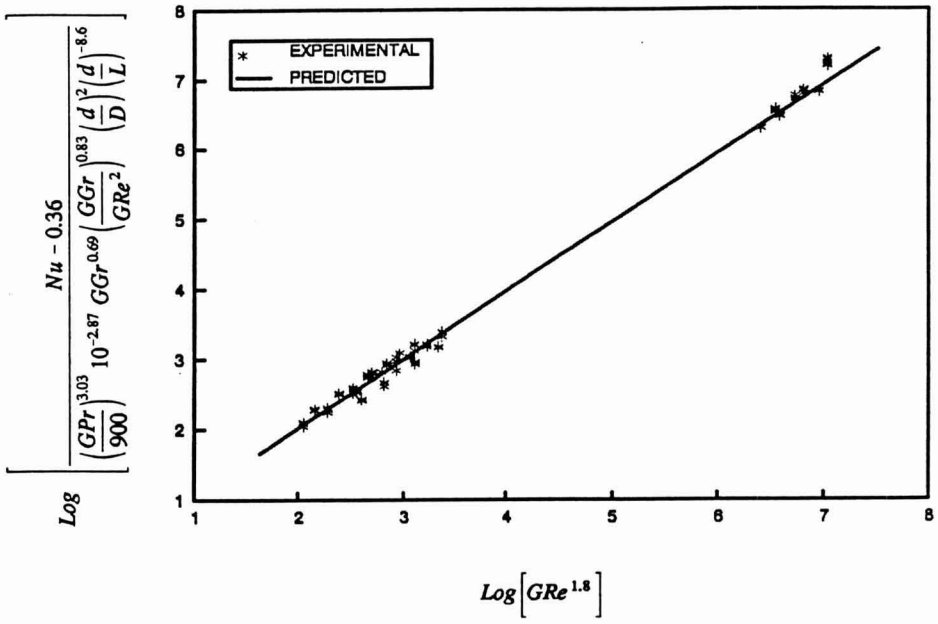

FIG. 1. PLOT OF DIMENSIONLESS CORRELATION FOR FORCED CONVECTION (GGr/GRe^2 RATIO BETWEEN 0.88 AND 2.0) HEAT TRANSFER TO FINITE CYLINDERS (EQ. 19): EXPERIMENTAL VERSUS PREDICTED

Mixed Convection to Finite Cylinders

Experimental data for cylindrical Teflon particles with GGr/GRe^2 greater than 2.0 was used in the modeling of mixed convection heat transfer and verified with data obtained for potato. A stepwise regression was performed, relating the Nusselt number to other dimensionless groups. The optimum correlation, which is valid for GGr/GRe^2 between 2 and 31; GGr between 216 and 1.6×10^8; GRe between 4.3 and 8751; and GPr between 1.6 and 800 was obtained as shown below:

$$\frac{Nu-0.36}{\left[\frac{d}{D}\right]^{0.31}\left[\frac{100d}{L}\right]^{-4.49}} = 18.24 GRe^{0.8} GPr^{2.0} GGr^{0.66} \qquad (20)$$

The R^2, PAE, PDM and PSD were 0.98, 1.1%, 17% and 21%, respectively. With the exception of the GGr/GRe^2 ratio which had less impact ($p > 0.05$), all dimensionless parameters had significant influence ($p < 0.05$) on Eq. (20). Increasing particle diameter for a given length (Eq. 20), decreases the Nusselt number. This is evident from the negative index associated with the diameter-to-length ratio in Eq. (20). Figure 2 shows a uniform distribution of the 560 experimental data points used in developing Eq. (20). Again the results are plotted as left hand side vs right hand side of Eq. (20) on a logarithmic format to illustrate the fitness of data. Similar trends were observed for plots of Nusselt number as a function of either the generalized Reynolds, Prandtl or the Grashof number.

The fluid-to-particle convective heat transfer coefficient is a boundary layer property and therefore depends on surface property of the particle used. Correlations developed with data obtained for Teflon somewhat under-predicted the results for potato, giving a total percentage average error (PAE) and percentage modulus (PDM) as high as -89%. In addition to differences in surface as well as thermal properties between Teflon and potato, some mass transfer can also take place between potato and the carrier fluid whereas for the Teflon particle it can be expected to remain inert under the heating conditions employed. Since natural convection contributes significantly to the overall heat transfer for mixed mode regimes, it may be necessary to consider the type of material in developing heat transfer correlations.

To account for the above differences, data for both potato and Teflon were combined, sorted by the GGr/Re^2 criterion and analyzed using a stepwise multiple regression to identify the significant parameters. An additional factor called "Thermal Diffusivity Ratio" which is defined as the ratio of particle-to-fluid thermal diffusivities (α_p/α_f) was introduced prior to data analysis and investigated. The reason for introducing this factor is due to the fact that thermal diffusivity indicates how fast heat propagates into a material as a function of

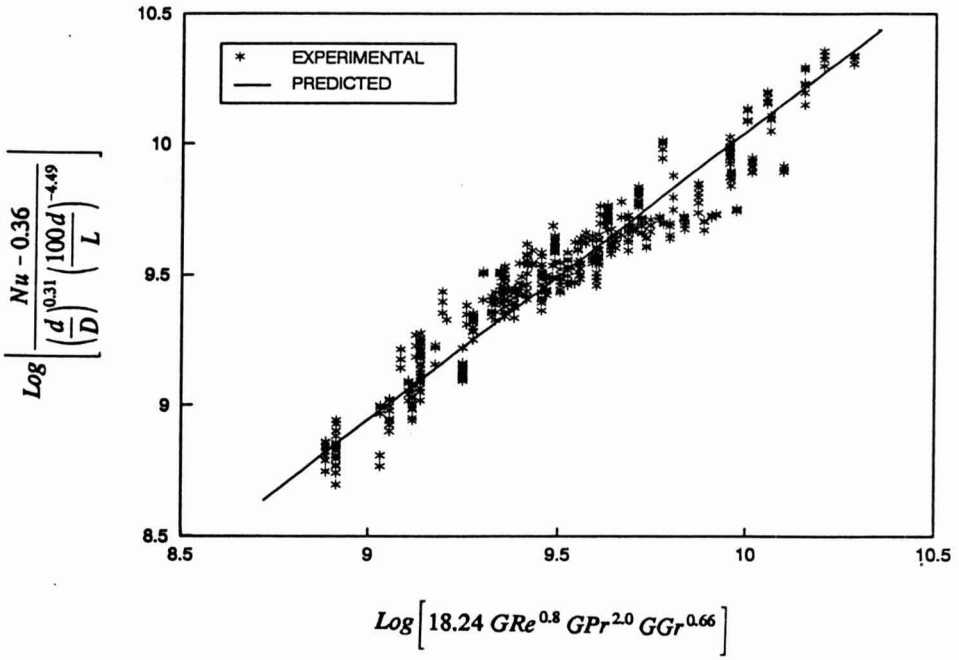

FIG. 2. PLOT OF DIMENSIONLESS CORRELATION FOR MIXED CONVECTION (GGr/GRe^2 RATIO BETWEEN 2.0 AND 3.1) HEAT TRANSFER TO FINITE CYLINDERS (EQ. 20): EXPERIMENTAL VERSUS PREDICTED

moisture content, temperature, composition and porosity. The diffusivity ratio was consistently found to have significant impact on the Nusselt number and also decreased the PAE, PDM and PSD associated with developed models. For GGr/GRe^2 between 0.88 and 1.8, the model which best fitted experimental data was:

$$\frac{Nu-0.36}{GRe^{2.5}\left(\frac{d}{D}\right)^{2}\left(\frac{\alpha_p}{\alpha_f}\right)^{4.09}}=10^{-3.53}GGr^{0.76}\left(\frac{d}{L}\right)^{-8.99}\left(\frac{GPr}{800}\right)^{3.86} \qquad (21)$$

The PAE, PDM and PSD associated with Eq. (21) were 4, 26 and 31%, respectively, with an R^2 value of 0.997. Eq. (21) is valid for GGr, GRe, GPr, d/L, d/D, and α_p/α_f from 265 to 1.1×10^8, 14 to 8038, 1.6 to 564, 0.625 to 1.0, 0.313 to 0.5, and 0.8 and 1.0, respectively. Apparently, the GGr/Re^2 ratio did not have any influence on the model due possibly to the introduction of α_p/α_f. However, ignoring both α_p/α_f ratio and the generalized Grashof number increased the PAE, PDM, and PSD to 9, 35 and 49%, respectively. Figure 3 shows an excellent fit between observed and predicted data (Eq. 21) for the pooled experimental data for Teflon and potato.

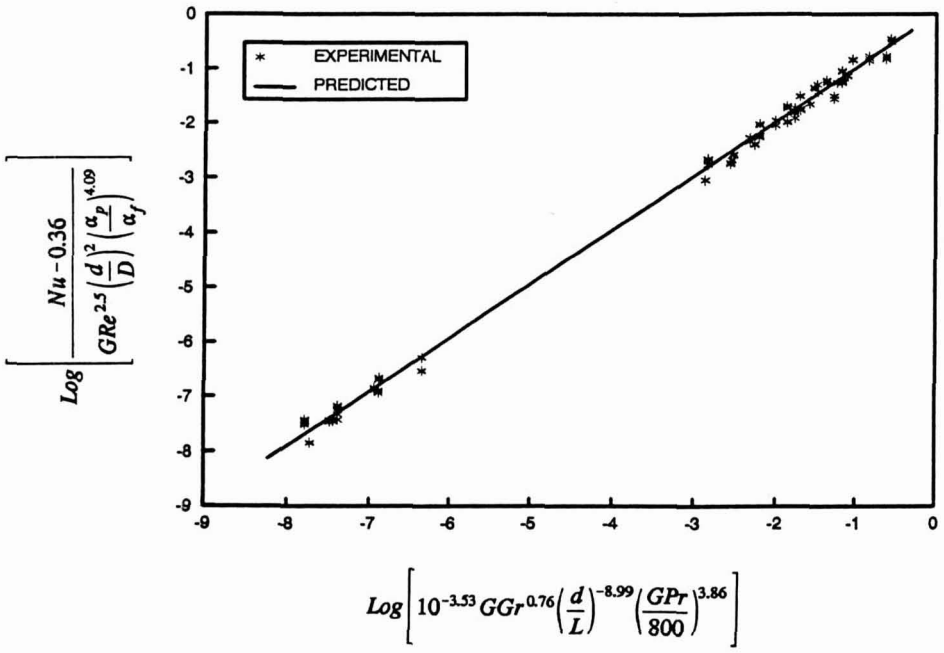

FIG. 3. PLOT OF DIMENSIONLESS CORRELATION FOR FORCED CONVECTION (GGr/GRe^2 RATIO BETWEEN 0.88 AND 2.0) HEAT TRANSFER TO FINITE CYLINDERS (EQ. 21) WITH THE DIFFUSIVITY RATIO USED AS AN INDEPENDENT DIMENSIONLESS PARAMETER: EXPERIMENTAL VERSUS PREDICTED

A similar correlation as well as excellent fit between observed and predicted data (shown in Fig. 4 for Eq.(22)] were obtained for GGr/GRe^2 between 2.0 and 31.3 using data for both Teflon and potato particles with GGr, GRe, GPr, d/L, d/D, and α_p/α_f ranging from 216 to 1.6×10^8, 4.3 to 8750, 1.6 to 800, 0.625 to 1.0, 0.197 to 0.5, and 0.8 to 1.0, respectively. The best correlation which showed a marked improvement in R^2 (0.99), PAE (8%), PDM (30%) and PSD (42%) was:

$$\frac{Nu-0.36}{GRe^{2.12}\left(\frac{d}{D}\right)^{-1.05}\left(\frac{\alpha_p}{\alpha_f}\right)^3}=10^{-2.06}GGr^{0.19}\left(\frac{d}{L}\right)^{-3.1}\left(\frac{GPr}{800}\right)^{2.39} \qquad (22)$$

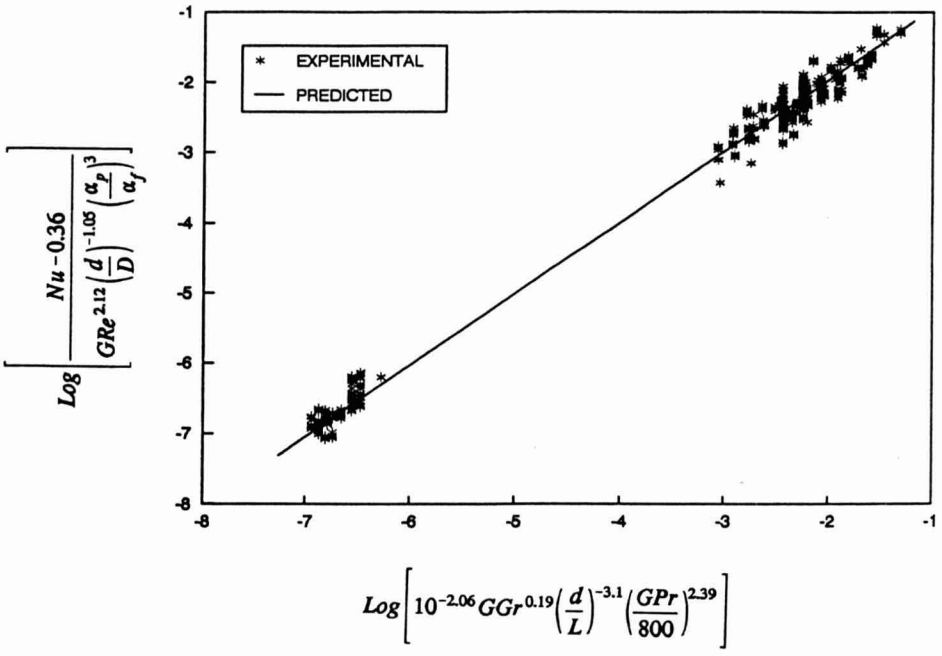

FIG. 4. PLOT OF DIMENSIONLESS CORRELATION FOR MIXED CONVECTION (GGr/GRe^2 RATIO BETWEEN 2.0 AND 3.1) HEAT TRANSFER TO FINITE CYLINDERS (EQ. 22) WITH THE DIFFUSIVITY RATIO USED AS AN INDEPENDENT DIMENSIONLESS PARAMETER: EXPERIMENTAL VERSUS PREDICTED

Comparison of the present models with published relationships is impossible due to lack of information on heat transfer to finite cylinders submerged in carrier fluids.

Spherical Particles

The GGr/GRe^2 for spherical particles ranged from 1.3 to 23.5, exceeding the limit proposed by Yuge (1960) for pure forced convection. Although the GGr/GRe^2 range obtained falls within the limits suggested by Johnson *et al.* (1988) for mixed convection, it did not conform with the general relationship between the Nusselt and generalized Grashof numbers for pure natural convection. A modified form of Eq. (2) and (4) were used as initial approximations to model pure force convection alone, giving the relationships:

$$Nu=2.0+0.07GRe^{0.62}GPr^{0.53}\left[\frac{d}{D}\right]^{0.16} \tag{23}$$

$$Nu=2.0+0.36(0.4GRe^{0.5}+0.06GPr^{0.67})GPr^{0.46}\left[\frac{d}{D}\right]^{0.33} \tag{24}$$

The PAE, PDM, and PSD for Eq. 23 and 24 were 0.34, 7.8, 9.4% and 0.3, 8, 9%, respectively with R^2 values of 0.84 and 0.99, respectively. Contributions from natural convection were accounted for by introducing both GGr and GGr/GRe^2 ratios in Eq. (24) and investigating, resulting in the relationship:

$$Nu=2.0+0.32(0.4GRe^{0.5}+0.06GPr^{0.67})GPr^{0.46}\left[\frac{d}{D}\right]^{0.17}\left[\frac{GGr}{GRe^2}\right]^{-0.04} \tag{25}$$

The PAE, PDM and PSD calculated with Eq. (25) were 0.32, 7.6 and 9.1%, respectively with an R^2 value of 0.99. Although Eq. (24) and (25) have the same R^2, the PDM and PSD associated with Eq. (25) are lower than Eq. (24). The range of applicability of Eq. (23), (24), and (25) are as follows: $1380 < GGr < 4.7 \times 10^7$; $7.7 < GRe < 2693$; $1.8 < GPr < 332$; and $0.25 < d/D < 0.38$. Again, comparison of the present models with published correlations is difficult because of the lack of information on mixed convection to submerged particles. In addition, attempts made to compare the above models with well-known correlations of Geankoplis (1978) and Whitaker (1972) for forced convection failed because they over-predicted the Nusselt number. This discrepancy can be expected because the relationships derived from the literature are for unbounded flow around a sphere. It is perhaps not appropriate to compare the present correlation with those presented by Sastry *et al.* (1990) and Zuritz *et al.* (1990) for forced convection in submerged particles because of differences in experimental procedures, and most importantly differences in the range of particle Re_p and Pr_f.

CONCLUSIONS

Dimensionless correlations for mixed and forced convection to finite cylindrical and spherical particles submerged in both Newtonian and non-New-

tonian fluids at temperatures between 90 to 110C are presented. The suitability of four characteristic dimensions were investigated in relation to developing predictive models for estimating the Nusselt number. Although each dimension gave excellent fit between experimental data and predicted values, extreme care is required if comparison is to be made with published correlations. Correlations developed with experimental data from Teflon was generally found to underestimate data for potatoes. This discrepancy was attributed to differences in heat capacities and the possibility of mass transfer across potato particles and the carrier fluid. Evidently, heat capacity and for that matter, the type of particle material, affects the Nusselt number by influencing operating buoyant forces. Introducing the diffusivity ratio was found to improve correlations developed with data obtained from both particles. In general, excellent correlations were obtained between predicted and observed data with coefficients of determination (R^2) ranging between 0.97 to 1.0.

NOMENCLATURE

d Diameter of the particle (m)
d_{cd} Characteristic dimension of particle (diameter of a cylinder or a sphere or volume to area ratio) (m)
C_p Specific heat (J/kgC)
D Diameter of the tube (m)
h_{fp} Convective heat transfer coefficient (W/m^2C)
g Acceleration due to gravity, m/s^2
k Thermal conductivity (W/mC)
L Length of the cylinder (m)
m Consistency coefficient (Pas^n)
n Flow behavior index
ΔT Temperature difference (°C)
V Volumetric flow rate (m^3/s)
u Average relative velocity $[4V/(\pi D^2)]$ (m/s)

α Thermal diffusivity $(k/\rho C_p)$
β Volumetric thermal expansion coefficient (C^{-1})
ρ Density (kg/m^3)
μ Viscosity of the fluid (Pa.s)

Subscripts

f Fluid
w Wall
∞ Infinite value

Dimensionless Parameters

GGr	Generalized Grashof number $[g\ \beta\ \rho^2\ \Delta T\ d_p^3]\ /\ [m\{(3n+1)/n\}^n\ 2^{n-3}\ \{D/u)^{1-n}\}]^2$
GPr	Generalized Prandtl number: $[C_p\ m[(3n+1)/n]^n\ 2^{n-3}\ (D/u)^{1-n}\}/k_f]$
GRe	Generalized Reynolds number: $[d_p\ u\ \rho/\{m\{(3n+1)/n\}^n\ 2^{n-3}\{D/u)^{1-n}\}]$
Gr	Grashof number: $[g\ \beta\ \rho^2\ \Delta T)\ d^3/\mu^2]$
Nu	Nusselt number: $[h_{fp}\ d_{cd}/k_f]$
Pr	Prandtl number: $[C_p\mu/k]$
Ra	Rayleigh number: [Gr.Pr]
Re	Reynolds number: $[u\ d\ \rho/\mu]$

ACKNOWLEDGMENTS

This research was supported by the Strategic Grants Program of Natural Sciences and Engineering Research Council of Canada. Financial support provided to the first author by the Canadian International Development Agency is acknowledged.

REFERENCES

ABDELRAHIM, K.A. and RAMASWAMY, H.S. 1995. High temperature/pressure rheology of carboxymethylcellulose (CMC). Food Res. Int. *28* (3), 285–290.

ALHAMDAN, A. and SASTRY, S.K. 1990. Natural convection heat transfer between non-Newtonian fluids and an irregular shaped particle. J. Food Process Engineering *13*, 113–124.

ALHAMDAN, A., SASTRY, S.K. and BLAISDELL, J.L. 1990. Natural convection heat transfer between water and an irregular shaped particle. Trans. ASAE. *33*(2), 620–624.

ASHRAE. 1981. ASHRAE Handbook. Fundamentals. American Society for Heating Refrigerating and Air Conditioning Engineers. New York.

ASTROM, A. and BARK, G. 1994. Heat transfer between fluid and particles in aseptic processing. J. Food Eng. *21*, 97–125.

AWUAH, G.B., RAMASWAMY, H.S. and SIMPSON, B.K. 1993. Surface heat transfer coefficients associated with heating of food particles in CMC solutions. J. Food Process Engineering *16*, 39–57.

AWUAH, G.B., RAMASWAMY, H.S. and SIMPSON, B.K. 1994. Comparison of two analytical methods for evaluating surface-to-particle heat transfer coefficients. Food Res. Intl. *28*, 261–271.

AWUAH, G.B., RAMASWAMY, H.S., SIMPSON, B.K. and SMITH, J.P. 1996. Fluid-to-convective heat transfer coefficient as evaluated in an aseptic processing holding tube simulator. J. Food Process Engineering *19*, 241-267.

BURMEISTER, L.C. 1983. Convective Heat Transfer. John Wiley & Sons. New York.

CHANDARANA, D.I., GAVIN, A. and WHEATON, F.W. 1989. Simulation of parameters for modelling aseptic processing of food containing particulates. Food Technol. *43*(3), 137–143.

CHANDARANA, D.I., GAVIN, A. and WHEATON, F.W. 1990. Particle/fluid heat transfer under UHT conditions at low particle/fluid relative velocities. J. Food Process Engineering *13*, 191–206.

CHAPMAN, A.J. 1989. *Heat Transfer*. Macmillan Pub., New York.

CHURCHILL, S.W. 1977. A comprehensive correlating equation for laminar, assisted forced and free convection. J. AIChE. *23*, 10–16.

CHURCHILL, S.W. and BERNSTEIN, M. 1977. A correlating equation for forced convection from gases and liquids to a circular cylinder in cross flow. J. Heat Transfer. *99*, 300–306.

CHURCHILL, S.W. and CHU, H.H.S. 1975. Correlating equations for laminar and turbulent free convection from a horizontal cylinder. Int. J. Heat Mass Transfer. *18*, 1049–1053.

FAND, R.M. and KESWANI, K.K. 1973. Combined natural and forced convection heat transfer from horizontal cylinders to water. Int. J. Heat and Mass Transfer. *16*, 1175–1191.

GEANKOPLIS, C.J. 1978. *Transport Processes and Unit Operations*. Allyn and Bacon, Boston, MA.

GNIELINSKI, V. 1983. Forced convection around immersed bodies. In *Heat Exchanger Design Handbook: Fluid Mechanics and Heat Transfer*. (Schlunder *et al.*, eds.) Hemisphere Pub., New York.

JOHNSON, A.G., KIRK, G. and SHIN, T. 1988. Numerical and experimental analysis of mixed forced and natural convection about a sphere. Trans. ASAE *31*(1), 293-299, 304.

KING, W.J. 1932. The Basic Laws and Data of Heat Transmission - III. Free convection. Mech. Eng. *54*, 347–353.

LARKIN, J.W. 1989. Use of a modified Ball's formula method to evaluate aseptic processing of foods containing particulates. Food Technol. *43*(3), 124–125.

LARKIN, J.W. 1990. Mathematical analysis of critical parameters in aseptic particulate processing systems. J. Food Process Engineering *13*, 155–167.

MAESMANS, G., HENDRICKX, M., DECORDT, S. and FRANSIS, A. 1992. Fluid-to-particle heat transfer coefficient determination of heterogeneous foods: A Review. J. Food Processing and Preservation *16*, 29–69.

MORGAN, V.T. 1975. The overall convective heat transfer from smooth circular cylinders. In *Advances in Heat Transfer*, (T.F. Irvine and J.P. Hartnett, eds.) Academic Press, New York.

OZISIK, M.N. 1985. *Heat Transfer: A Basic Approach*. McGraw-Hill Book Co., New York.

PFLUG, I.J., BERRY, M.R. and DIGNAN, D.M. 1990. Establishing the heat-preservation process for aseptically-packed low-acid food containing large particulates, sterilized in a continuous heat-hold-cool system. J. Food Proc. *53*(4), 312–321.

RAMASWAMY, H.S., TUNG, M.A. and STARK, R. 1983. A method to measure surface heat transfer from steam/air mixtures in batch retorts. J. Food Sci. *48*, 900–904.

SASTRY, S.K. 1986. Mathematical evaluation of process schedules for aseptic processing of low-acid foods containing discrete particulates. J. Food Sci. *51*, 1323–1328, 1332.

SASTRY, S.K., LIMA, M., BRIM, J., BRUN, T. and HESKITT, B.R. 1990. Liquid-to-particle heat transfer during continuous tube flow: Influence of flow rate and particle to tube diameter ratio. J. Food Process Engineering *13*, 239–253.

SKJOLDEBRAND, C. and OHLSSON, T. 1993. A computer simulation program for evaluation of the continuous heat treatment of particulate food products. Part 1: Design. J. Food Eng. *20*, 149–165.

SPARROW, E.M. and ANSARI, M.A. 1983. A refutation of King's rule for multidimensional external natural convection. Int. J. Heat Mass Transfer. *26*(9), 1357–1364.

WHITAKER, S. 1972. Forced convection heat transfer calculations for flow in pipes, past flat plates, single cylinders, and for flow in packed beds and tube bundles. J. AIChE *18*, 361–371.

YUGE, T. 1960. Experiments on heat transfer from spheres including combined and forced convection. J. Heat Transfer. *82*, 214–220.

ŽHUKAUSKAS, A.A. 1972. Heat transfer from a tubes in crossflow. Advan. Heat Transfer *8*, 93–160.

ŽUKAUSKAS, A. and ŽIUGŽDA, A.J. 1985. *Heat Transfer of a Cylinder in Crossflow*. Hemisphere Pub., New York.

ZURITZ, C.A., McCOY, S.C. and SASTRY, S.K. 1990. Convective heat transfer coefficients for irregular particles immersed in non-Newtonian fluids during tube flow. J. Food Eng. *11*, 159–174.

SIMPLIFIED PREDICTIVE EQUATIONS FOR VARIABILITY OF THERMAL PROCESS LETHALITY

KAN-ICHI HAYAKAWA, JIANJUN WANG[1] and PILAR R. DE MASSAGUER[2]

Food Science Department
New Jersey Agricultural Experiment Station
Cook College, Rutgers University
P.O. Box 231
New Brunswick, NJ 08903

Accepted for Publication December 12, 1995

ABSTRACT

A distribution free, analytical formula was derived for estimating variation in heating phase lethality as a function of variations in all independent parameters. Additionally, a regression formula was developed for estimating the coefficient of variation of thermal process lethalities for a fixed z value of 10C as a function of statistically significant parameters. Although process lethalities included both heating and cooling phases of processes, no cooling phase parameter was among the statistically significant parameters. Sample applications of both formulae were presented together with the results of a sensitivity analysis performed using the regression formula.

INTRODUCTION

Quantitative information on lethality variability is required for reliable thermal process design. Therefore, several researchers have developed predictive methods for the lethality variability of packaged food as reviewed in previous publications (Hayakawa *et al.* 1988 and Wang *et al.* 1991).

The first paper (Hayakawa *et al.* 1988) showed an experimentally validated Monte Carlo simulation method for estimating the variability represented by a coefficient of variation (W_{fp}), the ratio of standard deviation and the mean F_p value, when all independent biological, physical, and process parameters are statistically variable. Gamma distributions were used to represent the variabilities of process parameters since all parametric variates should be positive whereas most frequently used distribution, normal distributions, give both positive and negative parametric values.

[1] Currently Process Development Division, Ross Laboratory, Columbus, OH
[2] Currently Food Science Department, Faculty of Food Engineering, University of Campinas, Campinas, SP, Brazil

Journal of Food Process Engineering **19** (1996) 289–300.

The second paper (Wang *et al.* 1991) showed an experimentally validated regression formula for predicting W_{fp}, as a function of all significant parametric means and coefficient of variations, that was derived applying a previously developed simulation method together with statistical screening and regression analysis methods.

The present work is to develop simpler, alternative methods for estimating F_p variabilities of low acid food thermal processes. One is a statistical distribution free analytical formula and another a regression formula for estimating W_{fp} of a fixed mean z value of 10C since this z value is used widely for low acid food process design.

DERIVATION OF PREDICTIVE FORMULAS

Distribution Free Formula

Lethality gained during the heating phase, F_{ph}, of a thermal process is considered to derive a distribution free equation that is applicable when cooling phase lethality is relatively small. The analytical equation for estimating the heating phase lethality was obtained by Ball (1957) assuming negligible lethality of initial, nonlogarithmic (curvilinear) part of a heating curve (valid for most processes).

$$F_{ph}=(f_h/a)\exp\{a(T_1-T_r)/z\}[E_1(ag/z)-E_1(aj_hI_o/z)] \quad (1)$$

In the above, $E_1(\ )$ represents an exponential integral function defined as:

$$E_1(x) = \int_x^\infty e^{-u}/u \, du \quad (1a)$$

The values of $E_1(x)$ for different x's are widely available in mathematical handbooks (e.g., Abramowitz and Stegun 1964). These books show sharp $E_1(x)$ reduction with an increase in x.

The heating medium temperatures (T_1) of most low acid food processes range from 104 to 127C and initial food temperatures (T_o) from 10 to 70C (Wang *et al.* 1988).

Therefore, the initial temperature differences $I_o(= T_1-T_o)$ range from 34 to 117C. The j_h values of most low acid food packages or food particles at their centers range from 1 to 4 (Wang *et al.* 1988). Therefore, the minimum value of aj_hI_o/z, the expression in the second exponential integral of Eq. 1, is 7.8. Since $E_1(7.8)$ is 4.707×10^{-5}, the second integral may be eliminated for most processes.

$$F_{ph}=(f_h/a)\exp\{a(T_1-T_r)/z\}E_1(ag/z) \quad (2)$$

In the above, $g(= T_1 - T_g)$ depends on f_h, j_h, T_1, T_o, and t_b since one has:

$$g=j_h(T_1-T_o)10^{-t_b/f_h} \tag{3}$$

Additionally, the exponential integral $E_1(ag/z)$ is defined as follows, noting $g = T_1 - T_g$:

$$E_1\{a(T_1-T_g)/z\} = \int_{a(T_1-T_g)/z}^{\infty}(e^{-u}/u)du \tag{4}$$

The independent parameters for estimating F_{ph} that could deviate from set levels are: T_o, T_1, j_h, f_h, z, and t_b (note that T_r is a fixed constant). The influence of these parametric deviations on F_{ph} may be estimated using the partial derivatives of F_{ph} with respect to these parameters. These derivatives were estimated using the following equation for differentiating the exponential integral, obtained applying a Riemann integral property (Pearson 1983).

$$dE_1[y(p)]/dp = -\exp[-y(p)]/y(p)\cdot(dy/dp) \tag{5}$$

Therefore, one obtained:

$$\begin{aligned}
&\partial F_{ph}/\partial T_o = f_h L_g/(aI_o)\\
&\partial F_{ph}/\partial T_1 = aF_{ph}/z - f_h L_g/(aI_o)\\
&\partial F_{ph}/\partial j_h = -f_h L_g/(aj_h)\\
&\partial F_{ph}/\partial f_h = F_{ph}/f_h - L_g t_b/f_h\\
&\partial F_{ph}/\partial z = a(T_r-T_1)F_{ph}/z^2 + f_h L_g/(az)\\
&\partial F_{ph}/\partial t_b = L_g
\end{aligned} \tag{6}$$

Using the total differential of F_{ph} one obtained:

$$\begin{aligned}
|\Delta F_{ph}| < {} & |(\partial F_{ph}/\partial T_o)\Delta T_o| + |(\partial F_{ph}/\partial T_1)\Delta T_1| + |(\partial F_{ph}/\partial j_h)\Delta j_h|\\
& + |(\partial f_{ph}/\partial f_h)\Delta f_h| + |(\partial F_{ph}/\partial z)\Delta z| + |(\partial F_{ph}/\partial t_b)\Delta t_b|
\end{aligned} \tag{7}$$

Note that the absolute value of each term was taken since parametric deviations could be positive or negative. This ensures the upper bound of F_{ph} deviations.

Each parametric deviation term of Eq. 7 may be treated as a vectorial element in a multidimensional space. The equation represents the sum of vectorial elements. This sum is greater than the multidimensional, vectorial length. Therefore, one obtained a tighter upper bound of ΔF_{ph}, Eq. 8.

$$\begin{aligned}
|\Delta F_{ph}| < {} & [\{(\partial F_{ph}/\partial T_o)\Delta T_o\}^2 + \{(\partial F_{ph}/\partial T_1)\Delta T_1\}^2 + \{(\partial F_{ph}/\partial j_h)\Delta j_h\}^2\\
& + \{(\partial F_{ph}/\partial f_h)\Delta f_h\}^2 + \{(\partial F_{ph}/\partial z)\Delta z\}^2 + \{(\partial F_{ph}/\partial t_b)\Delta t_b\}^2]^{1/2}
\end{aligned} \tag{8}$$

From Eq. 6 and 8, one obtained:

$$\begin{aligned}
|\Delta F_{ph}| < {} & [[\{f_h L_g/(aI_o)\}\Delta T_o]^2 + [\{aF_{ph}/z - f_h L_g/(aI_o)\}\Delta T_1]^2\\
& + [\{f_h L_g/(aj_h)\}\Delta j_h]^2 + [\{F_{ph}/f_h - t_b L_g/f_h\}\Delta f_h]^2\\
& + [\{a(T_r-T_1)F_{pf}/z^2 + f_h L_g/(az)\}\Delta z]^2 + (L_g\Delta t_b)^2]^{1/2}
\end{aligned} \tag{9}$$

Theoretical Regression Formula

For the previous work (Wang *et al.* 1991), we assumed that z-distribution means changes from 7 to 12.5C. The z-mean was fixed to 10C for the present work, although it was variable around 10C, because of frequent use of this fixed value for the thermal process design. Dual steps parametric analyses were performed through an approach similar to the previous work (Wang *et al.* 1991). The first step was to identify parameters influenced significantly W_{fp} through screening Monte Carlo simulation and analysis and the second step to obtain an equation for estimating W_{fp} as a function of significant parameters through regression simulation and analysis. The identified significant parameters in the first step were: f_h, T_{l1}, W_z, W_{fh}, and F_p. No parameters related to the cooling phase of a process (f_c, j_c, and T_w and their coefficients of variations) were among the significant parameters although they influenced F_p. In the second step, all nonsignificant parameters were set to their frequently observed levels while the significant parameters were varied according to a statistical design (a fractional central composite design). Through regression analyses of results obtained from second step simulation, the following equation was obtained for estimating W_{fp} when $\bar{z}$ was fixed to 10C.

$$\begin{aligned} W_{fp} = {} & 37.7975 + 4.0029X_{fh} - 6.1851X_{tl} - 1.5010X_{wz} + 3.1002X_{wfh} \\ & + 1.3056X_{wjh} + 2.2739X_{fp} + 0.9157X_{fh}X_{wfh} - 1.2010X_{t1}X_{wfh} \\ & + 0.9075X_{tl}^2 + 0.1870X_{tl}^3 \end{aligned} \tag{10}$$

In the above equation, the parameters and parametric coefficient of variations were transformed to the following design variables, since the lower limit, frequent level, and upper limit of each parameter should be fixed to -4.0, 0.0, and 4.0, respectively, to use a central, composite design for the analysis.

$$\begin{aligned} X_{fh} &= 2.6816\ln(\bar{f}_h/60 + 6.4516) - 10.2930 \\ X_{t1} &= 15.7727\ln(160.30366 - \bar{T}_1) - 59.4352 \\ X_{wz} &= 11.8880\ln(27.5000 - W_z) - 34.2600 \\ X_{wfh} &= 8.5106\ln(W_{fh} + 6.3333) - 22.9744 \\ X_{wjh} &= 3.2688\ln(W_{jh} + 2.1667) - 8.6646 \\ X_{fp} &= 17.4793\ln(18.6889 - \bar{F}_p/60) - 45.7362 \end{aligned} \tag{11}$$

Note that five or more significant digits are retained in Eq. 11 since they are theoretical transformation equations, not regression equations. Equation 10 is applicable within -4.0 and +4.0 of each design variable. This corresponds to these parametric ranges $240 \leq f_h \leq 120{,}000$(s); $104 \leq T_1 \leq 126.7$(C); $3 \leq W_z \leq 15$(%); $2 \leq W_{fh} \leq 15$(%); $2 \leq W_{jh} \leq 46$(%); $89 \leq F_p \leq 468$(s). Additionally, the equation estimates W_{fp} more accurately within -1.0 and +1.0

of each design variable compared to the outside of this variable range. This corresponds to these parametric ranges: $1,530 \leq \bar{f}_h \leq 3,660$(s); $114.2 \leq \bar{T}_1 \leq 119.7$(C); $8.5 \leq \bar{W}_z \leq 11.4$(%); $5.52 \leq \bar{W}_{fh} \leq 8.66$(%); $8.27 \leq \bar{W}_{jh} \leq 17.07$(%); $251 \leq \bar{F}_p \leq 345$(s). Frequently observed parametric values were transformed to zeros of the design variables. These values of $\bar{F}_p$, $\bar{f}_h$, $\bar{T}_1$, $\bar{W}_z$, $\bar{W}_{fh}$, and $\bar{W}_{jh}$ were 300s, 2400s, 117C, 10%, 7%, and 12%, respectively.

Equation 10 is much simpler to use compared to the published regression equation consisting of 27 polynomial terms (Wang *et al.* 1991) when $\bar{z} = 10$C.

SAMPLE APPLICATION AND DISCUSSION

Equation 9 was applied to estimate F_{ph} variability for a conventional thermal process of packaged food. Assumed parametric values and variations were:

$$F_{ph}=360\text{s},\Delta t_b=15\text{s},f_h=1800\text{s},\Delta f_h=90\text{s}(5\%\text{ of }f_h),j_h=2.0,\Delta j_h=0.2(10\%\text{ of }j_h),$$
$$T_1=120\text{C},\Delta T_1=0.2\text{C},T_o=70\text{C},\Delta T_o=2.0\text{C},z=10\text{C},\Delta z=1.0\text{C}(10\%\text{ of }z)$$

The assumed parametric deviations were based on realistic variabilities reported in literature (Wang *et al.* 1991). A proper heating time of the above process was estimated, assuming a negligible cooling phase lethality, by a published method (Hayakawa and Downes 1981), 3,035s. When the assumed parametric values and their variations are substituted into Eq. 7, an estimated limiting value for ΔF_{ph} was 177s or 49.3% of the assumed F_{ph} value. When Eq. 9 was used, a ΔF_{ph} upper limit was 84.6s or 23.5% of F_{ph}, less than one half of Eq. 7 limit. The tighter Eq. 9 limit is more useful for examining F_{ph} deviations. It should be noted that both Eq. 7 and 9 show inequality relationships, ΔF_{ph} being less than values estimated by the right hand side expressions. Therefore, seemingly conflicting results are correct mathematically. Table 1 shows a relative F_{ph} deviation due to each parametric deviation (the percentage of each parametric F_{ph} deviation with respect to the total F_{ph} deviation) together with the percentage of the total F_{ph} deviation, the sum of all parametric deviations, with respect to the assumed F_{ph}. The two most significant contributors to ΔFp were Δf_h (31.1% of total F_p deviation) and Δz (26.5%).

An F_{ph} variation for a high temperature, short time (HTST) process was examined using the same equation. Assumed parametric values and variations were:

$$F_{ph}=360\text{s},\Delta t_b=15\text{s},f_h=240\text{s},\Delta f_h=12\text{s}(5\%\text{ of }f_h),j_h=1.1,$$
$$\Delta j_h=0.1(10\%\text{ of }j_h),T_1=145\text{C},\Delta T_1=0.2\text{C},T_o=85\text{C},$$
$$\Delta T_o=2\text{C},z=10.0\text{C},\Delta z=1.0\text{C}(10\%\text{ of }z).$$

TABLE 1.
INFLUENCE OF PARAMETRIC DEVIATION ON HEATING PHASE LETHALITY (F_{ph}) DEVIATION

Process	Relative F_{ph} deviation (%) due to the parametric deviations (% of total F_{ph} deviation)[1]						Total F_{ph} deviation limit (% of F_{ph}) estimated by [2]	
	T_o	T_l	j_h	f_h	z	t_h	Eq.7	Eq. 9
Conventional	8.5	8.5	21.3	31.1	26.5	4.1	49.2	23.5
HTST-I[3])	8.5	2.3	23.1	17.4	12.1	36.6	146.6	71.8
HTST-II[4])	0.7	1.9	37.5	28.3	19.7	11.9	90.2	47.3

[1] The percentages of total F_{ph} deviation limit estimated by Eq. 7 or 9. The percentages of both limits are identical since those of ΔF_{ph} estimated by Eq. 9 were normalized. The sum of percentages for each process is 100%.
[2] The percentage of the assumed F_{ph}, 360s.
[3] Assumed relative or absolute deviations identical to those of the conventional process.
[4] Smaller T_o, T_l and T_h deviations assumed.

It should be noted that the smaller f_h and j_h values were typical for a small food package or particle and that the assumed absolute or relative parametric deviations were identical to those for the conventional process application. As before, a heating time was estimated using the published method, t_b = 171s. The values of ΔF_{ph} estimated by Eq. 7 and 9 were 528s (146.6% of F_{ph}) and 258s (71.6%), respectively. Again, Eq. 9 limit was about one half of Eq. 7 limit. Table 1 shows that the two largest contributors were Δt_b (36.6% of ΔFp) and Δj_h (23.1%). The relatively large ΔF_p implies a need for tighter operational control compared to the conventional process as practiced in the industry. Since a tighter control produces smaller operational parametric deviations, the following were assumed in another sample application. ΔT_o = 0.1C, ΔT_l = 0.1C, Δt_b = 3s (all others unchanged). The value of ΔF_p estimated by Eq. 7 and 9 were 325s (90.2% of F_{ph}) and 170.1s (47.3%), respectively. The two largest contributors were Δj_h (37.5%) and Δf_h (28.3%), Table 1. These two deviations should be reduce to obtain lethality deviation comparable to the conventional process. This requires precise control of package or particle weights and shapes.

The regression equation, Eq. 10, was applied to two processes similar to those considered in the previous paper (Wang *et al.* 1991). The first was for a process of 211 × 300 cans of a conduction food simulator (8% bentonite aqueous suspension) and the second for a process of 307 × 409 cans of the same suspension. Table 2 shows experimentally determined parametric values.

Table 3 shows experimentally determined parametric values and parametric coefficients of variations required to use Eq. 10 together with the values of corresponding design variables estimated using Eq. 11.

TABLE 2.
KEY PROCESSING CONDITIONS OF CANNED 8% AQUEOUS BENTONITE SUSPENSION[1]

Can size	$\bar{T}_o$ (°C)	$\bar{T}_1$ (°C)	$\bar{T}_w$ (°C)	$\bar{t}_h$ (sec)	$\bar{F}_p$ (sec)
211 x 300	15.8	115.6	13.1	3,368	184
307 x 409	13.1	118.3	8.7	5,202	373

[1]Average values of experimentally determined values.

The estimated W_{fp} values of processes for the 211 × 300 and of 307 × 409 cans were 25.5 and 21.6%, respectively. The estimated values agreed well with those determined experimentally, 24.6% for 211 × 300 cans and 24.9% for the other cans (Wang *et al.* 1991) although the values of most design variables were outside of the accurate prediction ranges, with -1.0 and 1.0, Table 3.

Equation 10 estimates W_{fp} using three significant parametric mean values and three significant parametric variation coefficients. However, experimentally determined values of nonsignificant parameters and variation coefficients, not listed in Table 2, are given in Table 4 for both can sizes to show experimental processing conditions.

A sensitivity analysis was performed using Eq. 10. For this, one parameter was varied at a time while all others were kept at frequently observed levels, Fig. 1. In the figure, the abscissa is relative parametric deviation from its frequently observed level, r_d (r_d based on an original parameter, not a design variable). The figure shows that W_{fp} was influenced most strongly by T_1, followed by W_z and F_p (target lethality). Noting that an F_p was obtained integrating lethal rate L with respect to processing time, the strong influence of T_1 was due to an exponentially increased L with a T_1 increase (i.e., $L = \exp\{a(T - T_r)/z\}$ and $T = T_1 - j_h(T_1 - T_o) \bullet \exp(-at/f_h)$).

The strong W_z influence may be explained also in terms of W_z influence on lethal rate L. A z-distribution with a larger W_z value produced a larger fraction of large z values compared to a z-distribution of a smaller W_z value. It should be noted that randomly selected z-values in each z-distribution were used to determine the W_z influence on F_p variation and that the lethal rate L of an individual food temperature, T, was estimated using an equation similar to the

TABLE 3.
VALUES OF SIGNIFICANT PARAMETERS AND VARIATION COEFFICIENTS FOR SAMPLE CALCULATIONS USING EQ. 10[1]

Can size	$\bar{f}_h$ (sec)	$\bar{T}_1$ (°C)	W_z[2] (%)	W_{fh} (%)	W^{jh} (%)	$\bar{F}_p$ (sec)	W_{fp} estimated by Eq. 10 or determined experimentally[3]
211 × 300	1,754	115.6	11.1	4.350	4.412	184	22.5 (24.6)
	-0.7065	0.5019	-1.006	-2.815	-2.507	2.354	
307 × 409	2,962	118.3	11.1	3.145	4.848	373	21.6 (24.9)
	0.4928	-0.4807	-1.006	-3.834	-2.297	-1.597	

[1] The parametric values and variations obtained experimentally (Wang *et al.* 1991). The second row for each size shows the design variable values estimated using Eq. 11. For example, -0.7065 is the X_{fh} value of 211 × 300 cans.

[2] Assumed value.

[3] The first value for each can is Eq. 10 estimation and the second value enclosed within a parenthesis pair is experimentally determined (Wang *et al.* 1991).

TABLE 4.
EXPERIMENTALLY DETERMINED VALUES OF NONSIGNIFICANT PARAMETERS AND VARIATION COEFFICIENTS[1]

Parameters	Processes for 211 x 300 cans of 8% bentonite suspension	Processes for 307 x 409 cans of 8% bentonite suspension
$\bar{j}_h$ (-)	1.933	2.104
$\bar{f}_c$ (s)	2263	3870
j_c (-)	1.756	2.797
W_{fc} (%)	3.695	3.388
W_{jc} (%)	0.890	16.649
S_{t1} (C°)	0.46	0.46
S_{tw} (C°)	0.47	2.63
S_{to} (C°)	1.21	2.02
S_{th} (s)	12	12

[1]From Wang *et al.* (1991).

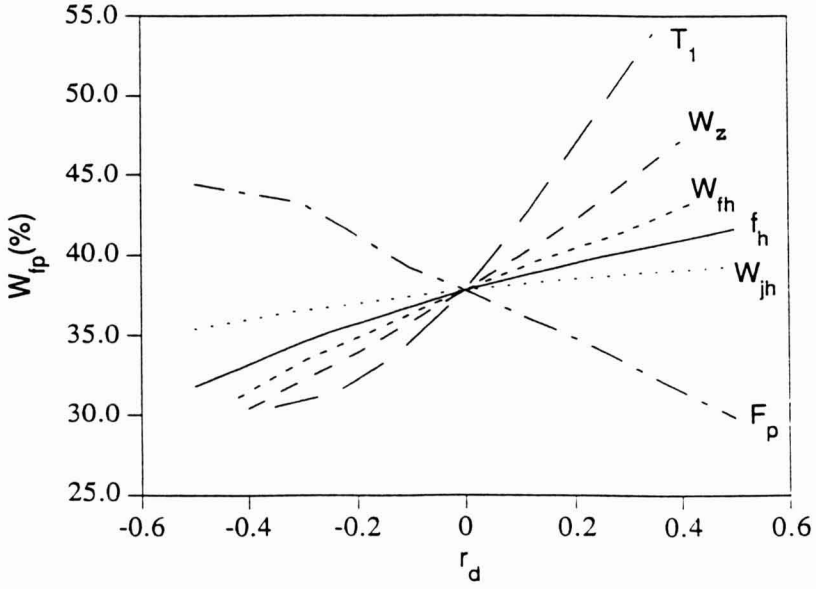

FIG. 1. SENSITIVITY ANALYSIS OF COEFFICIENT OF VARIATION OF THERMAL PROCESS LETHALITY

one given above, replacing $\bar{T}$ by T. In the present case, the exponent in this equation, a $(T - T_r)/ z$, was negative since $T < T_r$. Therefore, a larger z produced a smaller absolute of this negative exponent, which produced a larger L value. This resulted in an increased W_{fp}.

The influence of a target sterilizing value, $\bar{F}_p$, may be explained as follows. Food temperature became uniformly close to T_1 due to a longer heating time required with an increased $\bar{F}_p$. This resulted in reduced influence of all process parameters on W_{fp}.

The direct comparison of Eq. 9 and 10 is not possible since Eq. 9 estimates the *upper limit* of F_{ph} variation (a true deviation less than an estimated limit) and since Eq. 10 estimates variation coefficient of the entire process lethality, F_p, that includes heating and cooling phases. However, Eq. 9 was used to estimate F_{ph} variation coefficient of both can sizes. For this, F_{ph} values were estimated using data given in Tables 2, 3 and 4 and treating standard deviations as parametric deviations (standard deviation = variation coefficient × mean parametric value). Estimated F_{ph} values of 211 × 300 and 307 × 409 cans were 113 and 244s, respectively. Estimated upper limits of F_{ph} variation coefficients for 211 × 300 and 307 × 409 cans were 31.5 and 24.0%, respectively. Since a lesser number of parameters influenced F_{ph} variation compared to F_p variation, the standard deviation of F_{ph} is likely smaller than that of F_p. According to Table 3, experimentally determined F_p variation coefficients of 211 × 300 and 307 × 409 cans were 24.6 and 24.9%, respectively. Therefore, true variation coefficient of F_{ph} for both cans should be less than these experimentally determined values. The estimated upper limits were correct mathematically.

CONCLUSION

The statistical distribution free, analytical equation was obtained for estimating a variation in the heating phase lethality of a thermal process when there were deviations in all independent parameters. Additionally, the regression equation was developed to estimate the coefficient of variation of process lethality as a function of significant parameters.

The sample applications of the distribution free equation showed the heating phase lethality variation for the HTST process that was greater than that for the conventional process.

The values of W_{fp} estimated by the developed regression equation agreed well with those determined experimentally. The sensitivity analysis performed using the regression equation showed the strong influence of T_1, W_z and $\bar{F}_p$ on W_{fp}.

ACKNOWLEDGMENT

This publication D-10209-6-95 of New Jersey Agricultural Experiment Station supported by U.S. Hatch Act Fund, New Jersey State Fund, Mainframe computer time supported by Rutgers University Computing Services, Supercomputer time grant by National Science Foundation and by Cray Research, Inc. (both administered by Pittsburgh Supercomputing Center).

NOMENCLATURE

a	$= \ln 10$ (-)
CV	Coefficient of variation which is equal to the ratio of standard deviation and mean (-)
$E_1( )$	Exponential integral estimated for a value placed within parentheses, see Eq. 1a.
F_p	Sterilizing value of entire process that includes heating and cooling phases (s)
F_{ph}	Sterilizing value of heating phase of a thermal process (s)
f_c	Slope index of semilogarithmic cooling curve (s)
f_h	Slope index of semilogarithmic heating curve(s)
g	$= T_1 - T_g$ (C°)
I_o	$= T_1 - T_o$ (C°)
j_c	Intercept coefficient of linear portion of semilogarithmic cooling curve extrapolated to a zero cooling time (-)
j_h	Intercept coefficient of linear portion of semilogarithmic heating curve extrapolated to a zero cooling time (-)
L	$= \exp\{a(T - T_r)/z\}$
L_g	$= \exp\{a(T_g - T_r)/z\}$ (-)
r_d	= (parametric value - its frequent value)/frequent value. The parametric values are those of original parameters, not of transformed design variables. Relative parametric deviation from its frequent value (-).
T	Food temperature (°C)
S_{i1}, S_{tw}, S_{to}, S_{tb}	Standard deviations of T_1, T_w, T_o and t_b, respectively.
T_g	Food temperature at the end of thermal process heating phase (°C)
T_o	Initial food temperature (°C)
T_r	Reference temperature, 121.11 (°C)
T_1	Holding temperature of heating medium (°C)
t_b	Length of thermal process heating phase(s)
u	Dummy variable (-)

W_{fc}, W_{jc}, W_{fh}, W_{fp}, W_{jh}, W_z	Coefficient of variations of f_c, j_c, f_h, F_p, j_h, and z, respectively (-)
X_{fh}, X_{fp}, X_{t1}, X_{wfh}, X_{wjh}, X_{wz}	Design variables corresponding to $\bar{f}_h$, $\bar{F}_p$, $\bar{T}_1$, W_{fh}, and W_{jh}, and W_z, respectively. (-)
z	Slope index of thermal death time curve (°C)

Subscript

a bar '—' placed above a symbol ... parametric mean value.

REFERENCES

ABRAMOWITZ, M. and STEGUN, T. A., eds. 1964. *Handbook of Mathematical Functions*. pp. 238–243, National Bureau of Standards, Washington, D.C.

BALL, C.O. and OLSON, F.C.W. 1957. *Sterilization in Food Technology*. pp. 313–316, McGraw-Hill, New York.

HAYAKAWA, K. and DOWNES, T.W. 1981. New Parametric values for thermal process estimation by using temperatures and z values expressed in degree Celsius units. Lebemsm. Wiss. Technol. *14*, 60–64.

HAYAKAWA, K., de MASSAGUER, P.R. and TROUT, R.J. 1988. Statistical variability of thermal process lethality in conduction heating food-computerized simulation. J. Food Sci. *53*, 1887–1893.

PEARSON, C.E., ed. 1983. *Handbook of Applied Mathematics*. p. 101, Van Nostrand Reinhold, New York.

WANG, J., WOLFE, R.R. and HAYAKAWA, K. 1991. Thermal foods process lethality variability in conduction-heated foods. J. Food Sci. *56*, 1424–1428.

CALCULATION OF INITIAL FREEZING POINT, EFFECTIVE MOLECULAR WEIGHT AND UNFREEZABLE WATER OF FOOD MATERIALS FROM COMPOSITION AND THERMAL CONDUCTIVITY DATA[1]

EDGAR G. MURAKAMI[2] and MARTIN R. OKOS[3]

[2]*Food and Drug Administration/National Center for Food Safety and Technology, 6502 S. Archer Ave., Summit-Argo, IL 60501*

[3]*Purdue University, Department of Agricultural Engineering, West Lafayette, IN 47907*

Accepted for Publication November 12, 1995

ABSTRACT

A procedure was developed for simultaneous determination of the effective molecular weight, unfreezable water, and initial freezing point of foods based on composition and thermal conductivity data. Freezing properties were determined by trial and error and optimized by minimizing the difference between calculated and reported values of thermal conductivity. The procedure involved determination of the ice fraction at several temperature levels. Corresponding thermal conductivity values at each temperature level were then calculated. Results showed that calculated values of effective molecular weight, unfreezable water, and initial freezing point for various types of meat and fish are comparable to those published. The parallel-perpendicular model was found an excellent predictor of thermal conductivity of frozen meat and fish with muscle fibers oriented toward the direction of the heat flow.

INTRODUCTION

During freezing and thawing process operations, high moisture foods are exposed to temperatures that can make them susceptible to microbial growth. To determine if a food material has reached critical conditions during freezing and thawing, information is needed on temperature distribution as a function of time. In frozen particles, temperature distribution can be determined by numerical modeling, which requires data on freezing and thermal properties; however, data

[1] The contents of this paper are solely the opinions of the authors and do not necessarily represent the official views of the U.S. Food and Drug Administration.

[2] Author for correspondence.

Journal of Food Process Engineering **19** (1996) 301–320.

on these properties for various foods are seldom available. In this study, a method is proposed for the calculation of initial freezing point (T_f), unfreezable water (b), and effective molecular weight (ω_e) of frozen materials from thermal conductivity (k) and composition (X^w) data. Conversely, thermal conductivity can be calculated if those three freezing properties are known.

Freezing proceeds gradually, and in the presence of solutes the freezing point of the unfrozen fraction drops as the amount of water in the system decreases. The relationship between freezing point (T_f) and the amount of unfrozen water in the system can be expressed with the following (Heldman 1974):

$$\frac{L_f \omega_w}{R}\left[\frac{1}{T_{fw}}-\frac{1}{T_f}\right] = \ln(X_a) \tag{1}$$

The left-hand side of Eq. (1) is derived from the summation of chemical potentials of different phases of matter in the system, and the right-hand side is the mole fraction of the unfrozen water (X_a). The mole fraction of water in a solution depends on the weight fractions of unfrozen water ($X_w{}^w$) and dissolved solids ($X_{ds}{}^w$) in the system and their corresponding molecular weights (ω_w and ω_{ds}), respectively. The X_a is calculated by the following equation:

$$X_a = \frac{X_w^w}{X_w^w + X_{ds}^w(\omega_w/\omega_{ds})} \tag{2}$$

If all solids in the system are dissolved, the ω_{ds} can be computed from the weight fractions and molecular weights of all the solute in the system. This assumption was made in several previous freezing studies because dissolved solids are difficult to identify and quantify; however, it is unrealistic since only a fraction of the total solids actually dissolves in the unfrozen water. To account for the undissolved solids, Heldman (1974) suggested using total solids in the calculation and a parameter called effective molecular weight (ω_e), which serves as a correction factor for using total solids instead of undissolved solids in the equation. By replacing ω_{ds} with ω_e, Heldman (1974) calculated ω_e from Eq. (1) and (2) using the moisture content (MC) and the T_f of the system, and concluded that his procedure for calculating the ω_e is valid only in systems without a significant amount of unfreezable water. Other studies have used the concept of effective molecular weight and suggested several other methods for calculating it. Table 1 shows the published ω_e for some materials used in this study.

The definition of unfreezable water is often interchanged with that of bound water (Chen 1985). Unfreezable water has been defined as the amount of unfrozen water in the system at -40C. In contrast, bound water is the amount of water left in the system after drying. Pham (1987) and Chen (1985) reported that

the wide ranges of both bound and unfreezable water overlap each other. They are assumed equal in this study because the difference in their values has not been clearly established in the literature. The literature values of bound water for various food materials are listed in Table 2.

Several workers including Choi (1985) and Murakami and Okos (1988) have proposed the modeling of thermal conductivity (k) of foods based on composition. Choi (1985) reported that the k of food materials can be determined from the major components, such as protein, carbohydrates, fats, ash, water, and ice. He developed empirical equations of thermal properties for each food component as a function of temperature.

The objective of this study was to develop a method for calculating initial freezing point, effective molecular weight, and unfreezable water of food materials from composition and thermal conductivity data. This study will increase the database of food properties that are useful in numerical modeling of heat transfer in frozen foods.

TABLE 1.
LITERATURE VALUES OF ω_e FOR VARIOUS FOOD MATERIALS AT SPECIFIED LEVELS OF MOISTURE AND FAT CONTENTS

	MC (% wb)	Fat (%)	ω_e
Lean beef	74	---	662[a,b], 677[c], 724[d]
	50	---	677[e], 701[b], 702[a], 1071[d]
Cod fish	82	---	466[a,b], 494[d], 519[c]
	50	---	509[a,b], 519[e], 810[d]
Lamb kidneys	79.8	2.9	416[e]
Lamb loin	64.9	11.7	1023/684[f,e]
	52.5	28.4	1993[e], 779[e,f]
	44.4	39.4	3711[e], 1078[e,f]
Calf veal	77.5	4.4	1091[e]

[a] Heldman 1974; Chen 1985.
[b] Bartlett 1944; Chen 1985.
[c] Schwartzberg 1976; Chen 1985.
[d] Chen, 1985.
[e] Schwartzberg 1976.
[f] Based on nonfat solids.

TABLE 2.
LITERATURE VALUES OF b FOR VARIOUS FOOD MATERIALS

	b (sb)	References
Meat, fish	0.24-0.27	Duckworth (1971); Schwartzberg (1976)
	0.143-0.318	Pham (1987)
Lean beef[a]	0.34, 0.36	Reidel (1951,1957,1959); Chen (1985)
	0.25	Schwartzberg (1976); Chen (1985)
	0.06, 0.054	Bartlett (1944); Chen (1985)
	0.31, 0.389	Chen (1985)
Cod fish[b]	0.364, 0.39	Reidel (1951,1957,1959); Chen (1985)
	0.25	Schwartzberg (1976); Chen (1985)
	0.082, 0.075	Bartlett (1944); Chen (1985)
	0.342, 0.419	Chen (1985)

[a]Corresponding MC = 74 and 50% wb, respectively.
[b]Corresponding MC = 82 and 50% wb, respectively.

MATERIALS AND METHODS

Calculation of Parameters

Ice Fraction. In the proposed procedure, the amount of ice in the system (X_i^w) at any temperature is calculated from Schwartzberg's (1976) equation. Since unfreezable water is not available for the freezing process, Schwartzberg (1976) modified Heldman's (1974) equation by subtracting the amount of unfreezable water (bX_s^w) from the unfrozen fraction (X_w^w). The resulting equation is:

$$X_a = \frac{X_w^w - bX_s^w}{(X_w^w - bX_s^w) + (18/\omega_e)X_s^w} \tag{3}$$

Then, X_i^w is calculated from the following:

$$X_i^w = MC - X_w^w - bX_s^w \tag{4}$$

Note that at above freezing temperatures, MC is equal to X_w^w. Schwartzberg (1976) agreed with Heldman (1974) that the effective molecular weight (ω_e) serves as a correction factor for using the weight fraction of the total solids.

Thermal Conductivity. Modeling of thermal conductivity based on composition requires a structural model to relate the various food components (Murakami and Okos 1988). The two basic structural models are the parallel and

perpendicular models. In the parallel model, all food components are assumed to be arranged parallel to the direction of heat flow. In the perpendicular model, they are perpendicular to the heat flow. In this study, it was found that the published thermal conductivity values for frozen meat were lower than those calculated with the parallel model and higher than those calculated with the perpendicular model. For example, Pham and Willix (1989) reported that the thermal conductivity of lamb kidneys at -40C is 1.65 W/m-K. The predicted values are 0.64 W/m-K using the perpendicular model and 2.06 W/m-K for the parallel model. The predicted values using the parallel model are high since components with high thermal conductivity (i.e., ice and liquid water) can compensate for those with low thermal conductivity (i.e., protein and fat). In the perpendicular model, the total conductive heat has to pass through each component. Thus, the components with low thermal conductivity can serve as insulators. In this study, the structural model chosen for frozen foods is a parallel-perpendicular model, which combines the two basic structural models. In this model, frozen food materials are assumed as 2-phase systems of liquid and solid, which are arranged perpendicular to the direction of heat flow. Then, the solid phase is made up of the ice fraction and other nonwater components which are arranged parallel to the heat flow. The parallel-perpendicular model is expressed in the following equation:

$$\frac{1}{k} = \frac{(1 - X_1^v)}{k_s} + \frac{X_1^v}{k_1} \tag{5}$$

where:

$$k_s = \frac{\Sigma X_n^v k_n}{\Sigma X_n^v} \tag{6}$$

A parallel-perpendicular model with the solid and liquid phases in parallel arrangement and the solid phase components in perpendicular arrangement was also evaluated. This model was found to give high standard errors. The k model (Eq. 5 and 6) requires the volume fraction (X^v) of the components rather than their weight fractions (X^w). Because data on food composition are usually available in terms of weight fractions, the equivalent volume fractions must be calculated. Volume fractions can be calculated from weight fractions and densities (ρ) by the following conversion equation:

$$X_m^v = \frac{X_m^w/\rho_m}{\sum_{n=1}^{N}(X_n^w/\rho_n)} \tag{7}$$

Initial Freezing Point. The presence of ice in frozen foods dramatically increases the k of the system. Since the k of ice is as much as four times that of water, the accuracy of k models for frozen foods depends largely on the accuracy of ice content prediction. Figure 1 illustrates how the initial freezing point (T_f) influences the temperature-thermal conductivity (T-k) curve of a material. This figure was calculated using the parallel-perpendicular model used in this study and it is consistent with the figures published by Heldman and Gorby (1975) and Pham and Willix (1989). Figure 1 shows that when the system temperature drops below the T_f, its k increases rapidly. The higher the T_f, the sooner the ice forms, and consequently the higher is the k of the system. We used the T-k curve to estimate the starting values for T_f.

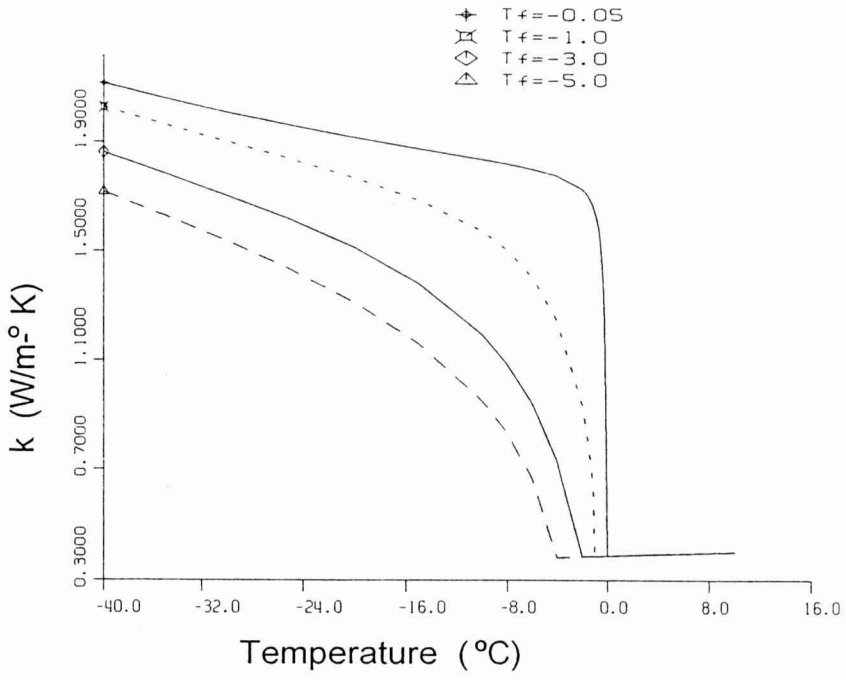

FIG. 1. CALCULATED k AS INFLUENCED BY T_f

Unfreezable Water. The effect of unfreezable water (b) on k is demonstrated in Fig. 2. This figure was derived by calculating Eq. (3), (5) and (6) at several values of b. As the b of the system increases, the slope of the T-k curve at the subfreezing temperatures decreases. Figure 2 shows that the difference between T-k curves with different values of b increases as the system temperature decreases; thus, if the b value is inaccurate, the error in the calculated k increases as the temperature decreases. The T-k curves were used to determine the starting values of b in the proposed procedure.

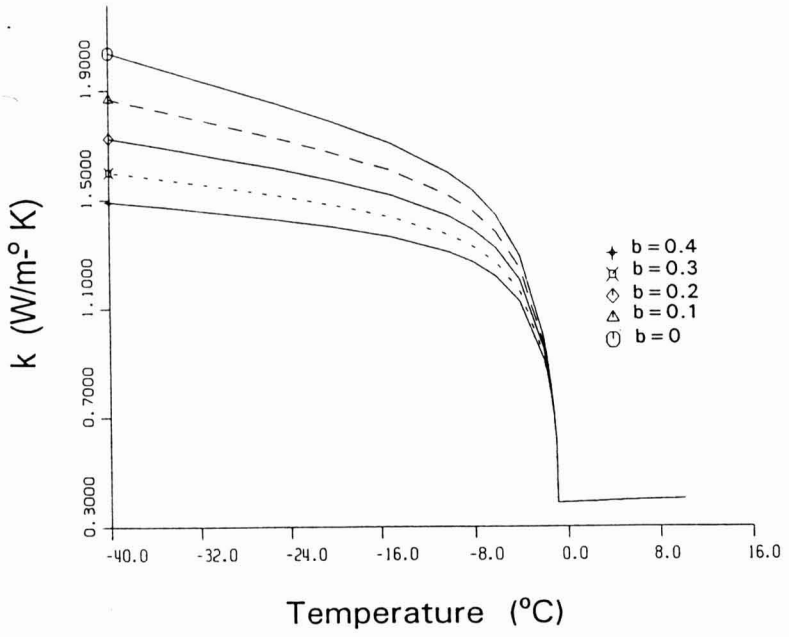

FIG. 2. EFFECT OF b ON THE k OF FROZEN FOODS

Food Composition. Published studies of food properties seldom include complete information on food composition. In this study, alternative sources for composition data were handbooks published by the U.S. Department of Agriculture (USDA) (Watt and Merrill 1975; Adams 1975). However, since the data on composition from these sources are not specific to the materials used in this study, they are referred to as the reference composition. Published data on food properties may be available for levels of moisture, protein, fat content, or other components ($X_{j,f}$) that differ from those in the reference composition ($X_{j,o}$). The weight fractions of the remaining components which are not given in the literature ($X_{m,f}$) were adjusted from their corresponding values in the reference composition ($X_{m,o}$) by the following equation:

$$X^{w}_{m,f} = \frac{X^{w}_{m,o}}{(1-\Sigma X^{w}_{j,o})}\left[1-\Sigma X^{w}_{j,f}\right] \tag{8}$$

For example, the reference composition of haddock is MC = 80.2% wb, proteins = 18.3%, fats = 0.1%, and ash = 1.4%. If a published study on the k of haddock uses materials with MC = 83.6% wb and fat = 0.08%, then their calculated protein and ash contents are 15.16 and 1.16%, respectively. Another importance of Eq. (8) is that the composition of foods at various MC levels can be determined even if proximate analysis is done at only one MC level.

The proximate analysis of materials used by Pham and Willix (1989) did not total 100% because of experimental errors. This was corrected by adjusting the MC so that the sum of the components was 100%, and the corrected proximate analysis was used as the reference composition.

Standard Error. To compare the predicted values ($\hat{k}_n$) to literature data (k_n) of thermal conductivity at various temperatures, we used the standard error (E) as a measure of fit. They were evaluated from the following equation (Choi 1985):

$$E = 100\left[\frac{\sum_{n=1}^{N}(k_n-\hat{k}_n)^2}{N}\right]^{1/2} \Bigg/ \left[\frac{\sum_{n=1}^{N}(K_n)}{N}\right] \tag{9}$$

In this study, E values $<10\%$ were considered acceptable.

Literature Data

Thermal conductivity data used in the study were obtained from the literature. Data were found for fresh lamb meat and offal, pork, veal, beef,

turkey, fish, and liquid foods in frozen states. Initial results of modeling in this study showed that the parallel-perpendicular model had unacceptably high standard errors when used in frozen liquids (i.e., 18% for sucrose solution, 20% for sugar solution and 12% for orange juice) and inconsistent results in frozen meats with fibers perpendicular to heat flow (i.e., 22% for pork and 6% for pork leg). The parallel-perpendicular model is inappropriate for frozen liquid foods since the solid phase (i.e., ice and fiber) is randomly arranged relative to the liquid phase, which is contradictory to the assumption of the parallel-perpendicular model. In the case of frozen meats with fiber perpendicular to the heat flow, the parallel-perpendicular model matches the physical configuration of the muscle and the spaces between them in which ice can form. However, there is insufficient data in the literature to evaluate the effectiveness of the model for these type of materials. Therefore, the food materials included in this study were limited to meat and fish with fibers parallel to the heat flow and those without specification of fiber orientation. Data on lamb meat and offal were generated from regression equations published by Pham and Willix (1989) (Table 3). Specific equations for various parts of lamb were chosen over the generalized equation because they provided more accurate values. Between -2.0 and 0C, the k values were calculated at an interval of 0.1C, since the T_f is most likely to fall within this range. Thirty-one data points were generated at T <0C. For other meats, the number of k data from the literature at freezing temperatures (N_{kf}) was limited, between 2 and 4 data points (Table 4). Data for meat other than lamb were those taken from Morley (1972), which he tabulated from several publications; those for fish were taken mostly from Jason and Long (1955). Pham (1990) suggested that at least two data points, both above and below the freezing point, were sufficient to make trend assessments.

TABLE 3.
CALCULATED VALUES OF T_f, b AND ω_e OF LAMB MEAT AND OFFALS
(THE k VALUES WERE CALCULATED FROM THE REGRESSION EQUATIONS OF PHAM AND WILLIX 1989)

	MC (% wb)	Fat (%)	b (sb)	T_f (°C)	ω_e	E (%)
Leg	73.6	4.8	0.40	-1.1	704	6.6
Leg, minced	73.9	4.9	0.40	-1.1	703	7.1
Hearts	69.8	13.0	0.40	-1.2	833	4.8
Hearts, minced	68.8	14.5	0.40	-1.1	972	2.5
Livers	68.9	7.1	0.40	-1.1	931	4.6
Livers, minced	67.7	4.5	0.40	-1.0	1097	3.5
Brains	79.0	8.3	0.40	-0.9	620	4.7
Kidneys	79.9	3.3	0.40	-0.9	560	4.3
Thymus	79.2	6.0	0.40	-0.8	714	4.9
Thymus, minced	75.9	9.1	0.30	-0.9	754	3.5

TABLE 4.
CALCULATED T_f, b AND ω_e OF VARIOUS MEAT PRODUCTS

	MC (% wb)	Fat (%)	N_{kf}	b (sb)	T_f (°C)	ω_e	E (%)	Ref.
Pork leg	75.1	7.8	4	0.27	-1.03	694	2.4	a
	72.0	6.1	3	0.20	-0.6	1048	0.8	b
Lamb leg	71.0	9.6	4	0.30	-1.2	710	6.2	a
Veal leg	75.0	2.1	4	0.25	-0.8	916	2.0	a
Beef, inside round	78.7	1.4	2	0.25	-1.6	420	2.2	a
	76.5	2.35	4	0.30	-1.8	383	4.6	a
Beef, sirloin	75.0	0.009	3	0.30	-0.9	785	2.6	b
Turkey breast	74.0	2.1	4	0.15	-1.2	586	0.8	c
Turkey leg	74.0	3.4	3	0.30	-1.3	540	1.3	b

a. Hill *et al.* 1967, as tabulated by Morley 1972.
b. Lentz 1961, as tabulated by Morley 1972.
c. Digitized from Lentz 1961.

A major problem in modeling studies that depend on literature data is assessing the accuracy of the models and data. In most cases, data for the same materials are an aggregate from several sources, causing possible test sample incompatibility. Moreover, since information on data precision is seldom reported, evaluation of predictive model accuracy is difficult with respect to the original data. This problem was also recognized by Heldman and Gorby (1975). In this study, most of the data on freezing and thermal properties were taken from different studies, except those taken from Pham and Willix (1989), which reported both k and freezing properties. Most literature data on unfreezable water and effective molecular weights were calculated from various mathematical models.

Calculation Scheme

The calculation procedure for initial freezing point, effective molecular weight, and unfreezable water combines both numerical and graphical techniques. Figure 3 illustrates the flow diagram of the proposed technique. The procedure is a numerical iteration in which k is calculated from assumed values of T_f and b; the calculation stops when the difference between the calculated and literature values of k is within a defined maximum limit. The data required are food composition and thermal conductivity values at both the freezing and nonfreezing temperatures. The k values at $T > T_f$ are used to establish visual trends for estimating the T_f and b.

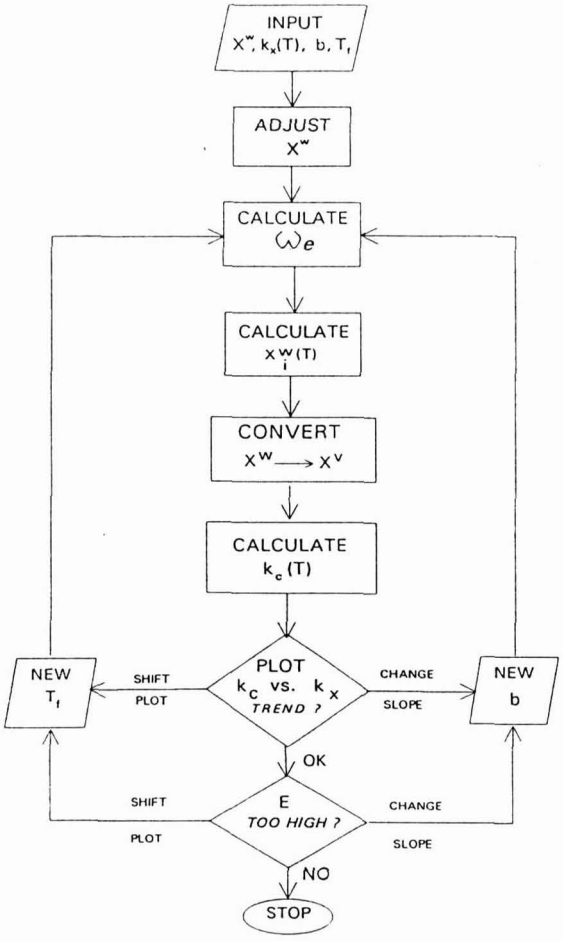

FIG. 3. FLOW DIAGRAM FOR CALCULATING ω_e, b, AND T_f.

The calculation is initiated by adjusting the reference composition to match the composition of the food material used in the published k data. The first values of T_f and b are visually estimated from the T-k curve. Then the effective molecular weight is evaluated from Eq. 1 and 3 by assuming that the amount of unfrozen water is equal to the initial moisture content. After the ice fraction is calculated at various temperatures, the k values as a function of temperature are calculated. The calculation is repeated with a new value of T_f until the optimum

value of T_f is found. The optimum value of T_f is determined by using an optimization procedure based on the observation that when the T_f is underestimated, the sum of the experimental k is greater than the sum of the calculated k, and when the T_f is overestimated, the calculated k values are higher than the experimental values. After the optimization, if the standard error between the calculated and literature k values is $< 10\%$, the calculation stops; otherwise, the calculation procedure restarts using new values of b and T_f, which are obtained graphically by comparing the T-k plots of the literature values and calculated values of k. The calculated k values are determined by using the latest values of b and T_f. If the calculated values of k are initially lower and cross those of the literature data, a higher value of unfreezable water is used. If the calculated T-k plot is always lower than the literature T-k, a lower value of T_f is chosen.

RESULTS AND DISCUSSION

Calculated Freezing Properties

Lamb. Tables 3-5 list the calculated ω_e, T_f and b of fresh lamb and offal, other assorted meats, and fish. The fat content of the products is given to allow calculation ω_e and b based on nonfat solids. For fresh lamb and offal, mincing did not affect b and T_f values, except for minced thymus, b = 0.3 (Table 3). The result that the calculated b value of minced thymus is lower than the thymus gland is consistent with the findings by Pham and Willix (1989). The ω_e of the minced products was higher than that of those not minced. The biggest difference was found in liver, where the ω_e increased by 17.9% after mincing. The fat content of the minced livers was almost half that of those not minced (see Food Composition section for calculation). Although their moisture content was almost identical, the measured protein content of the livers increased from 22.3 to 25.4% after mincing. Consequently, the minced livers may have more soluble proteins, and since proteins have high molecular weights, their presence increased the ω_e. The highest standard error among lamb meat and offal was 7.1%; the average error was 4.8%. In comparison, the general equation for lamb meat and offal developed by Pham and Willix (1989) had an error of $\pm$ 8%. Although their error may be calculated differently, the error comparison indicates that accuracy of the predicted k values in this study was within the range of the literature data.

Meat and Poultry. The b values for other meats ranged from 0.15 to 0.30 (Table 4). Turkey breast had the lowest b value at 0.15. The b values of pork legs and beef inside round increased with increasing fat content. The calculated T_f for assorted nondehydrated meats ranged from -0.6 to -1.3C, which is within the reported values for nondehydrated meat. The ω_e ranged from 383 to 1048.

Values for beef inside round, which has low fat content, were the lowest. The calculated b, T_f and ω_e values between the two samples of pork legs are different although their moisture contents are almost identical. The reason is the differences in their reported thermal conductivity values. For example, at -13.2C, Hill *et al.* (1967) and Morley (1972) reported that the thermal conductivity of pork leg is 1.42 W/m-K while Lentz (1961) and Morley (1972) reported that at -8.5C, it is 1.41 W/m-K. This can be attributed to the differences in either the fat contents of the sample or the accuracies in the published data. Nevertheless, it is found in this study that the standard errors for these two samples are low. Overall, the standard errors for the various types of meat products ranged from 0.8 to 6.2% (Table 4).

Fish. The unfreezable water in fish varies more than that in meat products, from 0.1 to 0.3 per solids basis (Table 5). Trout and catfish have the lowest value of unfreezable water; red fish has the highest. Therefore, in fish with high moisture content, e.g., red fish and haddock, a larger fraction of their water cannot be frozen. The calculated T_f and k for all fish are almost identical in spite of the wide differences in their moisture content. These values could be attributed to high moisture contents; the differences in the MC among fish were too small to influence the values of T_f and k. The standard error for all fish was between 1.9 and 2.7%.

TABLE 5.
PREDICTED T_f, b AND ω_e FOR VARIOUS FISH SAMPLES

	MC (%wb)	Fat (%)	N_{kf}	b (sb)	T_f (°C)	ω_e	E (%)	Ref.
Catfish	77.8	3.29	5	0.10	-0.8	693	2.4	a
Haddock	83.6	0.08	5	0.25	-0.7	517	2.7	a
Perch	79.1	0.90	5	0.15	-0.8	757	2.2	b
Red fish	84.7	0.80	5	0.30	-0.7	520	1.9	a
Trout	78.1	2.04	5	0.10	-0.8	703	2.4	a

a. Jason and Long 1955.
b. Lusk *et al.* 1964.

Comparison with Literature Values

Unfreezable Water. The proposed technique was validated by comparing the calculated ω_e, T_f, and b values to those reported in the literature (Tables 6-8). The ratio of calculated values to literature data indicates the accuracy of the proposed procedure. For unfreezable water, calculated values for fish and meat are within the range of the published values (Table 6). The calculated

TABLE 6.
COMPARISON BETWEEN THE CALCULATED AND LITERATURE VALUES OF b FOR VARIOUS MEAT AND FISH SAMPLES

	Calc.	Lit.	Calc./Lit.[a]	Ref.
Meat	0.2-0.3	0.143-0.36	1.0	TABLE 2
Fish	0.15-0.30	0.143-0.39	1.2	TABLE 2
Beef	0.25-0.30	0.219-0.318	1.0	TABLE 2
Lamb kidney	0.40	0.466	0.9	Pham 1987
Calf veal	0.25	0.29	0.9	Pham 1987
Haddock	0.25	0.143	1.7	Pham 1987
Perch	0.15	0.205	0.7	Pham 1987
Lamb Muscle	0.433-0.492	0.303-0.494[b]	1.2	Pham 1987
	0.3-0.4	0.144-0.31	1.5	Pham 1987; Pham and Willix 1989

[a] Based on median values.
[b] Calculated based on nonfat solids.

values for haddock and perch are not in agreement with those published by Pham (1987), which were calculated from enthalpy-temperature data. However, the b values calculated for these two fish species are within the generally recommended range for all fish and meat. For fresh lamb and offal, Pham and Willix (1989) recommended an unfreezable water of 0.4 based on protein content, in which the per solids equivalent would be lower than the calculated b values. Pham (1987) also suggested that the b value be calculated on the basis of nonfat solids, which actually bind the water in the system. This method can reduce incompatibility caused by difference in fat content. Using this method, Pham (1987) reported that the unfreezable water of lamb loin is between 0.303 and 0.494. In comparison, the calculated values for lamb leg in this study were between 0.433 and 0.492. Pham's (1987) lamb had fat contents of 11.7-9.4%, whereas the lamb legs used in this study had 4.8-9.6% fat.

Effective Molecular Weight. Table 7 compares the calculated and literature values of ω_e for various meats. In beef, the lower limit of the calculated values was lower than that of published values, whereas its upper limit was slightly higher. The ratio of calculated to published values is 0.8, and the difference in their medians is small. The worst ratio is 0.3 for lamb muscle, and the difference in their medians is 1660. The meats used in this comparison are the same as those used in the b comparison. Schwartzberg (1976) observed the same wide variations of the ω_e for various parts of lamb meat and calf veal and suggested that the ratio should be calculated by disregarding the fat content.

TABLE 7.
COMPARISON BETWEEN THE CALCULATED AND LITERATURE VALUES OF ω_e FOR VARIOUS FOOD MATERIALS

	Calc.	Lit.	Calc./Lit.[a]
Beef	383 - 785[b]	662 - 724[c,d]	0.8
Fish	517 - 757[e]	466 - 519[d,f]	1.3
Lamb muscle	703 - 710[g]	1023 - 3711[h,i]	0.3
	578 - 582[g,j]	684 - 1078[h,i,j]	0.7
Lamb kidney	560	416[i]	1.3
	474[j]	356[i,j]	1.3
Calf veal	916	1091[i]	0.8
	839[j]	878[i,j]	1.0

[a] Based on median.
[b] Sirloin and inside round, ave. MC=76.8% wb.
[c] Lean beef, MC=74% wb.
[d] Chen 1985.
[e] Catfish, Haddock, Perch, Red Fish & Trout.
[f] Cod.
[g] Lamb leg, fat=4.8%.
[h] Lamb loin, fat=11.7-39.4%.
[i] Schwartzberg 1976.
[j] Nonfat solids only.

When the effective molecular weights were recalculated on the basis of only nonfat solids, the ω_e ratio improved to 0.7 and the difference of their medians decreased to 301. In lamb kidneys, calculation of the ω_e from nonfat solids did not improve the comparison ratio, as the difference in the fat content among the products was very small (0.4%). In calf veal where the fat contents were 4.4 and 2.1%, the ω_e ratio improved to 1.0 when ω_e was calculated from nonfat solids.

Freezing Point. Table 8 compares the calculated and literature values of T_f. T_f values were calculated for materials that had an MC comparable to those used in the literature. The T_f were determined from the ω_e and b values calculated from this study (Table 8). Most of the literature data were evaluated from the equation of Chang and Tao (1981), the calculations of Chen (1985), Pham (1987), Succar and Hayakawa (1990), and the Mollier diagram of Riedel (Chen 1985). For nondehydrated materials, the biggest difference among the published values was < 0.2C, which was small for practical purposes. In general, the calculated freezing points were higher than those evaluated with Chang and Tao's (1981) equation but lower than published values. Haddock and cod, which have similar compositions, were compared at 82% wb. At the lower MC levels, haddock and the "lean fish meat" of Succar and Hayakawa (1990) were compared. The calculated freezing points of haddock were within the range of published values of the respective fish. In beef, the calculated values for sirloin

TABLE 8.
COMPARISON BETWEEN THE CALCULATED AND LITERATURE VALUES OF T_f FOR VARIOUS MEAT AND FISH PRODUCTS

	MC (% wb)	Calc. (°C)	Literature	Calc./Lit.
Fish	82.0	-0.83[a]	0.87[b,c], 0.9[b,d],-0.7[e],-0.8[f]	0.92-1.17
	75.0	-1.23	-0.82[e], -1.0[f],-1.29[g]	0.95-1.5
	66.0	-1.98	-1.95[f],-1.96[g]	1.0
Lean beef	80.0	0.64[h]	0.73[i],-0.74[e]	0.86-0.88
	74.0	-0.92[h]	1.0[d,j],-0.98[c,j]-1.0[i,j],-0.83[e]	0.92-1.11
	70.0	-1.19	-1.01[f],-1.20[g]	1.0-1.18
	63.0	-1.72	-1.63[g],-1.76[f]	0.98-1.06
	50.0	-3.24[h]	-2.6[c,j],-2.8[d,j],-3.6[i,j]	0.9-1.25
Calf veal	77.5	-0.63	-0.68[i],-0.78[e]	0.81-0.93
Haddock	83.6	-0.73	-0.89[i],0.69[e]	0.82-1.1
Perch	79.1	-0.68	-0.86[i],-0.76[e]	0.79-0.9

[a] Reference material is haddock, MC=83.6% wb.
[b] Cod.
[c] Chen 1985.
[d] Mollier Chart of Riedel as reported by Chen 1985.
[e] Chang & Tao (1981).
[f] Succar & Hayakawa (1990).
[g] Calc. by Succar & Hayakawa (1990) using Chen's (1985) procedure.
[h] Reference sample is beef sirloin, MC=75% wb and fat=0.9%.
[i] Pham 1987.
[j] Lean beef.

were compared with published values for lean beef. Except for beef at MC = 50% wb, the T_f values found in this study were close to those reported in the literature. Although the ω_e and b of beef and fish were evaluated at high MC, the calculated T_f for dried products is still within the reported values. For beef at 50% wb, the result is inconclusive because the reported values differ by 1.0C.

Sensitivity Analysis

Because ω_e is calculated from T_f and b, their influence on its value is important. A sensitivity analysis was done for three representative foods. Beef sirloin represented lean beef, haddock represented all fish, and lamb liver represented all non-muscle materials (Table 9). Results indicated that regardless of food type, the effect of T_f on the calculated ω_e was more than that of b. Moreover, the magnitude of influence of each parameter was not affected by material type. The average change in ω_e per unit change of b is $\pm$ 300, whereas for every 1.0C change of T_f ω_e changed by $\pm$ 1300. Because the accuracy of most temperature transducers is $\pm$ 0.5C, the calculated ω_e can vary by $\pm$ 650 due to error in temperature. Therefore, since the differences among the ω_e

values listed in Tables 4-6 are within this limit of error, it can be concluded that the calculated ω_e for fresh lamb and offal, and assorted meat and fish are not significantly different from one another.

TABLE 9.
SENSITIVITY ANALYSIS OF THE ω_e AND E AS AFFECTED BY T_f AND b

			$[E/E_o]$			
	$[\Delta\omega_e/\Delta T_f]^a$	$[\Delta\omega_e/\Delta b]^b$	$(T_f-0.5)$	$(T_f+0.5)$	(b-0.15)	(b+0.15)
Beef sirloin	1229	283	3.6	3.8	2.8	2.2
Haddock	1597	113	3.2	3.1	3.0	2.0
Lamb liver	1066	510	4.0	2.5	2.1	1.6

[a] Calculated at $\pm$ 0.5C of the tabulated T_f in Tables 4-6.
[b] Calculated at $\pm$ 0.15 of the tabulated b in Tables 4-6.

The effect of the accuracy of T_f and b on the standard error (E) of the calculated k was also analyzed (Table 9). E values were calculated for T_f values $\pm$ 0.5C and b values $\pm$ 0.15 of the values listed in Tables 3-5. These E values were then divided with the respective E values (E_o) for the tabulated values of b and T_f. On the average, a $\pm$ 0.5C error in the T_f value can cause E values to increase by 3.4 times, whereas an error of $\pm$ 0.15 in b can result in an increase in standard error of 2.3 times. Thus, an error of $\pm$ 0.5C in T_f is equivalent to $\pm$ 0.22 error in b. Since the average E of all the materials in Tables 3-5 is $<4\%$ and the accuracy of thermocouples is typically $\pm$ 0.5C, the tolerable E for k modeling can be as high as 14%. This finding indicates that all the predicted values in this study (Tables 3-5) are within an acceptable limit.

CONCLUSIONS

Based on the findings in this study, the following conclusions are drawn:

(1) The proposed calculation procedure for effective molecular weights, unfreezable water, and initial freezing point from thermal conductivity and food composition produces acceptable results ($E < 10\%$). The accuracy of this procedure depends largely on the accuracy of the thermal conductivity data.

(2) For a group of foods with large differences in fat content, the ratio of calculated values to literature values improved (closer to 1.0) when unfreezable water and effective molecular weight were calculated from nonfat solids. The ratio did not improve when variation of fat content of different foods in the group was small.

(3) Because standard errors for the foods studied were $< 10\%$, the parallel-perpendicular model is an adequate structural model for predicting the thermal conductivity of frozen meat with fibers that are parallel to heat flow.

(4) The calculated effective molecular weights of fresh lamb and offal, assorted meats, and fish are not significantly different from one another.

(5) Considering the accuracy of thermocouples, standard errors of up to 14% may be acceptable for thermal conductivity models for frozen foods.

NOMENCLATURE

b	Unfreezable water or bound water, based on fraction of solids (sb)
E	Standard error based on k values (%)
k	Thermal conductivity (W/m-°K)
k_n $\hat{k}_n$	Literature and calculated values of k at various temperature levels, respectively
L_f	Latent heat of fusion (333.8 m^3-Pa)
MC	Moisture content (% wet basis or % wb)
N, N_{kf}	Total number and N of k data at $T < T_f$
R	Universal gas constant (8.314 m^3-Pa/g-mole-°K)
T	Temperature
T_f, T_w	Initial freezing point (°C or °K) and freezing point of pure water (273.15°K)
X_a	Mole fraction of unfrozen water
X^w, X^v	Weight and volume fractions, respectively (decimal or %)
$X_{j,f}$	Values of certain food component of the material used in the measurement of thermal and freezing properties
$X_{j,o}$	Corresponding reference values of the $X_{j,f}$ components
$X_{m,f}$	Calculated values of the non $X_{j,f}$ components
$X_{m,o}$	Reference values of the non $X_{j,f}$ components
ω, ω_w	Molecular weight and molecular weight of water (18)
ρ	Density (kg/m^3)

Subscripts

c	Calculated
ds	Dissolved solids
e	Effective
I	ice
l	Liquid
n	Dummy
p	Protein
uf	Unfrozen water
s	solids or solutes
w	Water
o	Optimum
x	Experimental or literature

REFERENCES

ADAMS, C.A. 1975. *Nutritive Value of American Foods in Common Units.* Agriculture Handbook No. 456. Agricultural Research Service, U.S. Department of Agriculture, Washington, DC.

BARTLETT, L.H. 1944. A thermodynamic examination of the latent heat of food. Refrig. Eng. *47*, 377.

CHANG, H.D. and TAO, L.C. 1981. Correlation of enthalpies of food systems. J. Food Sci. *46*, 1493–1497.

CHEN, C.S. 1985. Thermodynamic analysis of freezing and thawing of foods: Ice content and Mollier diagram. J. Food Sci. *50*, 1163–1166.

CHOI, Y.H. 1985. Food thermal property prediction as affected by temperature and composition. Ph.D. Dissertation, Purdue University, W. Lafayette, IN.

DUCKWORTH, R.B. 1971. Differential thermal analysis of frozen food systems: the determination of unfreezable water. J. Food Technol. *6*, 317–327.

HELDMAN, D.R. 1974. Predicting the relationship between unfrozen water fraction and temperature during food freezing using freezing point prediction. Trans. ASAE *17*(1), 63–66.

HELDMAN, D.R. and GORBY, D.P. 1975. Prediction of thermal conductivity in frozen foods. Trans. ASAE *18*, 740–744.

HILL, J.E., Jr., LEITMAN, J.D. and SUNDERLAND, J.E. 1967. Thermal conductivity of various meats. Food Technol. *21*, 1143–1148.

JASON, A.C. and LONG, R.A.K. 1955. The specific heat and thermal conductivity of fish muscle. Proceedings of the International Congress on Refrigeration, 9th Congress *2*, 160.

LENTZ, C.P. 1961. Thermal conductivity of meats, fats, gelatin gels and ice. Food Techno. *15*, 243–247.

LUSK, G., KAREL, M. and GOLDBLITH, S.A. 1964. Thermal conductivity of some freeze-dried fish. Food Technol. *18* (10), 1625–1628.

MORLEY, M.J. 1972. Thermal properties of meat: tabulated data. Meat Research Institute Special Report No. 1. Meat Research Institute, Langford, Bristol, UK.

MURAKAMI, E.G. and OKOS, M.R. 1988. Modelling of thermal conductivity of nonporous foods. ASAE Paper No. 88-6579.

PHAM, Q.T. 1987. Calculation of bound water in food. J. Food Sci. *52*, 210–212.

PHAM, Q.T. 1990. Prediction of thermal conductivity of meats and other animal products from composition data. In *Engineering and Food*, Vol. 1, (W. Spiess and H. Schubert, eds.) pp. 408–423, Elsevier, New York.

PHAM, Q.T. and WILLIX, J. 1989. Thermal conductivity of fresh lamb meat, offals and fat in the range -40 to +30C: Measurements and correlations. J. Food Sci. *54*, 508–515.

SCHWARTZBERG, H.G. 1976. Effective heat capacities for the freezing and thawing of food. J. Food Sci. *41*, 152–156.

SUCCAR, J. and HAYAKAWA, K. 1990. A method to determine initial freezing point of foods. J. Food Sci. *55*, 1711–1713.

WATT, B.K. and MERRILL, A.L. 1975. *Composition of Foods: Raw, Processed, and Prepared*. Agricultural Handbook No. 8. Agricultural Research Service, U.S. Department of Agriculture, Washington, DC.

APPLICATION OF ARTIFICIAL NEURAL NETWORKS TO INVESTIGATE THE DRYING OF COOKED RICE

M.N. RAMESH[1], M.A. KUMAR and P.N.SRINIVASA RAO

Central Food Technological Research Institute
Mysore, India - 570 013

Accepted for Publication August 21, 1995

ABSTRACT

Commercially available neural networks software was applied for prediction of processing parameters with reference to the product quality of the dehydrated cooked rice. These results were verified with experimental data. The experimental results indicate good concurrence with the predicted data. A small capacity vibrofluidized bed drier was used to conduct the experimental studies. The inlet air temperature of 160C to 180C, the inlet air velocity of 3 to 6 ms $^{-1}$ and the resident time of 5 to 8 min were used in the study. The optimized process parameters were identified. The operation of the neural network model is discussed. The trained model can be applied in a nonlinear model predictive scheme to control the product moisture content.

INTRODUCTION

Convenience foods are one of the latest developments in food processing. Ready to serve products need special characteristics such as quick rehydration, simulated properties similar to original products and preservation of quality parameters.

Dehydrated cooked rice has been marketed widely in many places. The characteristics of dried cooked rice depend mainly on the drying process. Being sticky, it is absolutely essential that mobility has to be incorporated during the preliminary stages of drying. Combined vibratory motion for particle movement and intimate contact with hot air are the specific advantages of the vibrofluidized bed drier. A few of the drying processes in the fluidized bed-drying of grains are reported (Prasad *et al.* 1994; Uckan and Ulku 1986; Giner and Calvelo 1987). But their application in drying of cooked rice has not been reported much in the literature. The study of drying characteristics is essential for the follow up studies and process development. An efficient approach to co-relating the

[1]To whom correspondence should be addressed.

Journal of Food Process Engineering **19** (1996) 321–329. *All Rights Reserved.*

input and output parameters in the study of the drying characteristics is the modelling of the process.

Currently applied techniques for modelling the drying process involve a large number of mathematical equations and thermal properties of the food material being dried. The basic equations are developed to describe the process of simultaneous heat and mass transfer (Kamlan *et al.* 1994; Uckan and Ulku 1986; Thomas and Verma 1992; Palancz 1983). Also, the thermal properties are interdependent and are not accurate. Values for most of the food products are not available. As the moisture content varies during the process of drying these properties vary. Most of the time the application of these models for the prediction of drying parameters is very difficult as it involves the solution of differential equations. The transport of water in food materials is difficult to describe mathematically (Bruin and Luyben 1980).

Recently Artificial Neural Networks (ANN) were used to solve a wide variety of problems in science and engineering. A review of the applications has been cited by Guptha and Narsimhan (1993) and Lee and Chen (1993). A well trained ANN model is a built-in predictive model for the specific application. Unlike other modelling techniques such as simultaneous heat and mass transfer, kinetic models, diffusion model, phase model and regression analysis, an ANN can accommodate more than two variables to predict two or more output parameters. ANN differ from conventional programs in their ability to learn about the system to be modelled without a need of any apriori knowledge on the relationships of the process variables (Linko *et al.* 1993). In the present study ANN is applied in the area of drying of food products with special reference to the prediction of drying parameters of cooked rice with its rehydration properties in view.

The Neuroshell™ Version 4.0 supplied by Ward Systems Group Inc. (228 W. Patrick Street, Fredrick, Maryland 21701, USA) has been used in this study. The ANN model consists of three layers, one input layer, one hidden layer and one output layer. The hidden layer contains four neurons.

EXPERIMENTAL SET UP

The experimental set up (Fig. 1) consisted of a drying chamber (1), a plenum chamber (2), a blower (3), an electrical heating unit (4) and a temperature controller. The dimensions of the drying chamber were 0.5 m long × 0.15 m wide × 0.15 m high. The plenum chamber had a similar dimension with an entry for air at the center. The drying chamber and the plenum chamber were connected with a perforated sheet. The dryer had an inlet chute to feed the material to be dried and an outlet chute to collect the dried material. A weir was provided within the drying chamber to restrict the flow of the product and to control the residence time of drying.

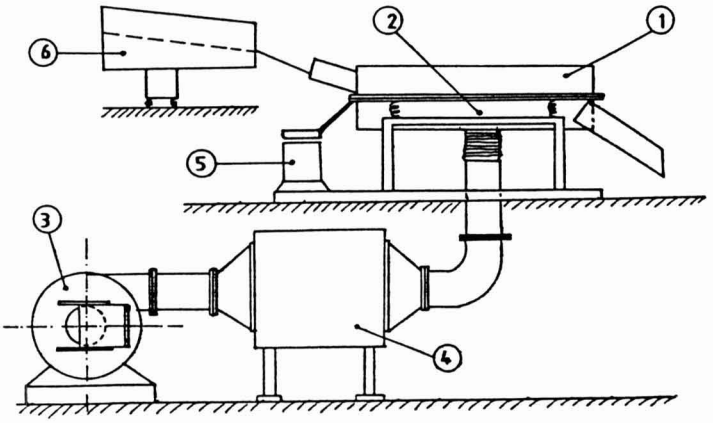

FIG. 1. EXPERIMENTAL SETUP
(1) Drying Chamber
(2) Pleanum Chamber
(3) Blower
(4) Electrical Heating Unit
(5) Electromechanical Vibrating Unit
(6) Vibratory Feeder

The inlet air velocity was controlled by a sliding door at the blower inlet. The air heating unit between the plenum chamber and the blower consisted of 30 heating elements of 2 kw each with individual switches to control the inlet air temperature. A thermostat was used to control the temperature to an accuracy of $\pm$ 3C. The temperature was measured before feeding the material using a mercury in glass thermometer.

MATERIALS AND METHODS

The 250 g of cleaned and graded SONA MASURI, a high amylose variety rice was washed thoroughly to remove dust particles and adhering bran and soaked in cold water for 25 to 30 min to an equilibrium moisture content of 30% wet basis (Indudhara Swamy *et al.* 1971). Soaked rice was steamed for 15-18 min in an autoclave without pressure to completely gelatinize it. The moisture content after cooking was 75 $\pm$ 2 % wb. It was washed and soaked in cold water for 15-20 min to arrest further cooking and to remove the starch adhering to the surface. Excess water was drained by pouring the contents over

a mesh. The total cooked rice was 850 $\pm$ 25 g. After the dryer was brought to steady state conditions of required inlet temperature and air velocity the cooked rice was fed into the dryer. The material was dried for a specific period of time to control the residence time. The experiment was repeated for various parameter settings of inlet air temperature, air velocity and residence time.

The main attribute applied to evaluate the product obtained with different drying parameters is the rehydration characteristic. The dehydrated rice was reconstituted by adding boiling water of 1:5 ratio. After 5 min of soaking, the excess water was drained and the surface moisture was removed by gently pressing the rice grains in between filter papers. The moisture pick up was determined by oven method at 110C for 8 h.

The observation revealed that at high temperatures of above 180C the dehydrated cooked rice became brownish, possibly due to polyphenol oxidase (Kim *et al.* 1986). At temperatures below 160C the drying took longer periods of time leading to poor rehydration characteristics. The inlet air velocities of less than 3 ms^{-1} did not fluidize the cooked rice. The residence time of less than 5 min caused incomplete drying. The inlet conditions were varied over a wide range. Since the final product was not acceptable, they are not reported.

During rehydration, it was observed that all the water added for rehydration (ratio of 1:5) was absorbed and there was no hard core. These properties were similar to that of a commercially available product. It was also observed that as the rehydration time increased, the moisture pick up also increased. But to compare the sample with the commercial product, the same rehydration time of 5 minutes was used. With lower water ratio of 1:2 the rice did not rehydrate completely. Hence, the water ratio was increased to 1:5.

RESULTS AND DISCUSSION

A three-layer perceptron model consists of one input layer, one hidden layer and one output layer. The nodes in the input layer transmit the input fed to them, and the number of nodes is equal to the number of input variables. The number of output nodes is decided by the type of predictions required of the model. The number of hidden layer nodes depends on the type of input, such as whether the decisions are linearly separable, convex or nonconvex (Guptha and Narsimhan 1993).

To train an ANN model, a set of input patterns with known or desired outputs were fed in succession. The values of the input and output parameters required for training the network were determined by experimentation as described above. These values are given in Table 1. The three input nodes were inlet air temperature in °C, inlet air velocity in ms^{-1} and residence time of cooked rice in the drier in minutes. The output node was the moisture content attained after 5 min of rehydration in boiling water.

TABLE 1.
VALUES OF PARAMETERS PROVIDED FOR LEARNING (ACTUAL VALUES)

Case No.	Inlet Air Temp °C	Air Velocity ms^{-1}	Residence time (min)	Rehydration Moisture Content (% wb)[a]
1	172.5	6.20	7	58.1
2	167.5	6.05	6	63.3
3	162.5	6.05	8	67.6
4	172.5	4.25	6	70.0
5	172.5	4.25	8	68.0

[a] Rehydration time of 5 mins in boiling water with rice water ratio of 1:5

On completion of learning, the NNM is capable of reproducing the correct output when any input similar to the pattern it has learned is presented. As the first layer passes its values to the second layer and the second layer to the third layer, the values are weighed to represent connection strengths. To positively influence a connection, the weights are raised. To negatively influence a connection, the weights are lowered. This adjustment of weights is done iteratively until a desired output pattern is closely attained. The back propagation method is applied for this iterative process (Rumelhart *et al.* 1986). The network connection weights are shown in the Fig. 2.

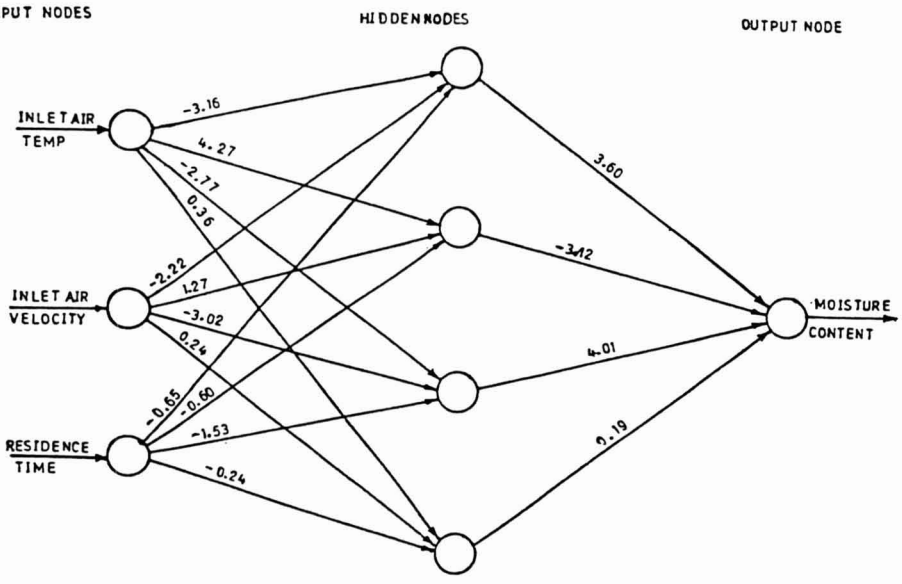

FIG. 2. NETWORK CONNECTION WEIGHTS

The actual experimental values and predicted values of moisture content after the learning process are given in Table 2 and have been plotted in Fig. 3.

TABLE 2.
ACTUAL AND PREDICTED VALUES OF REHYDRATION MOISTURE CONTENT (% wb)

Case No.	Inlet Air Temp. °C	Air velocity ms^{-1}	Residence Time min	Predicted Values	Actual Values
1	170.0	3	5	75.60	74.30
2	170.0	3	6	74.30	73.50
3	175.0	3	5	75.70	75.00
4	180.0	3	5	76.00	76.00
5	170.0	4	6	73.74	73.60
6	187.5	3	6	63.52	62.50
7	175.0	5	5	63.12	62.00
8	187.5	5	6	54.86	53.00

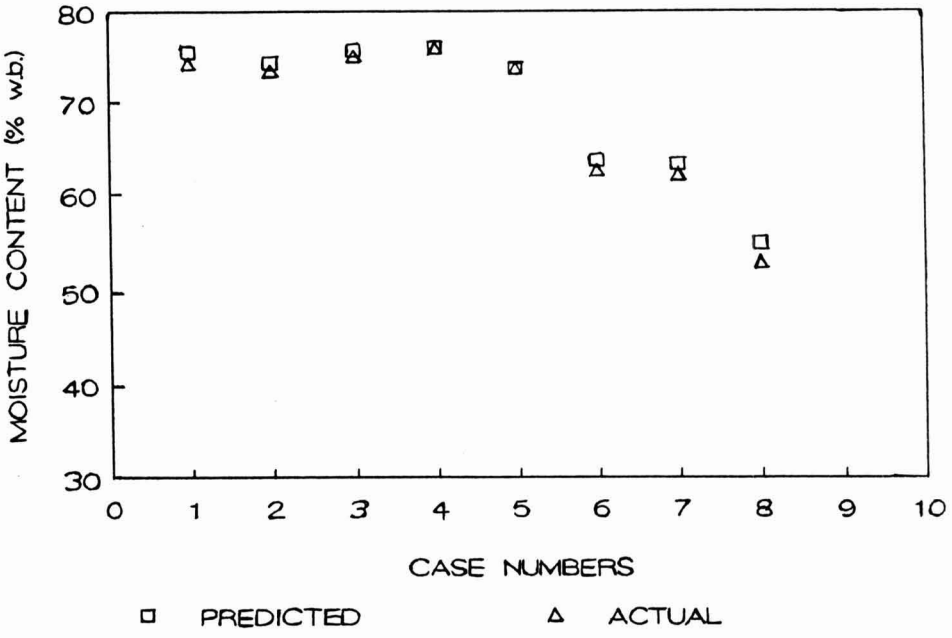

FIG. 3. PREDICTED AND ACTUAL MOISTURE CONTENT

From the table it can be concluded that higher temperature with a maximum limit of 180C, lower air velocity with a minimum fluidization velocity and lower

residence time of not less than 5 min leads to higher rehydration moisture content. This high temperature-short time process causes moisture to be removed from the surface of the cooked rice at a rate which is sufficiently faster than the diffusion of moisture from the interior of the grain to the surface. These conditions set the grains in their enlarged expanded size without shrinkage, and give a porous structure for rapid rehydration (Daniels 1970).

From the graph of predicted versus actual rehydration moisture content (Fig. 3) it is clear that the predictions are close to the actual experimental values. The slight deviations may be due to the 3 different parameters involved in each case. The deviations can still be reduced by providing more sets during the training/learning phase.

CONCLUSION

An artificial neural network model has been used in this work to predict the moisture content attained after rehydrating dried cooked rice. Generally, promising results have been obtained by using the trained artificial neural network model as an alternative tool for the prediction of the drying parameters. The investigation indicates that the predictions from the model are close to the actual values. Hence a simple, rapid method of predicting the desired outputs by a few initial experiments can be developed by Neural Networks. Tedious methods can be avoided when only desired outputs are required within a short time. This model can also be used to develop process control for the complete drying system. As a further study this model can be developed to provide on-line adaptation to changing process conditions (Linko *et al.* 1993). The most significant advantage is that the process parameters can be optimized to get the best set of parameters to obtain the targeted output values of rehydration moisture content. Thus, it has been shown that Artificial Neural Network is a potential tool to develop a built-in model for determining the process parameters especially when the existing models cannot accommodate more than two process variables.

Finally, the optimized parameters of the batch drying process with respect to the maximum rehydrated moisture content of 76% w.b were standardized as below. The rehydration moisture content of dehydrated rice should be as close as possible to that prepared conventionally, which will be 75 $\pm$ 2% wb moisture (Battacharya and Sowbhagya 1971).

Inlet air temperature - 180C
Inlet air velocity - Minimum fluidization velocity (3 m/s)
Residence time - 5 min

ACKNOWLEDGMENTS

The authors wish to thank Mr. A Ramesh, Head PEPD, Dr. M. S. Thakur and Mr. Y.M. Indhudara Swamy for their encouragement.

APPENDIX

Definition and brief explanation of basic terminologies:

Perceptron: Please refer to Fig. 2. Each circle represents a single node (neuron), having inputs and outputs. Each input 'x' is multiplied by a weight 'w' and sums the weighted inputs. Such systems are called perceptrons.

Linearly separable: Any function which can be represented by means of a single layered network are termed as linearly separable. This is applicable to simple logics with direct applications. Linear separability limits single-layer networks to classification problems.

Convex and nonconvex: If the solution set of the problem under investigation is within a defined boundary and is convergent, then it is said to be convex or a closed system. If it is non-convergent and has no defined boundaries, it is said to be nonconvex, or an open system.

REFERENCES

BATTACHARYA, K.R. and SOWBHAGYA, C.M. 1971. Water uptake by rice during cooking. Cer. Sci. Today, *16* (12), 420–423.

BRUIN, S. and LUYBEN, K.ch.A.M. 1980. Drying of food materials - A review of recent development. In *Advances in Drying*, Vol. 1, (A.S. Mujumdar, ed.) pp. 169, 175, 179. Hemisphere Pub. Co., Washington.

DANIELS, R. 1970. Quick cooking rice. In *Rice and Bulgar Quick Cooking Process*, pp. 75, Noyes Data Corp., Park Ridge, New Jersey.

GINER, S.A and CALVELO, A. 1987. Modelling of wheat drying in fluidized beds. J. Food Sci. *52*(5), 1358–1363.

GUPTHA, G. and NARSIMHAN, S. 1993. Application of neural network for gross error detection. Ind. Eng. Chem. Res. *32*, 165–170.

INDUDHARA SWAMY, Y.M, ALI, S.Z and BATTACHARYA, K.R. 1971. Hydration of raw and parboiled rice and paddy at room temperature. J. Food. Sci. and Tech. *8*(1), 20-22.

KANNAN, C.S., SUBBA RAO, S. and VARMA, Y.B.G. 1994. A kinetic model for drying of solids in batch fluidized beds. Ind. Eng. Chem. *33*, 363–370.

KIM, H.I. and SEIB, P.A. 1986. Milling hard red winter wheat to farina, Comparison of cooking quality and colour of farina and semolina spaghetti. Cer. Food World, *31* (11), 810–819.

LEE, M.-J. and CHEN, J.-T. 1993. Fluid property predictions with the aid of neural networks. Ind. Eng. Chem. Res. *32*, 995-999.

LINKO, P., UEMURA, K. and EERIKAINEN, T. 1993. Neural networks in fuzzy extrusion control. In ICHEME symposium series No. 126, pp. 401-410.

PALANCZ, B. 1983. A mathematical model for continuous fluidized bed drying. Chem. Eng. Sci. *38*(7), 1045–1059.

PRASAD, B.V.S., CHANDRA, P.K. and BAL, S. 1994. Drying parboiled rough rice in stationary, semi-fluidized and fluidized conditions, Trans ASAE. *37* (2), 589-594.

RUMELHART, D.E., HINTON, G.E. and WILLIAMS, R.J. 1986. Learning representations by back-propagating errors. Nature *323*, 533–540.

THOMAS, P.P. and VARMA, Y.B.G. 1992. Fluidized bed drying of granulated food materials. Powder Technol. *69*, 213–222.

UCKAN, G. and ULKU, S. 1986. Drying of corn grains in a batch fluidized bed drier. In *Drying of Solids: Recent Developments* (A.S. Mujumdar, ed.) pp. 91–96, Wiley, New York.

RHEOLOGICAL CHARACTERIZATION OF COFFEE MUCILAGE

CARLOS E. OLIVEROS

Researcher, CENICAFE, Colombia

and

SUNDARAM GUNASEKARAN[1]

Professor
Biological Systems Engineering Department
460 Henry Mall
University of Wisconsin
Madison, WI 53706

Accepted for Publication April 16, 1995

ABSTRACT

Rheological behavior of mucilage obtained from two varieties of coffee grown in Colombia (Caturra and Colombia) was studied as a function of ripe cherry content (RCC) and postharvest time (PHT). A Brookfield HB DV-III viscometer was used in concentric cylinder geometry over a shear rate range of 4.8 to 120 s^{-1}. The power-law model was used to describe the shear stress versus shear rate data, and the consistency index (K) and flow behavior index (n) were determined. The mucilage is a highly viscous and pseudoplastic ($n < 0.3$) fluid. The K increased and n decreased as the RCC and PHT increased. The mucilage of the Caturra variety was more viscous and shear thinning than that of the Colombia variety. Microstructural examination of the mucilage revealed that certain weak structures as phloem vessels found in the mucilage may be destroyed upon application of shear stress and may contribute to the pseudoplastic nature of the mucilage. Diffusion of tannin from the pulp to mucilage with delay in postharvest processing may be responsible for increased apparent viscosity with increased PHT.

INTRODUCTION

Postharvest processing of coffee (*Coffea arabica*) in Colombia involves depulping, fermenting, washing and drying. The fermentation step facilitates the

[1] Address for correspondence.

Journal of Food Process Engineering **19** (1996) 331–342.

removal of mucilage during washing. Coffee mucilage or mesocarp is a thin layer (about 0.4 mm) contained between the pulp (epidermis) and coffee parchment (Fig. 1). The coffee embryo is embedded in the mucilage (Dentan 1985). The mucilage is rich in pectin and sugars and represents 17% by mass of the whole coffee cherries (Carbonell and Vilanova 1952; Coste 1959). Most quality defects of coffee are attributed to inadequate control during fermenting and drying. These conventional postharvest operations account for about 10% of the total cost of coffee production in Colombia (Junguito 1978). Additional economical losses are due to uncontrolled fermenting. Thus, alternate postharvest processes have been under investigation for several years.

The CENICAFE (Centro Nacional de Investigaciones de Café) in Colombia has developed a mechanical demucilaging process with favorable results in terms of quality and cost (Oliveros 1993). In addition, water required to wash off the mucilage is also significantly reduced. Mechanical detachment of mucilage is obtained by shearing forces applied on the beans using a rotating cylinder with fingers within a cylindrical chamber. Coffee variety, degree of cherry ripeness and postharvest time, the time elapsed between harvesting and depulping, are known to affect efficiency of mechanical removal of mucilage.

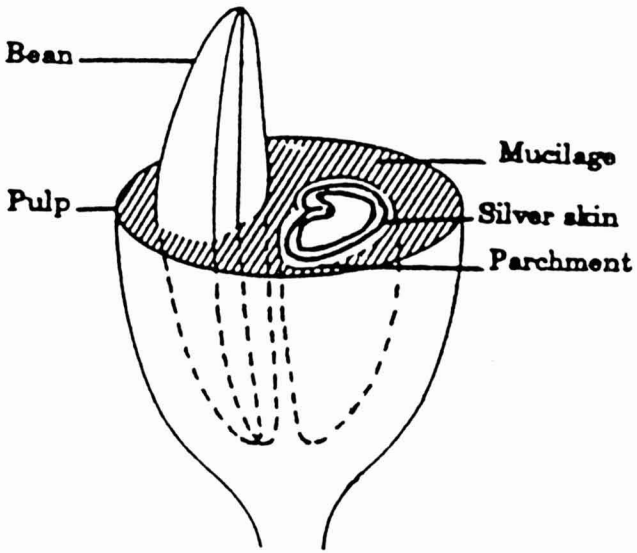

FIG. 1. CROSS SECTION OF A COFFEE CHERRY

Information on the rheological properties of coffee mucilage is required for proper design and analysis of a mechanical remover. However, such information is not available in the literature. Therefore, experiments were conducted to characterize the rheological behavior of coffee mucilage. Specific objectives of the investigation were to determine: (1) the viscosity of the mucilage and the power-law parameters, consistency index (K) and flow behavior index (n) as a function of the ripe cherry content (RCC) and postharvest time (PHT); and (2) the microstructural changes occurring when shear stresses are applied to the mucilage.

Rheology of Non-Newtonian Fluids

For Newtonian fluids, the shear stress and (σ) and shear rate ($\dot{\gamma}$) are linearly related, i.e.,

$$\sigma = \eta\dot{\gamma} \tag{1}$$

where η is the fluid viscosity. However, most biological fluids are non-Newtonian and do not obey the behavior described by Eq. 1. The shear stress is shear-rate dependent and, in several cases, time dependent (Cheng and Evans 1965, Tiu and Boger 1974; Rao 1977). In addition, rheological behavior of biological material is also influenced by biomass concentration (Tanglertpaibulb and Rao 1987; Allen and Robinson 1990; Manohar *et al.* 1990). Therefore, more complex models are required. The Herschel-Bulkley and Casson's models are extensively used to fit σ and $\dot{\gamma}$ data (Rao 1977).

Herschel-Bulkley Model:

$$\sigma = \sigma_y + K\dot{\gamma}^n \tag{2}$$

Casson's Model:

$$\sigma_y = \sigma_y^{1/2} + Kc\dot{\gamma}^{1/2} \tag{3}$$

where: σ_y = yield stress
K = consistency index
n = flow behavior index
K_c = Casson's constant.

For fluids exhibiting low yield stress a power-law model is used. The power-law model can be considered a special case of the Herschel-Bulkley model.

Power-law model:

$$\sigma = K\dot{\gamma}^n \tag{4}$$

Based on the magnitude of n and σ_y fluids can be grouped as: Newtonian ($n = 0$, $\sigma_y = 0$); Bingham ($n = 0$, $\sigma_y > 0$); pseudoplastic ($0 < n < 1$, $\sigma_y = 0$); Bingham-pseudoplastic ($0 < n < 1$, $\sigma_y > 0$); and dilatant ($n > 1$, $\sigma_y = 0$). For power-law fluids, an apparent viscosity (η_a) is reported.

$$\eta_a = K\dot{\gamma}^{n-1} \tag{5}$$

Fluids composed of high molecular weight substances such as mucilage exhibit non-Newtonian behavior (Rao 1977). They behave in a more complex manner while mixing than Newtonian fluids (Hoogendorn and Den Hartog 1967). Microstructural observations have been used to understand the rheological behavior of fluids (Metzner 1985; Goto *et al.* 1986; Jiménez *et al.* 1989; Arnfield and Murray 1992). Thixotropic behavior and decrease in the non-Newtonian behavior in fresh pulped tomato was found associated with destruction of its structure (Jiménez 1989). High correlation between dynamic rheological properties such as modulus, loss tangent, and storage modulus and the development of crosslinked network in proteins have been observed (Arnfield and Murray 1992). Effect of shape and elastic properties of particles suspended in Newtonian and polymeric fluids have been found associated with flow behavior (Goto *et al.* 1986). From these the importance of microstructural observations in analyzing the rheological behavior of fluids, mainly suspensions, is evident.

MATERIALS AND METHODS

Fresh coffee cherries were obtained and subjected to hydraulic classification in order to eliminate light materials. The cherries were visually inspected and classified into three degrees of ripeness: overripe, ripe, and unripe. Then two samples with different ripe cherry content (RCC) were prepared: (1) 100% ripe cherries, (2) 70% ripe and 30% unripe and overripe cherries. The second sample with 30% unripe and overripe cherries simulated actual field-harvested cherries having varying degrees of ripeness. The above procedure was performed for two levels of postharvest time (PHT): three and six hours. These times were chosen to closely match the current factory schedule for a batch process. Thus, a 2^3 factorial design (three variables each at two levels) was used for sampling. A sample of five kilograms of coffee cherries was taken for processing. The cherries were depulped using a mechanical depulper and demucilaged using a prototype at CENICAFE, Colombia. The demucilaging

process is described in detail by Oliveros (1993). The mucilage was separated from the beans by adding water at the rate of 0.3 L/kg of depulped coffee. Each treatment was repeated a minimum of seven times.

For rheological parameter characterization, a Brookfield HB DV-III viscometer was used in the concentric cylinder geometry with a small sample adapter (model SSA15/7RPY) suitable for the viscosity in the 0.1 to 10^5 Pa-s range. The small sample adapter has a cylindrical chamber 6.32 mm in diameter and a spindle 4.71 mm in diameter. Several shear rates ranging from 4.8 to 120 s^{-1} (rpm in the range 10 to 250) were used, and the corresponding shear stress data were obtained. The data were acquired via a personal computer using Rheocalc software (Brookfield Engineering Labs, Inc). The mucilage sample of 3.3 mL was used for each test. The sample temperature was held constant at 21 $\pm$ 1C by recirculating water in the small sample adapter. Before and after the application of shear stress, i.e., shear viscosity measurements, mucilage samples were drawn for microstructure evaluation. The microstructure was observed in a stereoscopic light microscope at 20X magnification.

RESULTS AND DISCUSSION

Rheological Characterization

The shear stress versus shear rate data obtained for different mucilage samples of Colombia and Caturra varieties are plotted in Fig. 2. As expected, for high molecular weight fluids (Rao 1977) the mucilage exhibited a pseudoplastic behavior (concave downward curve with zero yield stress, i.e., $0 < n < 1$, $\sigma_y = 0$). The effect of the experimental variables, RCC and PHT are more pronounced for the Caturra variety than for the Colombia variety especially at higher shear rates.

Apparent viscosity (η_a) values (Eq. 5) for the Caturra variety are plotted as a function of shear rate on a log-log scale in Fig. 3. The trend was similar for the Colombia variety. As can be seen, there was a substantial drop in viscosity with increasing shear rate. The change in viscosity was much smaller when the shear rate exceeded 100 s^{-1} indicating a tendency to approach a constant value. In general, pseudoplastic fluids exhibit shear thinning behavior over a long shear rate range. Since we did not perform experiments at higher shear rates, it is not possible to estimate the actual shear rate at which the minimum η_a, is reached. For both varieties, η_a increased with increased PHT. This has implications on the demucilaging process (demucilaging rate and power consumption).

The consistency index (K) and the flow behavior index (n) values were obtained using the power-law model (Eq. 4). The data conformed to the model very well as determined by the high coefficient of determination values ($r^2 > 0.9$). The data did not fit the Herschel-Bulkley Model (assuming a possible yield

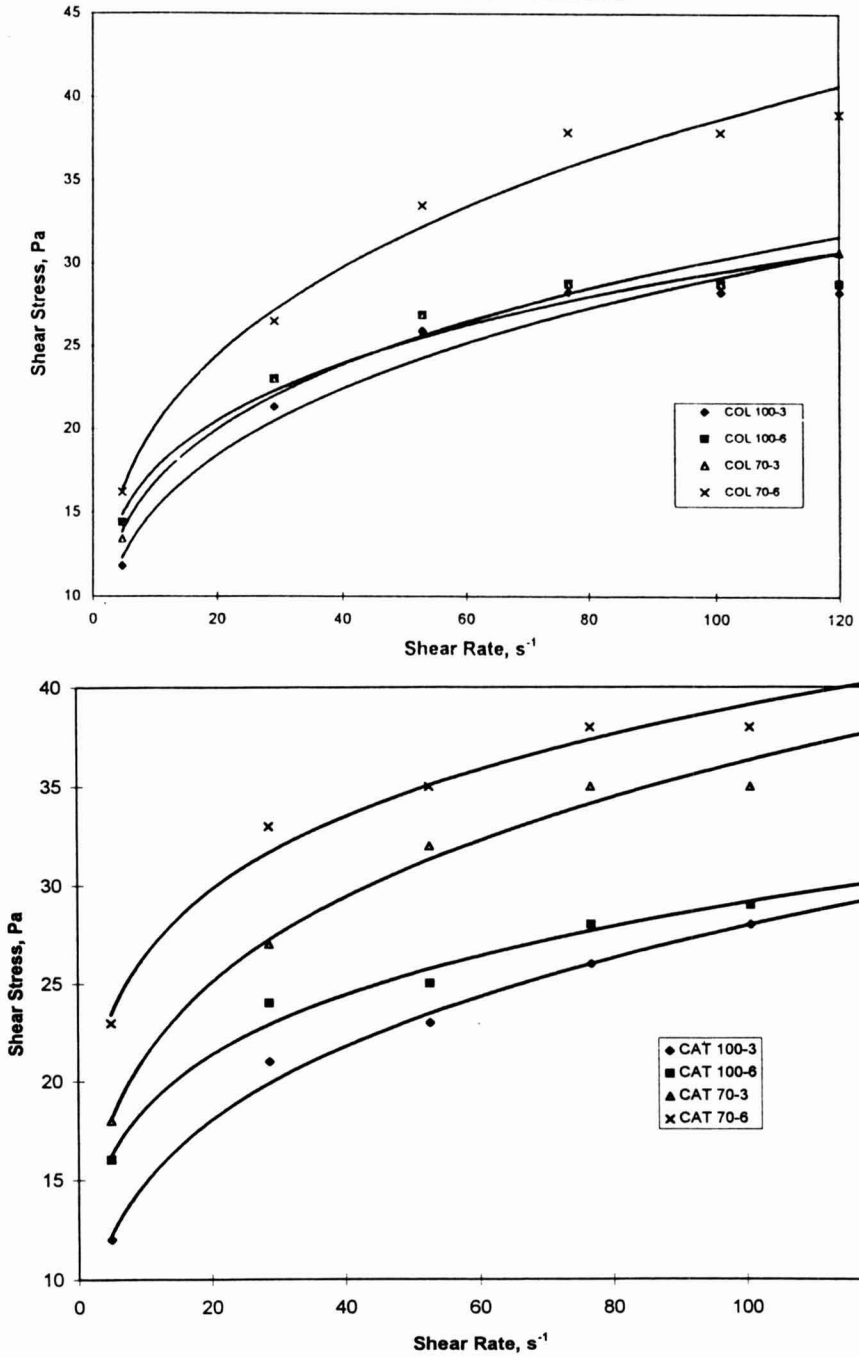

FIG. 2. SHEAR STRESS VERSUS SHEAR RATE DATA OBTAINED FOR MUCILAGE OF (A) COLOMBIA (COL) AND (B) CATURRA (CAT) COFFEE CHERRIES
Mucilage was obtained from cherries of different ripeness (100 or 70%) and after different durations since harvest (3 or 6 h).

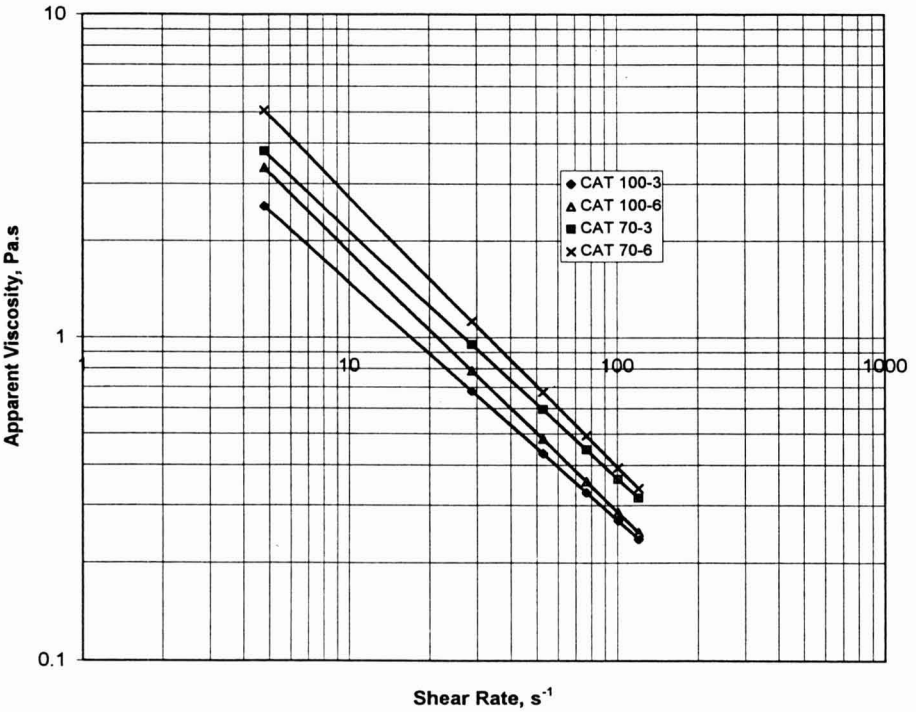

FIG. 3. APPARENT VISCOSITY VERSUS SHEAR RATE DATA FOR MUCILAGE OF CATURRA (CAT) COFFEE CHERRIES
Mucilage was obtained from cherries of different ripeness (100 or 70%) and after different durations since harvest (3 or 6 h).

stress) well ($r^2 < 0.8$). Therefore, the mucilage was described by the power-law model. The mean values for all treatments are summarized in Table 1. The coefficient of variation (cv) for the data was generally high but is acceptable considering the inherent inhomogeneity of the samples. In general, for both varieties, the n values decreased when unripe and overripe cherries were present and increased when processing had been delayed six hours after harvest. The mean K and n values from each treatment were compared using a Tukey's test at 99% probability. The analysis indicated that the K values are significantly different for each variety, RCC and PHT. However, the n values are significantly different only for each variety and PHT. In general, the mucilage of the Caturra variety was more viscous (larger K values) and more pseudoplastic (smaller n values) than that of the Colombia variety.

The mean K and n values were also subjected to ANOVA to determine the effects of the experimental variables and their interaction. The results (Tables 2 and 3) indicate that the K values are significantly different (at 99% probabili-

ty) for variety, RCC and PHT. However, the n values are significantly different only for variety and PHT. The interaction effects were not statistically significant for either K or n values.

TABLE 1.
MEAN VALUES* OF CONSISTENCY INDEX (K) AND FLOW BEHAVIOR INDEX (n) FOR COFFEE MUCILAGE AND THE CORRESPONDING COEFFICIENT OF VARIATION (cv)

Sample**	n	cv (%)	K	cv (%)
CAT 100-3	0.26[a]	31.15	8.17[e]	34.03
CAT 70-3	0.23[a]	27.23	12.62[g]	33.43
CAT 100-6	0.19[b]	28.29	11.96[f]	39.61
CAT 70-6	0.16[b]	40.58	18.90[h]	42.43
COL 100-3	0.29[c]	13.15	7.49[i]	20.87
COL 70-3	0.26[c]	16.41	8.57[k]	45.06
COL 100-6	0.23[d]	16.49	10.04[j]	11.89
COL 70-3	0.27[d]	23.99	11.07[l]	31.38

* Values followed by different letters are statistically significant at a 99% probability.
** Sample description: variety CAT = Caturra, COL = Colombia, RCC (%)-PHT (h).

TABLE 2.
ANALYSIS OF VARIANCE (ANOVA) FOR CONSISTENCY INDEX, K

Source	DF	SS	MS	F value
Variety	1	3.44E08	3.44E08	18.06*
RCC	1	4.01E08	4.01E08	21.10*
PHT	1	4.20E08	4.20E08	22.05*
Variety*RCC	1	1.11E08	1.1E08	5.85
Variety*PHT	1	6.72E07	6.72E07	3.53
RCC*PHT	1	0.0	0.0	0.0
Variety*RCC*PHT	1	2.82E08	2.82E08	1.48

*Significant at 99% of probability.
DF: Degree of Freedom; SS: Sum of Squares; MS: Mean Square.

TABLE 3.
ANALYSIS OF VARIANCE (ANOVA) FOR FLOW BEHAVIOR INDEX, n.

Source	DF	SS	MS	F value
Variety	1	6.73E-2	6.73E-2	18.88*
RCC	1	1.05E-2	1.05E-2	2.95
PHT	1	7.29E-2	7.29E-2	20.43*
Variety*PHT	1	8.88E-2	8.88E-2	2.47
RCC*PHT	1	2.09E-2	2.09E-2	5.86
Variety*RCC ~ PHT	1	2.82E08	2.82E08	1.48

*Significant at 99% of probability.

The highly shear-thinning nature of the mucilage implies that during the operation of the mechanical remover, there will be agitated fluid near the rotating blades and fairly stagnant areas relatively far from the blades. This situation may be overcome either by narrowing the gap between the rotating and stationary elements or by adding water to reduce the apparent viscosity and the shear-thinning behavior.

Microstructural Changes

Mucilage obtained from coffee cherries is not a pure fluid. In addition to its natural chemical constituents (pectin, sugars, water, etc.), it contains parts of cell structures initially surrounding the mesocarp on its borders, the pulp and the parchment. Some structures located in these borders (such as cell walls and phloem vessels in the pulp) and the parchment and the spermoderm or "silver skin" in the vicinity of coffee beans are detached and partially destroyed during the demucilaging process and are found in the mucilage. Micrographs in Fig. 4 are of coffee mucilage obtained from demucilaging after six hours but before shear viscosity tests have been conducted. It can be observed that the mucilage contains much of the epidermis cells and phloem vessels. Some natural materials found in the pulp such as tannins can diffuse through the mesocarp to internal structures of the cherry. This causes the typical brown discoloration of the parchment when the postharvest processes are delayed. The dark specks seen in Fig. 4 are due to tannins.

In the microstructure of the mucilage after shear viscosity tests, no significant damage in structures of the particles was observed at shear rates below 100 s^{-1}. However, at higher shear rates, the phloem vessels were apparently destroyed since epidermal cells could be found after the mucilage was agitated in the viscometer for 30 s at a shear rate of 100 s^{-1} (Fig. 5).

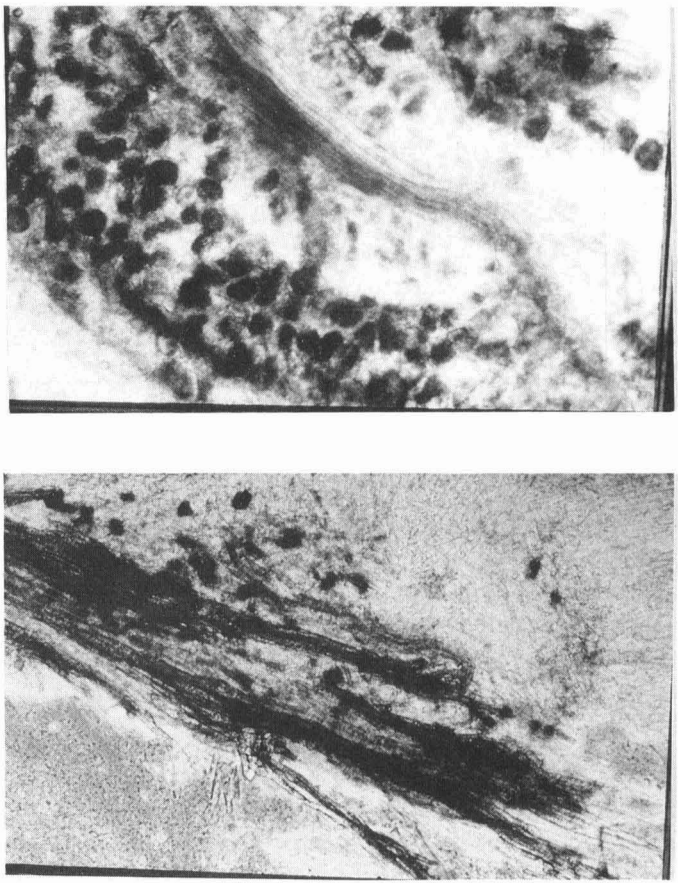

FIG. 4. MICROGRAPHS (20X) OF COFFEE MUCILAGE OBTAINED FROM CHERRIES PROCESSED 6 H AFTER HARVESTING BEFORE SHEAR STRESSES WERE APPLIED VIA SHEAR VISCOSITY MEASUREMENTS

(A) Epidermal cells are seen with intact phloem vessels. (B) Part of the mucilage showing only the phloem vessels. The dark specks presumably are due to tannins diffusing from the pulp.

As noted by Allen and Robinson (1990) and Jiménez *et al.* (1989), destruction of weak structures by the action of shearing forces, phloem vessels in this case, could be attributed to the highly pseudoplastic behavior of the mucilage. In addition, as mentioned previously, the diffusion of tannins from the pulp to the parchment, passing through the mucilage, adds significant amounts of small granules to the mucilage. This increases the concentration of solids in the mucilage and increases its viscosity. The higher apparent viscosity η_a of mucilage observed at six hours of PHT compared to three hours of PHT (Fig. 3) supports this explanation.

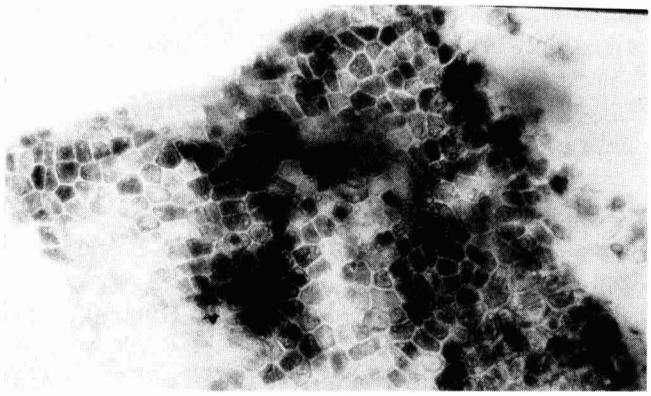

FIG. 5. MICROGRAPHS (20X) OF THE COFFEE MUCILAGE OBTAINED FROM CHERRIES PROCESSED 6 H AFTER HARVESTING AFTER SHEAR STRESSES WERE APPLIED VIA SHEAR VISCOSITY TESTS (30 S OF AGITATION IN THE BROOKFIELD VISCOMETER AT A SHEAR RATE OF 100 S^{-1}) WERE APPARENTLY DESTROYED DUE TO THE APPLIED SHEAR STRESSES
The dark specks presumably are due to tannins diffusing from the pulp.

CONCLUSIONS

Mucilage of Colombia and Caturra variety coffee cherries is highly viscous and pseudoplastic. The experimental shear rate-stress data follows the power-law model very well. The mucilage of the Caturra is more viscous and pseudoplastic than that of the Colombia variety. The variety, ripe cherry content and postharvest time have statistically significant effects on the K and n values. The interaction effects (among the experimental variables) were not found significant. The η_a of the mucilage decreases with the shear rate exhibiting a tendency to stabilize at shear rates exceeding 100 s^{-1}. Destruction of certain microstructural elements in the mucilage could be attributed to the high pseudoplasticity of the mucilage. Diffusion of tannins from the pulp into the mucilage may be resulting in the higher apparent viscosity of the mucilage with increased delay in postharvest processing.

REFERENCES

ALLEN, G.D. and ROBINSON, C. 1990. Measurements of rheological properties of filamentous fermentation broths. Chem. Eng. Sci. *45*, 37–48.

ARNTFIELD, S.D. and Murray, E.D. 1992. Heating rate affects thermal properties and network formation for vicilin and ovalbumin at various pH values. J. Food Sci. *57*(3), 640-646.

CARBONELL, R.J. and VILANOVA, M.T. 1952. Beneficiado rápido y eficiente del café mediante el uso de soda caústica. Bol. tec. No. 13, Centro Nacional de Agronomía, El Salvador.

CHENG, D.C.H. and EVANS, F. 1965. Phenomenological characterization of the rheological behavior of inelastic thixotropic and antithixotropic fluids. Brit. J. Appl. Phys. *16*, 1599.

COSTE, R. 1959. Cafetos y cafés en el mundo. Tomo segundo. p. 383, G.P. Masionneuve & Larouse, Paris.

DENTAN, E. 1985. The microscopic structure of coffee bean. In *Coffee-brewing, Biochemistry and Production of Beans and Beverage* (M.N. Clifford and K.C. Willson, eds.) Van Nostrand Reinhold/AVI, New York.

GOTO, S., NAGAZONE, H. and KATO, H. 1986. The flow behavior of fiber suspensions in Newtonian polymer solutions. II. Capillary flow. Rheologica Acta *25*, 119–129.

HOOGENDOORN, C.J. and DEN HARTOG, A.P. 1967. Model studies on mixers in the viscous flow region. Chem. Eng. Sci. *22*, 1689.

JIMÉNEZ, L., FERRER, L. and PANIEGO, L.M. 1989. Rheology, composition and sensory properties of pulped tomatoes. J. Food Eng. *9*, 119–128.

JUNGUITO, R. 1978. Economía Cafetera Colombiana. Fondo Cultural Cafetero. Bogotá, Colombia.

MANOHAR, B., RAMAKRISHNA, P. and RAMTEKE, R.S. 1990. Effect of pectin content on flow properties of mango pulp concentrates. J. Texture Studies *21*, 179–190.

METZNER, A.B. 1985. Rheology of suspensions in polymeric liquids. J. Rheology *29*(6), 739–775.

OLIVEROS, C.E. 1993. Analysis of mechanical demucilaging of depulped coffee beans. Unpublished PhD. thesis. University of Wisconsin-Madison, Madison.

RAO, M.A. 1977. Rheology of liquid foods -- a review. J. Texture Studies *8*, 135–167.

TANGLERTPAIBULB, T. and RAO, M.A. 1987. Rheological properties of tomato concentrates as affected by particle size and methods of concentration. J. Food Sci. *52*(1), 141–145.

TIU, C. and BOGER, D.V. 1974. Complete rheological characterization of time-dependent food products. J. Texture Studies *5*, 329–338.

THERMAL DIFFUSIVITY MEASUREMENTS OF WHEAT FLOUR AND WHEAT FLOUR DOUGH

T.R. GUPTA

Department of Food Engineering
Central Food Technological Research Institute
Mysore-570 013, India

Accepted for Publication February 22, 1996

ABSTRACT

A simple technique was used to measure thermal diffusivity of whole wheat flour and whole wheat flour dough at various levels of moisture and temperatures. The experimental values showed good agreement with the calculated values. It was found that thermal diffusivity of dough increases with moisture and temperature below 60C, but above 60C its value decreases. This is attributed to physico-chemical changes, e.g., starch geletinization and protein coagulation. Due to these changes swelling and softening of dough occur, which reduce the ability of dough to diffuse thermal energy, thus lowering the value of the thermal diffusivity. Based on the experimental value of wheat dough at various moisture levels and temperatures, the following equation is proposed:

$$\alpha = (7.957 - 0.6346\,M + 0.217\,T + 0.008\,M^2 - 0.00176\,T^2 - 0.00051\,M\,X\,T)\,X\,10\text{-}7$$

INTRODUCTION

To design a continuous oven for baking and puffing of Chapati (round disc generally prepared from whole wheat flour dough and consumed as staple food in South Asia, e.g., India, Pakistan etc.), thermal properties such as specific heat, thermal conductivity and thermal diffusivity of wheat flour and wheat dough are required. Data on specific heat and thermal conductivity of these materials have been reported previously (Gupta 1990, 1993). The present communication deals with the determination of thermal diffusivity of whole wheat flour and whole wheat flour dough at various levels of moisture and temperatures, as these data are not available in the literature. Thermal diffusivity of a substance is defined as

Journal of Food Process Engineering **19** (1996) 343–352.

$$\alpha = k/\varrho c \quad (1)$$

The thermal diffusivity of food materials depends on its moisture content, temperature, composition and porosity.

For the determination of thermal diffusivity of food materials Singh (1982) has reviewed various approaches. It can be calculated from the relation (1) provided values of k, ϱ and c are known or can be measured experimentally.

Several researchers (Hayakawa and Abraham 1973; Bhowmik and Hayakawa 1979) have suggested methods for determining the thermal diffusivity of food materials, the values of which were obtained from an equation given by Carslaw and Jaeger (1947) and were solved based on boundary conditions applicable in respective cases. Use of thermal conductivity probe has been described for measurement of thermal diffusivity (Suter *et al.* 1975). These researchers have used simple apparatus suggested by Dickerson (1965), which is universally adopted. In the present work a similar type of apparatus has been used. This method is based on transient heat transfer methods requiring only time temperature data.

In the present work thermal diffusivity of whole wheat flour and whole wheat flour dough has been determined experimentally. The value of α for these materials has also been calculated from Eq. (1), using the data on specific heat and thermal conductivity of these materials determined experimentally and reported earlier (Gupta 1990, 1993). Calculated values of thermal diffusivity of these food materials have been compared with the experimental values obtained in the present work. In the present study since the apparatus is a cylinder of large L/D ratio with ends made of teflon, it represents an infinite cylinder. The following is an empirical equation suggested by Ball and Olson (1957) for an infinite cylinder:

$$t = f \log_{10}(jT-To) \; / \; T-Th \quad (2)$$

where $f = 0.398\ r^2 / \alpha$ for infinite cylinder, r is radius of infinite cylinder in cm, j is the leg factor, for infinite cylinder its value is 1.6 (Ball and Olson 1957).

Here
- Th = Temperature of heating medium in C
- To = Initial temperature of sample in C
- T = Temperature at center of the tube in C

The boundary conditions are as follows:

at
- $r = 0, T = To$
- $r = a, T = T$
- $r = r, T = Th$

The following are the assumptions:

(1) Temperature at the surface of the thermal diffusivity apparatus which is immersed in the constant temperature water bath is constant and equal to the temperature of water.
(2) At the measured temperature, it is assumed that thermal diffusivity is constant.
(3) The food sample is considered to be homogeneous for the measurement purposes.

MATERIALS AND METHODS

Apparatus

The thermal diffusivity apparatus shown in Fig. 1 was made of copper shell of 50 mm outside diameter (O.D.), 200 mm long and 1.0 mm thick with teflon flanged caps of 87 mm diameter (dia.) and 12 mm thick at both ends to simulate an infinite cylinder.

Copper, being rigid and having high thermal conductivity value facilitates in high heat transfer coefficient, thus reducing the time taken to reach steady state. At the center of a top teflon flange a 5 mm dia. hole was drilled to insert a thermocouple (T) as shown in Fig.1. This thermocouple was fixed with a suitable adhesive to top teflon flange to obtain a leak proof joint and was meant to measure center temperature (T and To) of the test sample whose thermal diffusivity is to be determined. The hub portion of top flange was 48 mm in diameter and 12.0 mm in length. This extension in top flange was provided to prevent heat loss from the top of the shell. The top and bottom flanges were held together with 4 bolts of 6 mm diameter and 240 mm in length, to obtain a leak proof assembly. At the bottom flanged cap a 1 mm wide and 2 mm deep groove was made at 49 mm pitch circle diameter (pcd) to house the copper shell which was joined to bottom flanged cap with adhesive to get a leak proof joint.

Adjacent to the outside surface of the shell another thermocouple (Ti) was put in the constant temperature water bath (not shown in the figure) which measured the outside surface temperature (Th) of the shell. Both the thermocouples were made of pt-100 and were connected to a data logger to record, To, the initial temperature, Th, the temperature of heating medium after time t, and T, the temperature of test material at the center of the tube after time t, at intervals of 1, 2 or 5 min according to test requirements and measured with a resolution up to $\pm = 0.1$ C. An electrically heated sheathed coil and mechanical stirrer maintained the water bath temperature with an accuracy of $\pm$ 0.1C (not shown in the figure).

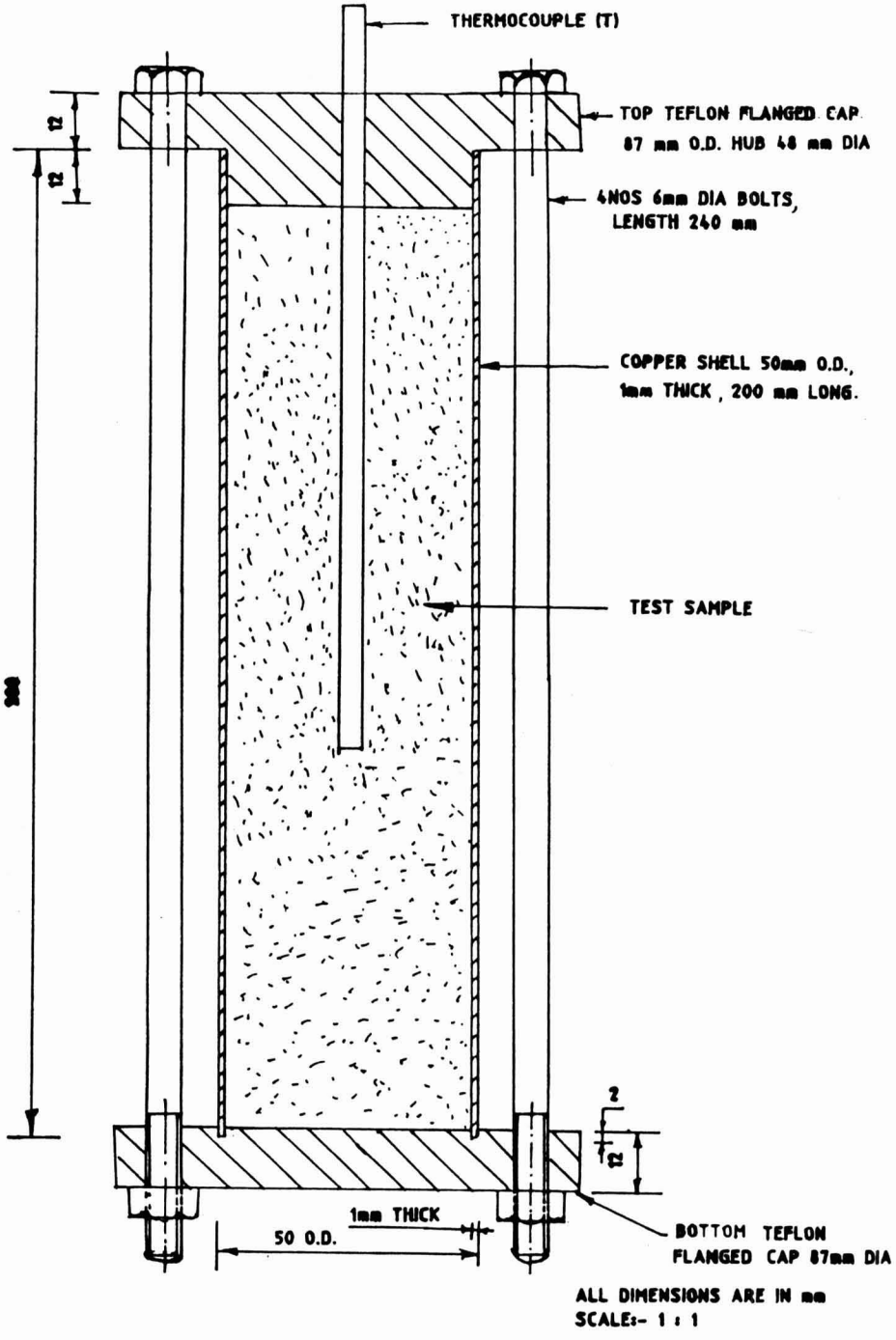

FIG. 1. SECTIONAL VIEW OF DIFFUSIVITY APPARATUS

Experimental Procedure

The copper shell of the thermal diffusivity apparatus (TDA) with the bottom flange in place was filled with a known quantity of the sample material whose thermal diffusivity was to be determined. The quantity of test material was 200 g in the case of wheat flour while in the case of wheat dough it was 360 g. The dough was prepared manually. The change in quantity was due to difference in bulk density of test materials. The top cap with thermocouple was inserted in the copper tube and top and bottom flanged caps were secured tight through bolts to obtain a leak proof assembly. The initial temperature To of the test sample was recorded with the help of thermocouple (To). The complete assembly was immersed in the constant temperature water bath so as to maintain the top flanged cap above water level. The bath itself was maintained at a temperature at which the thermal diffusivity of test sample was to be determined. The thermocouple (Ti) was immersed into constant temperature water bath near the thermal diffusivity apparatus. In the beginning temperature T and Ti were recorded at an interval of 1 min, and after 15 min (approximate) at an interval of 2 min when the rate of temperature rise of the test sample slowed down. After 30 min (approximate) when the rate of temperature rise was further slowed down the temperature was recorded at an interval of 5 min. The time and temperature data were collected at constant bath temperatures of 45, 55 and 65C for whole wheat flour(M-13.27%) and whole wheat flour dough at moisture level of 42%, 45.69% and 47.42% (wet basis). The experiments were repeated at each temperature three times. The experimental values were reported in the Table 1. The standard deviation was found $\pm$ 5%.

A $\log_{10} \times 1.6$ (T-To)/(T-Th) versus time curve were plotted and a typical plot for wheat dough at a moisture level of 47.42% and 55C is shown in graph Fig. 2. The nature of the graph was linear. The slope of the straight line gave value of f according to Eq. 2 which was equal to $0.398\ r^2/\alpha$ for infinite cylinder as given by Ball and Olson (1957). The value of α calculated at different temperatures and moisture levels is shown in Table 1.

RESULTS AND DISCUSSION

Thermal diffusivity values of whole wheat flour and whole wheat flour dough at various moisture levels and temperatures determined experimentally in the present method have been shown in Table 1. The thermal diffusivity values of these food materials have also been calculated by the formula $\alpha = k/\varrho c$. The value of c and k for wheat flour and dough have already been determined experimentally (Gupta 1990, 1993). The experimental and calculated values are in fair agreement. The maximum deviation between experimental and calculated values of wheat flour is 33.5%, where as maximum deviation between

TABLE 1.
THERMAL DIFFUSIVITY VALUES OF SUBSTANCES DETERMINED EXPERIMENTALLY BY PRESENT METHOD

Sl. No.	Substances	Moisture content % wet basis	Bulk Density kg/m^3	To C	Shell temp C	Value of α in m^2/s $\times$ 10^{-7} Cal.	Exp.	Deviation %	Value of α in m^2/s $\times$ 10^{-7} estimated	reported	% Deviation
1.	Whole wheat flour	13.27	0.615	29.8	45	1.049	0.815	+22.3		1.01	-19.3
		13.27	0.615	28.9	55	1.212	0.905	+25.3			-10.3
		13.27	0.615	25.9	65	1.383	0.920	+33.5			-8.9
2.	Whole wheat flour dough	42.00	1.076	28.2	45	1.013	0.7132**	+29.59	0.653		-8.4
		42.00	1.076	30.1	55	1.258	0.764	+39.26	0.8476		+10.9
		42.00	1.076	29.0	65.3	0.762	0.713	+6.43	0.6887		-3.4
3.	Whole wheat flour dough	45.69	1.076	24.8	45	1.1900	0.713	+40.08	0.8169		+14.5
		45.69	1.076	27.3	55	1.1484	1.097	+5.08	1.9918		-9.0
		45.69	1.076	26.2	66	0.871	0.820	+5.85	0.8142		-0.7
4.	Whole wheat flour dough	47.42	1.076	26.9	45	1.26	1.013	19.6	0.9683		-4.4
		47.42	1.076	27.2	55	1.48	1.12	+24.32	1.345		+20.0
		47.42	1.076	24.3	65	0.919	0.918	+0.1	0.948		+3.2

* Value of wheat flour, M, 11%, bulk density, 0.713, temperature range 23.3-50 C, as reported by Poulsen 1982

** Experimental values of α are average of three replicates for each temperature and moisture

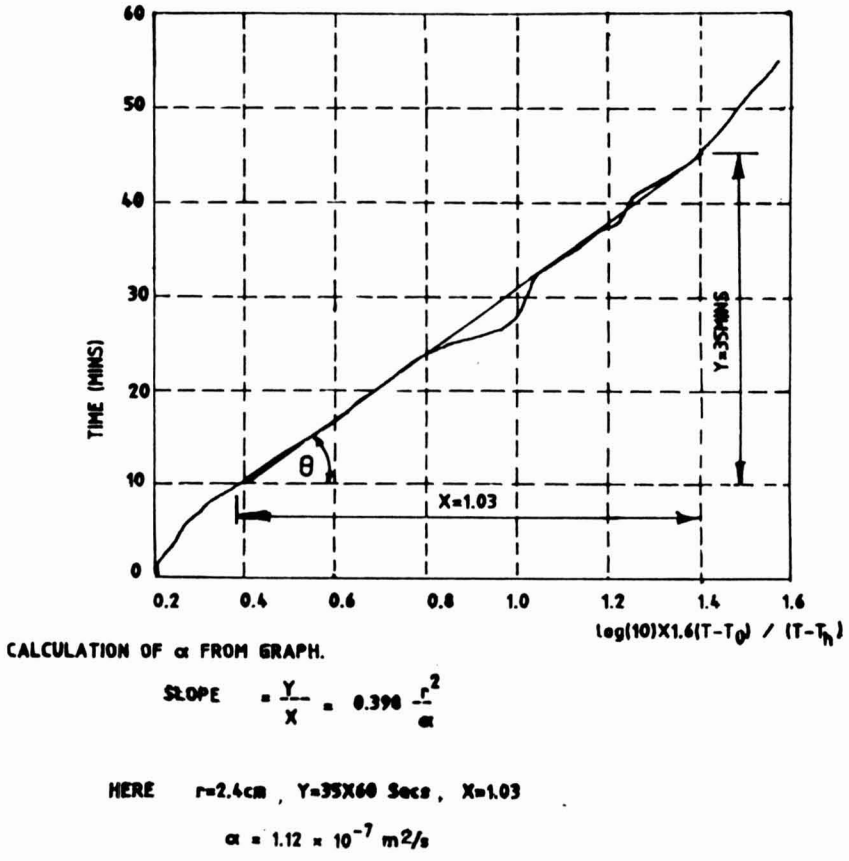

FIG. 2. DETERMINATION OF THERMAL DIFFUSIVITY α OF WHEAT DOUGH (M = 47.42%) AT 55C

experimental and reported values of wheat flour is 19.3%. With the increase of temperature, thermal diffusivity of wheat flour dough increases as shown in Fig. 3. However the value of thermal diffusivity decreases at 65C. This is attributed to physico chemical changes, e.g., starch gelatinization and protein coagulation taking place at and above 65C. Due to these changes, swelling and softening of dough occur which reduce the ability of dough to diffuse thermal energy, thus lowering the value of thermal diffusivity. The same trend has been observed in calculated value also.

Figure 3 also shows the effect of moisture on thermal diffusivity. The value of thermal diffusivity increases with moisture which is in agreement with the model suggested by Martens as reported by Singh (1982).

i.e., $\alpha = \{0.057363\ M + 0.000288\ (T + 273)\} \times 10^{-6}$

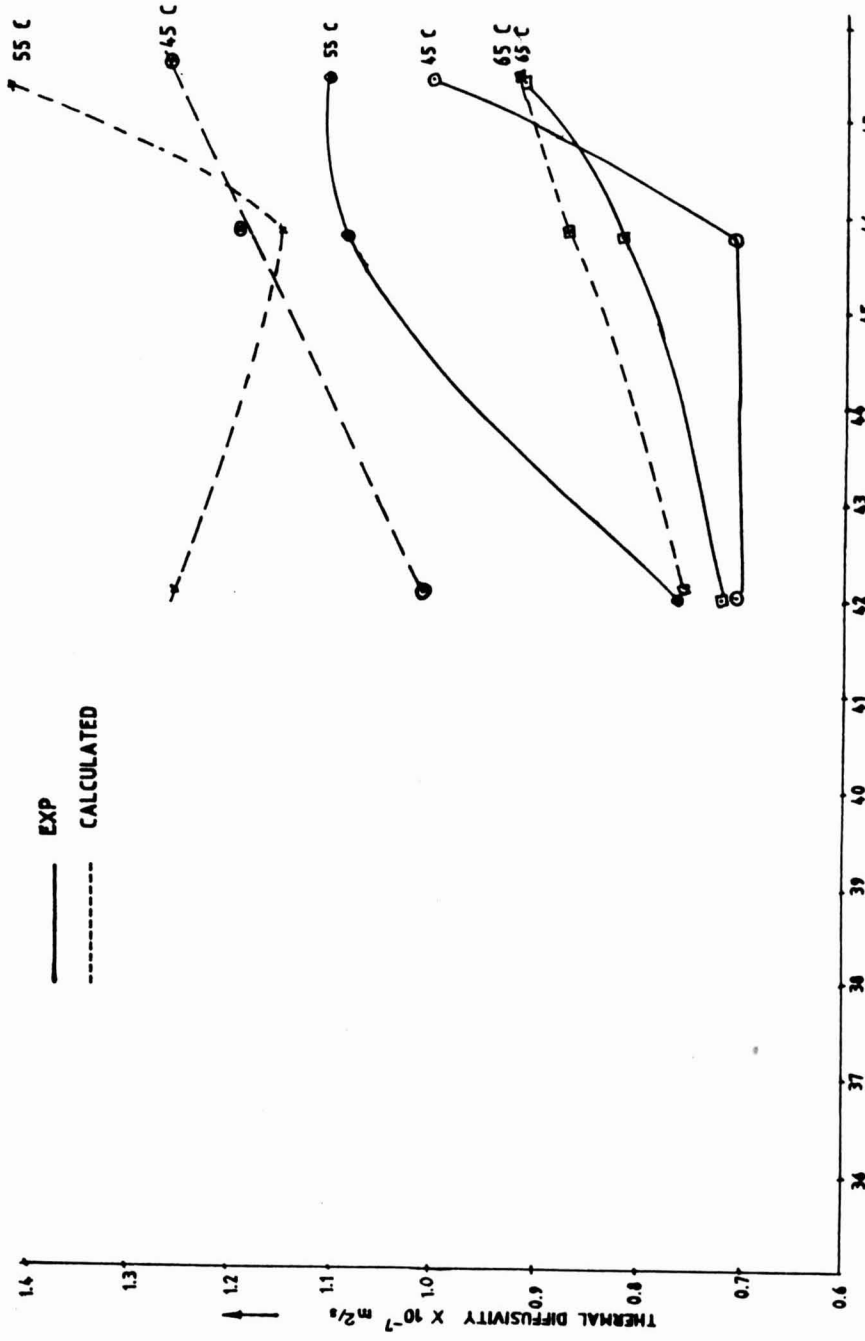

FIG. 3. EFFECT OF MOISTURE AND TEMPERATURE ON THERMAL DIFFUSIVITY OF WHOLE WHEAT FLOUR DOUGH

The finding of Kazarian and Hall (1965) for corn, and Lacklair *et al.* (1957) for tobacco (for M > 20% in both the cases) as reported by Mohsenin (1980) also confirms this. The reason for the increase in thermal diffusivity with moisture may be because heat conducted quickly due to the increase in thermal conductivity value of the dough at higher levels of moisture. Though the value of specific heat also increases with moisture but its contribution is less as compared to thermal conductivity.

Based on the experimental values at various moisture and temperature levels (Table 1), the following equation is proposed to estimate the thermal diffusivity of wheat dough having bulk density value of 1.076 kg/cu.m.

$$\alpha = (7.257 - 0.6346\ M + 0.217\ T + 0.008\ M^2 - 0.00176\ T^2 - 0.00051\ M*T) \times 10^{-7} \quad \ldots\ldots\ldots\ldots\ldots\ldots R^2 = 0.84$$

The maximum deviation between the present model and experimental values of thermal diffusivity was 20% at moisture and temperature values of 47.42% and 55C, respectively.

NOMENCLATURE

α	=	Thermal diffusivity	m^2/s
K	=	Thermal conductivity	w/m C
C	=	Specific heat	J/kg C
ϱ	=	Density	kg/m^3
t	=	Time	s
M	=	Percentage moisture content(wet basis)	%
T	=	temperature	C
R	=	Regression coefficient	
L	=	Length of cylinder	m
D	=	Diameter of cylinder	D

ACKNOWLEDGMENT

The author gratefully acknowledges encouragement given by Director Dr. V. Prakash and Shri A. Ramesh, Head, Department of Food Engineering, CFTRI, Mysore. Helpful suggestions by Dr. N.G. Karanth are also acknowledged.

REFERENCES

BALL and OLSON. 1957. *Sterilisation in Food Technology*, McGraw-Hill Book Co. London.

BHOMICK, S.R. and HAYAKAWA, K.-I. 1979. A new method for determining the apparent thermal diffusivity of thermally conductive food, J. Food Sci. *44*(2), 469.

CARSLAW, H.S. and JAEGER, J.C. 1947. *Conduction of Heat in Solid*, Oxford University Press, London.

DICKERSON, Jr., R.W. 1965. An apparatus for the measurement of thermal diffusivity of foods. Food Technol. *19*(5), 198.

GUPTA, T.R. 1990. Specific heat of Indian unleavened flat bread (Chapati) at various stages of cooking. J. Food Process Engineering, *13*, 217–227.

GUPTA, T.R. 1993. Thermal conductivity of Indian unleavened flat bread (Chapati) at various stages of baking. J. Food Process Engineering, *16*, 227–235.

HAYAKAWA, K.-I. and BAKAL, A. 1973. New computational procedure for determining the apparent thermal diffusivity of a solid body approximated with an infinite slab. J. Food Sci. *38*, 623.

KULACKI, F.A. and KENNEDY, S.C. 1978. Measurement of the thermophysical properties of common cookie dough. J. Food Sci. *43*, 380–384.

MCCURRY, T.A. 1968. The determination of a numerical technique for determining thermal diffusivity utilising data obtained through the use of a refined line source method. Advanced project report, Auburn University.

METAL, S.N. *et al.* 1986. Thermophysical characteristics of yeast dough, Izvestiga Vysshikh Uchobnykh Zavedenu Pishcshevaya Teknoljiya, *4*, 107–108.

MOHSENIN, N.N. 1980. *Thermal Properties of Food and Agricultural Materials*. Gordon and Breach Science Pub., New York.

NIX, G.H., LOWERY, G.W., VACHON, R.I. and Tanger, G.E. 1967. Direct determination of thermal diffusivity and conductivity with a refined line source technique. Progress in Aeronautics and Astronautics. Thermophys. Spacecraft Planet. Bod. *20*, 865–878, Academic Press, New York.

POULSEN, K.P. 1982. Thermal diffusivity of foods measured by simple equipment. J. Food Eng. *1*, 115–122.

RASK, C. 1989. Thermal properties of dough and bakery products - A review of published data. J. Food Eng. *9*, 167–193.

SINGH, R.P. 1982. Thermal diffusivity in food processing. Food Technol. *36*(2), 87.

SUTER, D.A. 1972. Heat of respiration and specific heat of peanuts. Unpublished Ph.D. Thesis, Oklahoma State University, May.

SUTER, D.A., AGARWAL, K.K. and CLARY B.L. 1975. Thermal properties of peanut pods, hulls and kernals. Trans. ASAE, *18*, 370–375.

THERMAL INACTIVATION OF PECTINESTERASE IN PAPAYA PULP (pH 3.8)

M.M. DOS A. MAGALHÃES

Dept° Engenharia Química - Centro de Tecnologia
Universidade Federal do RN, Campus Universitário
59072-970 Natal, RN, Brazil

AND

R.M. TOSELLO and P.R. DE MASSAGUER

Dept° Ciencias de Alimentos - Fac. Engenharia de Alimentos - Unicamp
C.P. 6121, 13081-970, Campinas, SP, Brazil

Accepted for Publication February 22, 1996

ABSTRACT

In order to establish the thermal process required by acified papaya pulp (pH 3.8) var "formosa", a study was carried out on the kinetics of thermal inactivation of the heat resistant enzymes present in the pulp. Since no peroxidase activity was detected, the study was focused on pectinesterase.

The heat inactivation curves at 75, 77 and 80C showed a change in slope indicating the presence of two different portions of the enzyme, one heat labile and the other heat resistant. The decimal reduction times (D value) of pectinesterase were 0.8, 0.3 and 0.2 min for the heat labile portion and for the heat resistant portion 16.7, 7.2 and 3.7 min, respectively.

The temperature-dependency factor for the heat labile portion was 9.2C and 7.8C for the thermostable portion, while the activation energies were 258.3 and 304.4 Kj/mol. These values were within the range of 167.5-418.7 Kj/mol reported in the literature for the thermal inactivation of enzymes. Thermal destruction studies with Clostridium pasteurianum, conducted at the same temperatures used for the inactivation of the enzyme, showed that the heat resistant portion of pectinesterase presented greater thermal resistance and should be used as target for the establishment of the required process.

INTRODUCTION

The use of papaya pulp as a base product for the formulation of mixed juices desserts and baby food is presently increasing, even though papaya is still mainly consumed as fresh fruit.

Journal of Food Process Engineering **19** (1996) 353–361. *All Rights Reserved.*

Brazil has a large production of papaya (*Carica papaya* L.) participating with 37% of the world production. A great portion of this fruit, which is a rich source of vitamin C and provitamin A could be preserved from spoilage by processing. The processing schedule required for papaya at its natural pH (4.2-5.65) has a deteriorative effect on texture and flavor.

In order to obtain a stable product and eliminate the gelatinization of the pulp, thermal treatment associated with acidification under pH level 4.2 is recommended. At this pH level, spoilage is caused by gram-positive, nonspore forming bacteria eg. *Lactobacilli*, or by yeast with a heat resistance lower than pectinesterase, naturally present in the fruit (Peralta *et al.* 1973). For such acid product, *Cl. Pasteurianum* is commonly used as target organism to establish the process required.

In 1978, Ling and Lund described a method for estimating the kinetics parameters for thermal inactivation of enzymes system containing no more than two fractions of isoenzyme.

In 1981, Nath and Ranganna reported a 2.5 D process for papaya pieces in syrup (pH 3.8) to ensure a safe acceptable product. This process was based on the thermal inactivation of the pectinesterase, and no indication was made in this research of the presence of pectinesterase isoenzymes of different thermal stabilities. In 1991, Seymour *et al.* reported a thermolabile (PEPTL) and thermostable (PEPTR) pectinesterases from grapefruit pulp following the work of Versteeg *et al.* (1980) and Ling and Lund (1978).

In this work we carried out investigation to determine the kinetics of thermal inactivation of heat resistant enzymes in papaya pulp and compare its resistance with that of *Cl. pasteurianum* in order to establish the thermal process required for acidified papaya pulp (pH 3.8).

MATERIALS AND METHODS

Preparation of Papaya Pulp

Papaya var "formosa" was used; ripeness was evaluated by visually selecting the fruit. After end-cutting, peeling and straining of the seeds the fruit was cut and blended for 5 min. Brix, pH, peroxidase (Silva and Nogueira 1984) and pectinesterase activity were determined at this point (Kertesz 1955). Followed by straining and acidification with citric acid to pH 3.8, the pulp was filled in plastic bags and stored at -18C. When required, the pulp was thawed and used.

Determination of the Thermal Resistance of *Cl. pasteurianum* in Papaya Pulp (pH 3.8)

Prior to resistance determination, the ability of *Cl. pasteurianum* to grow and produce gas in acidified papaya pulp (APP) was tested by inoculating

exhausted tubes of sterile papaya pulp with 5 mL of activated spore suspension (100C/2 min) and sealed with vaspar. Gas production after incubation at 30C was observed from 2-15 days. A spore suspension of *Cl. pasteurianum* FTPTA 0203 sporulated on liver infusion broth (DIFCO) by the successive transfer method (Reed *et al.* 1951) and quantified in liver broth (DIFCO) by Most Probable Number method, after 2 min activation at 100C was used. A 3-neck flask with inlets of thermometer, mechanical stirrer and samples, containing 792 mL of AAP (pH-3.8) were used. When the pulp reached the desired temperature, 8 mL of activated spores suspensions (10^6 sp/mL) were inoculated in the 3-neck flask. Immediately, a sample was withdrawn for initial counting. Other samples were withdrawn for counting of survivors at intervals of 1.0, 2.0, 5.0, 10.0, 15.0 and 20.0 min. They were subcultured in liver broth (DIFCO) by Most Probable Number methods. These tests were achieved using a water bath with controlled temperature of 75, 77 and 80C precision $\pm$ 0.50. On this method heating and cooling lags were negligible (Stumbo 1973). The D values were calculated by the inverse negative slope of the regression of the survivors curves.

Thermal Inactivation of Pectinesterase in APP

The 2 mL of APP were pipetted in each of 12 unsealed TDT tubes (9 $\times$ 27 mm) and heated in an oil bath at 75, 77 and 80C ($\pm$ 0.5°C). Extraction of pectinesterase was carried out with 10 mL of a 10% sodium chloride solution/TDT tube (Aung and Ross 1965). Residual activity of PE was determined (Kertesz 1955).

RESULTS AND DISCUSSION

Table 1 shows the characterization of papaya pulp. No peroxidase activity was detected in the 10 samples examined.

TABLE 1.
CHARACTERIZATION OF "FORMOSA" PAPAYA PULP[1]

pH	Soluble (BRIX)	Enzymatic Activity[2] Peroxidase	Pectinesterase	PE[3]
5.0	9.7	none	26.5 - 57.5	41.2

[1] Values are means of 10 samples tested.
[2] PEU $\times$ 10^4/mL where PEU = units of PE.
[3] PE = mean activity of PE.

A large variation in the content of pectinesterase was observed. This fact may be explained by the variety used since each variety has its own enzymatic content and also may be affected by variation in ripeness.

For the thermal inactivation curves (Fig. 1) the residual percent of PE as a function of heating time was plotted for each temperature.

No first order reaction behavior was observed (Fig. 1). The PE in papaya pulp has two different behaviors: a fast inactivation at short times, and a slow inactivation at long heating times. For the determination of kinetics parameters for thermostable portion of PE, the straight line portion of each heating curve, at long heating times was treated with linear regression and from the slope M:

$$M = \frac{K_R}{2.303} \tag{1}$$

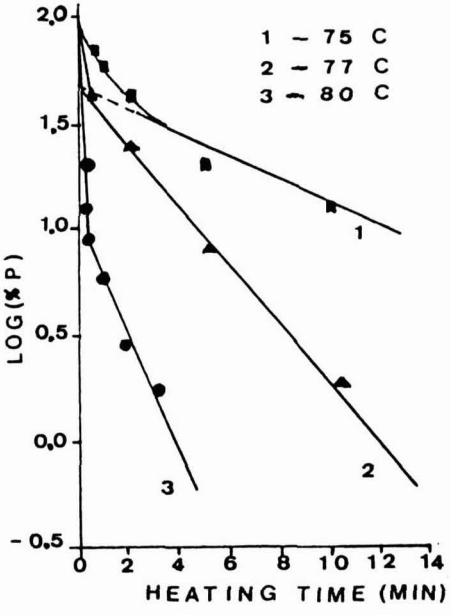

FIG. 1. THERMAL INACTIVATION OF PE IN APP (pH 3.8)

The rate constant K_R for thermal inactivation of PEPTR was determined. By extrapolating the regression line, the intercept A was found:

$$A = \frac{K_R \cdot E_{RO}}{K_L \cdot E_{LO}} + K_R \cdot E_{RO} \quad (2)$$

Where K_L and K_R are the rate constants for thermal inactivation of heat labile and heat resistant portion of the enzyme, respectively, and E_{LO}, E_{RO} are the concentrations of the heat labile and heat resistent isoenzymes at zero heating time ($_R$ and $_L$ = resistant and labile).

A semilog plot of percent activity minus the intercept (% P-A) versus time was plotted to analyze the kinetics of heat labile portion of PE (Fig. 2). The slope of straight line for each temperature was used to determine the rate constant K_L, from Fig. 2:

$$M = -\frac{K_L}{2.303} \quad (3)$$

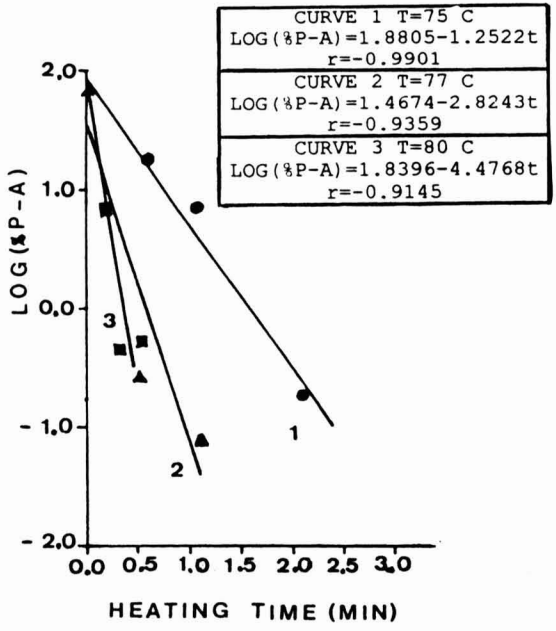

FIG. 2. MODIFIED THERMAL INACTIVATION CURVES FOR THE PEPTL

From the rate constant K_R and K_L, D values were easily calculated (see Table 2) for both portions of PE (Ling and Lund 1978).

TABLE 2.
D, Z AND E_A VALUES OF HEAT LABILE AND HEAT RESISTANT PORTION OF P_E IN APP (pH 3.8)

Temp (C)	D (min)		Z (C)		E_A (K$_j$/mol)	
	PEPTL	PEPTR	PEPTL	PEPTR	PEPTL	PEPTR
75	0.8	16.7				
77	0.3	7.2	9.2	7.8	258.3	304.4
80	0.2	3.7				

PEPTR

75C - log (%P) = 1.6159 - 0.0598 t r = - 0.9465
77C - log (%P) = 1.6707 - 0.1382 t r = - 0.9979
80C - log (%P) = 1.0086 - 0.2685 t r = - 0.9936

Temperature-dependency factors (Z) were determined for PEPTL and PEPTR, and the thermal resistance curves are shown in Fig. 3.

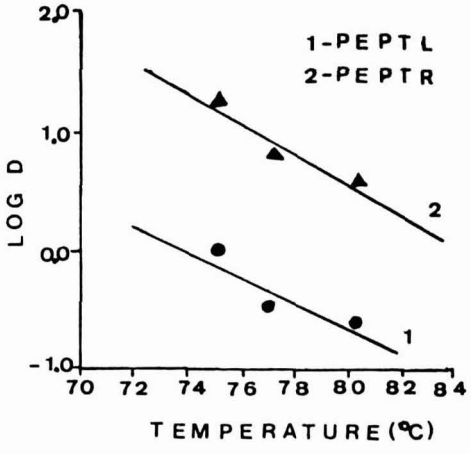

FIG. 3. THERMAL RESISTANCE CURVES FOR PE IN APP (pH 3.8)

The thermal destruction of *Cl. pasteurianum* showing logarithmic order of death is represented in Fig 4. Figure 5 represents the thermal destruction curve for *Cl. pasteurianum* in APP (pH 3.8). Activation energies (E_A) of the microorganism and the enzyme were established as Ramaswamy *et al.* (1989).

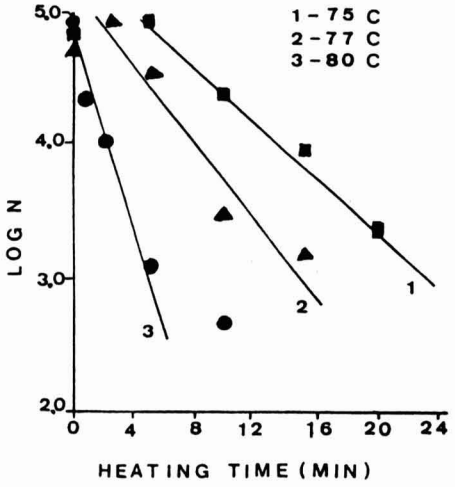

FIG. 4. THE SURVIVOR CURVE FOR *CL. PASTEURIANUM* IN APP (pH 3.8)

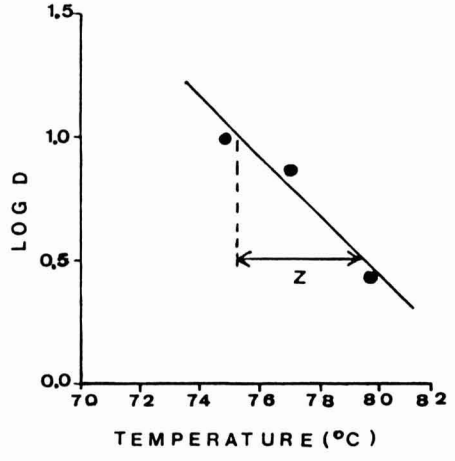

FIG. 5. THERMAL DESTRUCTION CURVE FOR *CL. PASTEURIANUM* IN APP (pH 3.8)

The comparison of thermal inactivation parameters for heat resistent portion of PE and *Cl. pasteurianum* in APP are shown in Table 3.

TABLE 3.
COMPARISON OF THERMAL INACTIVATION PARAMETERS FOR HEAT RESISTANT PORTION OF PE AND *CL. PASTEURIANUM* IN APP (pH 3.8)

Temp (C)	D (min)		Z (C)		E_A (Kj/mol)	
	Cl. pasteur.	PEPTR	*Cl. pasteur.*	PEPTR	*Cl. pasteur.*	PEPTR
75	9.7	16.7				
77	7.1	7.2	8.8	7.8	270.88	304.38
80	2.7	3.7				

Our results for D values, are close to those reported by Seymour *et al.* 1991 and (Versteeg *et al.* 1980) for citric fruit. These authors found and purified various fractions of PE with different thermal stability. However, Nath and Ranganna (1981), reported higher D values for PE, (D_{77C} = 13.97 min), in a papaya syrup homogenate (pH 3.8). The presence of sugar may be responsible for increasing the resistance. The same authors indicated that *Cl. pasteurianum* did not grow in sterile papaya pulp (pH 4.0). In the present work we found that this organism can grow and produce gas when inoculated in the pulp.

For PEPTR, Versteeg *et al.* (1980) reported a Z = 6.5C and a Z = 11C for the heat labile fraction we found a Z = 7.8C and 9.21C for PEPTR and PEPTL, respectively.

The values of activation energies determined are within the range reported by (Reed 1975) for the thermal inactivation of enzymes (167.5-418.7 Kj/mol) and are higher than the activation energy required to initiate the destruction of *Cl. pasteurianum* (270.88 Kj/mol).

CONCLUSIONS

Through thermal inactivation kinetics, two portions of PE may be detected in papaya pulp, one heat labile and the other heat resistant.

The resistance of the thermostable portion of PE in acidified papaya pulp was higher when compared to that of *Cl. pasteurianum*. Therefore, the kinetics parameters of the enzyme may be used to establish the required thermal process. We set an $F^{7.8C}_{80C}$ = 1.22 D_{PEPTR} and determined a process of 4.5 min at 80C to inactivate the enzyme and ensure a safe product.

REFERENCES

AUNG, T. and ROSS, E. 1965. Heat sensitivity of pectinesterase in papaya puree and catalase-like activity in passion fruit juice. J. Food Sci. *30*, 144–147.

KERTESZ, Z.I. 1955. Pectic enzymes. In *Methods in Enzymology*, Vol I, (S.P. Colowick and N.O. Kaplan, eds.) pp. 158–162, Academic Press, New York.

LING, A.C. and LUND, D.B. 1978. Determining kinetic parameters for thermal inactivation of heat resistent and heat labile isoenzymes from thermal destruction curves. J. Food Sci. *43*, 1307–1310.

NATH, N. and RANGANNA, S. 1981. Determination of thermal process schedule for acidified papaya. J. Food Sci. *46*, 201–211.

PERALTA, E.I., ALABASTRO, E.F., LEGASPI, G.R.A. and APOLINARIO, K.M. 1973. Growth characteristic and thermal resistance of spoilage organism isolated from canned peachy papaya given minimal heat treatment. Philippine J. Sci. *102*, 69–80.

RAMASWAMY, H.S., VAN DE VOORT, F.R. and GHAZALA, S. 1989. An analysis of TDT and Arrhenius methods for handling process and kinetic data. J. Food Sci. *54*, 1322–1326.

REED, G. 1975. *Enzymes in Food Processing*. Academic Press, New York.

REED, J.M., BOHRER, C.W. and CAMERON, E.J. 1951. Spores destruction rate studies on organisms of significance in the processing of canned foods. Food Res. *16*(5), 383–408.

SEYMOUR, T.A., PRESTON, J.F., WICKER, L., LINDSAY, J.A., WEI, C. and MARSHALL, M.R. 1991. Stability of pectinesterase of marsh white grapefruit pulp. J. Agric. Food Chem. *39*, 1075–1079.

SILVA, E. and NOGUEIRA, J.N. 1984. Estudo da atividade da polifenoloxidase e da peroxidase em algumas frutas e hortalicas. O Solo, *76*, 43–51.

STUMBO, C.R. 1973. Thermal resistance of bacteria. In *Thermobacteriology in Food Processing*. 2nd Ed. pp. 43–120. Academic Press, New York.

VERSTEEG, C., ROMBOUTS, F.M., SPAANSEN, C.H. and PILNICK, W. 1980. Thermostability and orange juice cloud destabilizing properties multiple pectinesterases from orange. J. Food Sci. *45*, 969–998.

F N P PUBLICATIONS IN FOOD SCIENCE AND NUTRITION

Journals

JOURNAL OF FOOD LIPIDS, F. Shahidi
JOURNAL OF RAPID METHODS AND AUTOMATION IN MICROBIOLOGY, D.Y.C. Fung and M.C. Goldschmidt
JOURNAL OF MUSCLE FOODS, N.G. Marriott, G.J. Flick, Jr. and J.R. Claus
JOURNAL OF SENSORY STUDIES, M.C. Gacula, Jr.
JOURNAL OF FOODSERVICE SYSTEMS, C.A. Sawyer
JOURNAL OF FOOD BIOCHEMISTRY, J.R. Whitaker, N.F. Haard and H. Swaisgood
JOURNAL OF FOOD PROCESS ENGINEERING, D.R. Heldman and R.P. Singh
JOURNAL OF FOOD PROCESSING AND PRESERVATION, D.B. Lund
JOURNAL OF FOOD QUALITY, J.J. Powers
JOURNAL OF FOOD SAFETY, T.J. Montville
JOURNAL OF TEXTURE STUDIES, M.C. Bourne and M.A. Rao

Books

HACCP: MICROBIOLOGICAL SAFETY OF MEAT AND POULTRY, J.J. Sheridan, R.L. Buchanan and T.J. Montville
OF MICROBES AND MOLECULES: FOOD TECHNOLOGY AT M.I.T., S.A. Goldblith
MEAT PRESERVATION: PREVENTING LOSSES AND ASSURING SAFETY, R.G. Cassens
S.C. PRESCOTT, M.I.T. DEAN AND PIONEER FOOD TECHNOLOGIST, S.A. Goldblith
FOOD CONCEPTS AND PRODUCTS: JUST-IN-TIME DEVELOPMENT, H.R. Moskowitz
MICROWAVE FOODS: NEW PRODUCT DEVELOPMENT, R.V. Decareau
DESIGN AND ANALYSIS OF SENSORY OPTIMIZATION, M.C. Gacula, Jr.
NUTRIENT ADDITIONS TO FOOD, J.C. Bauernfeind and P.A. Lachance
NITRITE-CURED MEAT, R.G. Cassens
POTENTIAL FOR NUTRITIONAL MODULATION OF AGING, D.K. Ingram *et al.*
CONTROLLED/MODIFIED ATMOSPHERE/VACUUM PACKAGING OF FOODS, A.L. Brody
NUTRITIONAL STATUS ASSESSMENT OF THE INDIVIDUAL, G.E. Livingston
QUALITY ASSURANCE OF FOODS, J.E. Stauffer
THE SCIENCE OF MEAT AND MEAT PRODUCTS, 3RD ED., J.F. Price and B.S. Schweigert
HANDBOOK OF FOOD COLORANT PATENTS, F.J. Francis
ROLE OF CHEMISTRY IN PROCESSED FOODS, O.R. Fennema *et al.*
NEW DIRECTIONS FOR PRODUCT TESTING OF FOODS, H.R. Moskowitz
ENVIRONMENTAL ASPECTS OF CANCER: ROLE OF FOODS, E.L. Wynder *et al.*
FOOD PRODUCT DEVELOPMENT AND DIETARY GUIDELINES, G.E. Livingston, R.J. Moshy and C.M. Chang
SHELF-LIFE DATING OF FOODS, T.P. Labuza
ANTINUTRIENTS AND NATURAL TOXICANTS IN FOOD, R.L. Ory
UTILIZATION OF PROTEIN RESOURCES, D.W. Stanley *et al.*
VITAMIN B_6: METABOLISM AND ROLE IN GROWTH, G.P. Tryfiates
POSTHARVEST BIOLOGY AND BIOTECHNOLOGY, H.O. Hultin and M. Milner

Newsletters

MICROWAVES AND FOOD, R.V. Decareau
FOOD INDUSTRY REPORT, G.C. Melson
FOOD, NUTRITION AND HEALTH, P.A. Lachance and M.C. Fisher

GUIDE FOR AUTHORS

If the manuscript has been produced by a word processor, a disk containing the manuscript would be greatly appreciated. Word Perfect 5.1 is the preferred word processing program. The original and THREE copies of the manuscript should be sent along with the disk to the editorial office. The typing should be double-spaced throughout with one-inch margins on all sides.

Page one should contain: the title, which should be concise and informative; the complete name(s) of the author(s); affiliation of the author(s); a running title of 40 characters or less; and the name and mail address to whom correspondence should be sent.

Page two should contain an abstract of not more than 150 words. This abstract should be intelligible by itself.

The main text should begin on page three and will ordinarily have the following arrangement:

Introduction: This should be brief and state the reason for the work in relation to the field. It should indicate what new contribution is made by the work described.

Materials and Methods: Enough information should be provided to allow other investigators to repeat the work. Avoid repeating the details of procedures that have already been published elsewhere.

Results: The results should be presented as concisely as possible. Do not use tables *and* figures for presentation of the same data.

Discussion: The discussion section should be used for the interpretation of results. The results should not be repeated.

In some cases it might be desirable to combine results and discussion sections.

References: References should be given in the text by the surname of the authors and the year. *Et al.* should be used in the text when there are more than two authors. All authors should be given in the Reference section. In the Reference section the references should be listed alphabetically. See below for style to be used.

RIZVI, S.S.H. 1986. Thermodynamic properties of foods in dehydration. In *Engineering Properties of Foods*, (M.A. Rao and S.S.H. Rizvi, eds.) pp. 133-214, Marcel Dekker, New York.

MICHAELS, S.L. 1989. Crossflow microfilters ins and outs. Chem. Eng. *96*, 84-91.

LABUZA, T.P. 1982. *Shelf-Life Dating of Foods*, pp. 66-120, Food & Nutrition Press, Trumbull, CT.

Journal abbreviations should follow those used in Chemical Abstracts. Responsibility for the accuracy of citations rests entirely with the author(s). References to papers in press should indicate the name of the journal and should only be used for papers that have been accepted for publication. Submitted papers should be referred to by such terms as "unpublished observations" or "private communication." However, these last should be used only when absolutely necessary.

Tables should be numbered consecutively with Arabic numerals. The title of the table should appear as below:

TABLE 1.
ACTIVITY OF POTATO ACYL-HYDROLASES ON NEUTRAL LIPIDS, GALACTOLIPIDS AND PHOSPHOLIPIDS

Description of experimental work or explanation of symbols should go below the table proper. Type tables neatly and correctly as tables are considered art and are not typeset. Single-space tables.

Figures should be listed in order in the text using Arabic numbers. Figure legends should be typed on a separate page. Figures and tables should be intelligible without reference to the text. Authors should indicate where the tables and figures should be placed in the text. Photographs must be supplied as glossy black and white prints. Line diagrams should be drawn with black waterproof ink on white paper or board. The lettering should be of such a size that it is easily legible after reduction. Each diagram and photograph should be clearly labeled on the reverse side with the name(s) of author(s), and title of paper. When not obvious, each photograph and diagram should be labeled on the back to show the top of the photograph or diagram.

Acknowledgments: Acknowledgments should be listed on a separate page.

Short notes will be published where the information is deemed sufficiently important to warrant rapid publication. The format for short papers may be similar to that for regular papers but more concisely written. Short notes may be of a less general nature and written principally for specialists in the particular area with which the manuscript is dealing. Manuscripts that do not meet the requirement of importance and necessity for rapid publication will, after notification of the author(s), be treated as regular papers. Regular papers may be very short.

Standard nomenclature as used in the engineering literature should be followed. Avoid laboratory jargon. If abbreviations or trade names are used, define the material or compound the first time that it is mentioned.

EDITORIAL OFFICE: DR. D.R. HELDMAN, COEDITOR, *Journal of Food Process Engineering*, Food Science/Engineering Unit, University of Missouri-Columbia, 235 Agricultural/Engineering Bldg., Columbia, MO 65211 USA; or DR. R.P. SINGH, COEDITOR, *Journal of Food Process Engineering*, University of California, Davis, Department of Agricultural Engineering, Davis, CA 95616 USA.

JOURNAL OF FOOD PROCESS ENGINEERING VOLUME 19, NUMBER 3

CONTENTS